Voice Coil Controlled Inspiration and Expiration Valves

PER BERGQVIST
LINUS KEMMLER

KTH Industrial Engineering
and Management

Master of Science Thesis
Stockholm, Sweden 2012

Voice Coil Controlled Inspiration and Expiration Valves

Per Bergqvist
Linus Kemmler

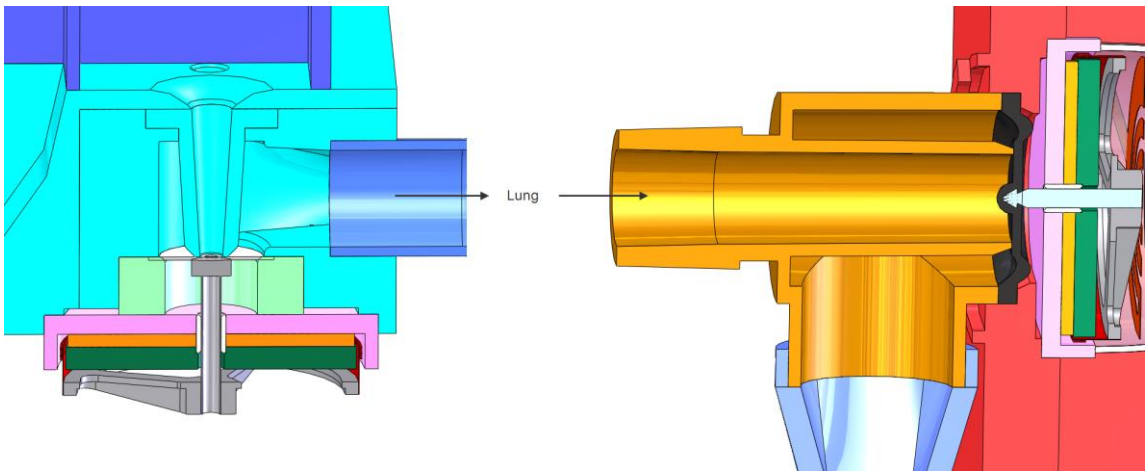

Master of Science Thesis MMK 2012:58 MDA 440
KTH Industrial Engineering and Management
Machine Design
SE-100 44 STOCKHOLM

KTH Industriell teknik och management

Examensarbete MMK 2012:58 MDA 440

Talspole kontrollerad inspiration och exspirations ventiler

Per Bergqvist
Linus Kemmler

Godkänt	Examinator	Handledare
2012-08-23	Jan Wikander	Mats Hanson
	Uppdragsgivare	Kontaktperson
	Maquet	Carl Troili

Sammanfattning

Masteruppsatsen utfördes på Maquet Critical Care i Solna, Stockholm. Maquet Critical Care är marknadsledande inom högpresterande ventilatorer. En ventilator är en maskin som hjälper patienter att andas. Två av de viktigaste komponenterna i en ventilator är de två ventilerna som är placerade närmast patienten, nämligen inspirations- och exspirationsventilen.

Huvudsyftet med denna masteruppsats är att få både en teoretisk och praktisk insikt av de inspirations- och exspirationsventilerna som skulle utvecklas. Utöver detta har en ventilatorprototyp utvecklats med hjälp av dessa ventiler.

Utifrån teoretisk kunskap är målet med uppsatsen att uppfylla ett antal krav på ventilerna och ventilatorn. Dessutom kommer uppsatsen att leda till riktlinjer för fortsatt forskning och utveckling av de framtagna ventilerna.

För att möjliggöra användandet av ventilerna i en ventilator kom Maquet med många olika krav. Kraven var fördelade inom flödeskaraktäristik, effektförbrukning, dynamisk prestanda och kostnad.

I arbetsmetoden som användes ingick en förstudie av flödesdynamik, ventiler och ventilatorer. Ventilernas design utvecklades med hjälp av flödessimuleringar. De tillverkade ventilmodellerna testades, dels för att verifiera krav och dels för att få en insikt om flödesimuleringarnas tillförlitlighet.

De aktuatorer som skulle användas var talspolar. I denna uppsats vi har använt oss av en standardaktuator men för att få maximal prestanda har en undersökning angående en optimerad talspole gjorts. För att få insikt i ventilernas dynamiska prestanda, utvecklades en dynamisk modell av talspolen och ventilsätet. Bandbredden för denna modell har verifierats med bandbredden på uppmätta ventiler.

För att realisera en tryckstyrd ventilation behövde inspirations- och exspirationsventilerna synkroniseras. Denna synkronisering och reglering implementerades i Matlab/Simulink och exekverades med dSPACE.

Alla verifierade krav har uppfyllts och har resulterat i två ventiler som maximat förbrukar 2 Watt. Den tryckstyrda ventilationen exekverades på den framtagna ventilatorprototypen och dess prestanda uppfyller ställda krav.

Två specialiseringar har också blivit undersökta. Dessa är inom flexure baserad upphängning av talspole samt hur gasen genom ventilator kan modelleras på lämpligast sätt.

KTH Industrial Engineering and Management

Master of Science Thesis MMK 2012:58 MDA 440

Voice coil controlled inspiration and expiration valves

Per Bergqvist
Linus Kemmler

Approved	Examiner	Supervisor
2012-08-23	Jan Wikander	Mats Hanson
	Commissioner	Contact person
	Maquet	Carl Troili

Abstract

This master thesis was performed at Maquet Critical Care located in Solna, Stockholm. Maquet Critical Care is a market leader in high performance medical ventilators. A ventilator is a medical device that helps patients to breathe. Two of the most vital components of a ventilator are the valves that are closest to the patient. These are the inspiration valve and the expiration valve.

The main purpose with this thesis is to get, theoretical as well as practical insights into the inspiration- and expiration valves to be developed. On top of this a ventilator using the developed valves was to be developed.

On the base of theoretical knowledge, the aim of the thesis is to achieve a set of valve and ventilator requirements on developed prototypes. On top of this the thesis should be able to deliver advice and guidelines for possible future research on these valves.

In order to use valves in a ventilator there were many requirement posed on the valves. These requirements included flow characteristics, power consumption, dynamic performance and cost.

The methodology used included a pre study of fluid dynamics, valves and ventilators. Initial valve designs were developed with the use of flow simulations. The valve models were manufactured and tested as well as being compared to the flow simulations.

The actuators used for the valves were voice coils. In this thesis a standard actuator was used to control the valves but in order to get the maximum performance an investigation into optimized voice coils were performed. In order to get insight into the control of the valves, a dynamic model of the voice coil were developed. This model was verified to have the same bandwidth as the measured voice coils and valve assembly.

In order to realize a pressure controlled ventilation mode the inspiration valve and expiration valve were synchronized. The control algorithms were implemented in Matlab/Simulink with dSPACE.

The tested requirements were fulfilled, resulting in valves that have a maximum power consumption of 2 Watts. The pressure controlled ventilation was executed on the developed demonstration ventilator. The performances of this ventilator were desirable and fulfilled the ventilator requirements.

Two specializations topics have also been investigated, in the areas of flexure based voice coil suspension and gas modeling.

Acknowledgements

This master thesis was performed at Maquet Critical Care in Solna, Stockholm in 2012, and it concludes a Master of Science degree in Engineering Design with Mechatronics as the major subject at Royal Institute of Technology in Stockholm. This has been an extremely good experience as a last step before graduation.

We want to thank everyone at Maquet Critical Care particular our supervisor Carl Troili for all support and help. We would also like to thank Leif Back, Staffan Henriksson, and Jukka Kaijalainen for their excellent support in manufacturing the electronics and mechanical components of the various prototypes.

Thanks also to Mario Loncar for giving us the opportunity to do Master Thesis at Maquet Critical Care and thanks to our supervisor at Royal Institute of Technology Mats Hanson.

Thank you all very much.

Per Bergqvist and Linus Kemmler

Stockholm, August 2012

Nomenclature

Notations

Symbol	Description
r	Radius [m]
p	Pressure [Pa]
Q	Flow $[m^3/s]$
ν	Kinematic viscosity $[m^2/s]$
ρ	Density $[kg/m^3]$
T	Temperature [K]
V	Volume $[m^3]$
ΔP	Pressure drop $[hPa]$
F	Force $[N]$
Re	Reynolds number
m	Mass $[kg]$
E	Young's modulus $[N/m^2]$
B	Magnetic flux density$[T]$
i	Current$[A]$
d	mechanical damping constant $[N \cdot s/m]$
k	mechanical spring constant $[N/m]$
C	electrical capacitance [F]
L	electrical inductance [H]
R	electrical resistance [Ω]

Abbreviations

ADC	Analog to digital converter
atm	Atmospheric
Bpm	Breaths per minute
CAD	Computer Aided Design
CFD	Computational fluid dynamics
cmH20	Centimetre of water
DAC	Digital to analog converter
DC	Direct current
FEA	Finite element analysis
FEMM	Finite Element Method Magnetics
lpm	Litre per minute
PEEP	Positive End Expiratory Pressure
PaP	Peak airway Pressure
PTFE	Polytetrafluoroethylene
UTS	Ultimate Tensile Strength
VCM	Voice coil motor

List of Figures

Table of Contents

1 Introduction

A ventilator is a medical device that helps critically ill patients to breathe. Maquet Critical Care is one of the market leaders in the high performance ventilator segment with their Servo-i ventilator.

This thesis investigates novel technologies for the gas delivery system of a high end intensive care ventilator.

The technical solution that has been investigated in this thesis has been focused on the two valves that control the flow of gas to and from the ventilated patient, namely the inspiration valve and the expiration valves. The primary driving force for the investigation into these valves, are to search for possibilities to design valves that can be produced at a lower cost, consume less energy and be reduced in size compared to the valves used in the Servo-i.

The main purpose of this thesis is to show that these new valves have the ability to achieve these goals. On base of theoretical knowledge, the aim of the thesis was therefore to develop technology able to fulfil a set of requirements posed on the valves. These valves in combination with a control algorithm will implement a basic pressure controlled breathing mode.

1.1 Background

This section is aimed at describing the basic working principle of a ventilator and the general role of the inspiration valve as well as the expiration valve. The main emphasis in this section has been on describing how and why improvements could be made to the inspiration and expiration valves.

1.1.1 Ventilation principles

There are two types of ventilation: assisted or controlled ventilation. When using assisted ventilation the ventilator helps the patient to breath when the patient assign a breath. Controlled ventilation means that the ventilator determines when and how often a patient makes a breath. Ventilators use a variety of pressure and flow sensors in order to make sure it ventilates the lung in a defined way. There are many different types of ventilation modes. Two basic ways to ventilate the lung are Volume Controlled Ventilation (VCV) seen in Figure 1. This delivers a specified volume at each breath.

The other is Pressure Controlled Ventilation (PCV) seen in Figure 2. Ventilator delivers a specified constant pressure to the patient.

There are many more features and modes that a ventilator can handle but these have not been in focus in this thesis and we will only use Pressure Controlled Ventilation.

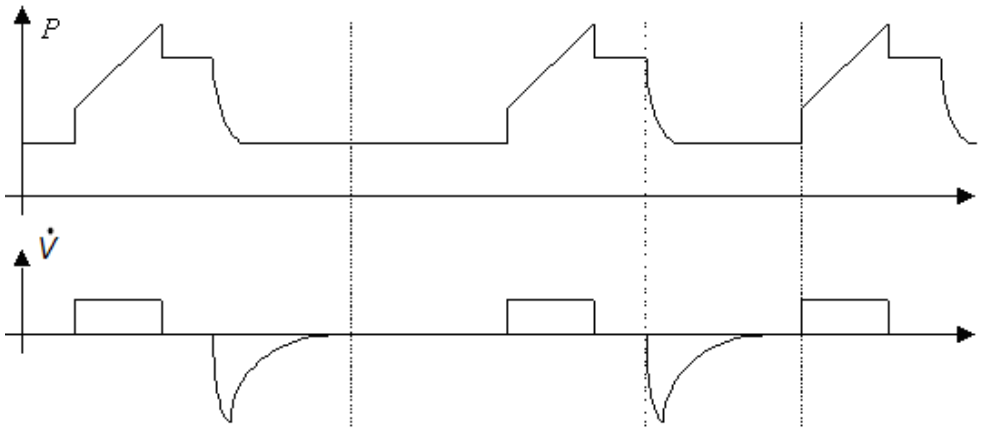

Figure 1: Ideal pressure and flow curves with volume controlled ventilation.

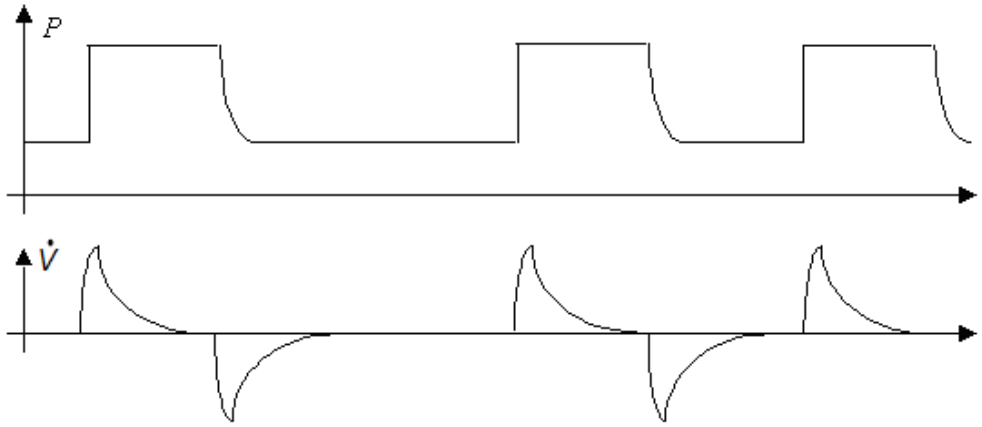

Figure 2: Ideal pressure and flow curves with pressure controlled ventilation.

Settings

To configure a ventilator some basic settings need to be defined:

- Patient type - Type of patient: adult, infant and neonatal.
- Positive End Expiratory Pressure (PEEP) - Overpressure in the lung to keep it from collapse during expiration.
- Pip - Peak inspiratory pressure.
- Pap - Pressure above PEEP
- Bpm - Breath frequency.
- Tidal volume - The amount of gas enter the patient.

1.1.2 Different Types of Ventilators

Ventilators can be used for a diverse range of patients and diseases. From the highly sophisticated devices are used in the intensive care departments wards down to less complicated devices used for ventilatory support in home care. Maquet Critical Care specializes in high performance medical ventilator for use in the intensive care department Their current ventilator is called Servo-i and can be seen in 3.

Figure 3: The ventilator Servo-i.

There are many ways to control the delivery of gas to a patient and the ventilation process, more details of this has been elaborated on in the report *EVU 124966 WGI Ventilatorer* [14]. The techniques described in the aforementioned document utilizes pressurised gas or some type of compressor to build up the pressures needed by the ventilator.

1.1.3 Basic Principle of a Valve Based Ventilator

A ventilator is used to control the respiration of a patient that has some type of respiratory deficiency. By the use of synchronized valves, the pressure in or flow to and from, the lung can be controlled in order to make the patient breathe. A basic and simplified description of ventilator is described below and seen in Figure 4.

In Figure 4 the gas present at the inlet to the inspiration valve, has a relatively high pressure in relation to the atmosphere as well as the patients lung. Hence opening the inspiration valve, gives a flow going from left to right through the inspiration valve in Figure 4. Given that the expiration valve is closed, the

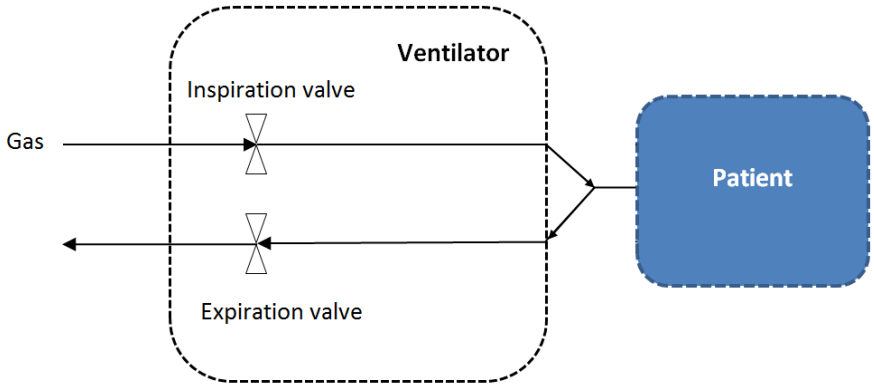

Figure 4: The basic working principle of a ventilator connected to a patient.

flow goes into the patients lung hence making - or helping - the patient inhale. By opening the inspiration valve less or more the flow will correspondingly be lower or higher. The valve itself can be thought of as a fluid resistance with flow going through it and a pressure drop over it. This is in analogy with the current through and voltage over an electric resistor.

As flow enters, the pressure in the lung increases. By closing the inspiration valve, a desired volume inserted into the lung - or a desired pressure in the lung - can be achieved. The lung pressure at this time is higher than the atmospheric pressure.

Opening the expiration valve then starts the exhalation. Since the inspiration valve is closed and the lung pressure is high a flow will pass through the expiration valve.

The next breath in turn, will begin by opening the inspiration valve and closing the expiration valve. The path which the gas travels through the ventilator and patient is defined as the gas chain throughout this thesis.

1.1.4 Gas Mixing Principles

In order to control the oxygen level in the delivered air, there is a need to mix oxygen and air. Two different principles for gas mixing - serial and parallel mixing - are shown in Figure 5.

The main difference is at what stage the air and oxygen are mixed in the ventilators. Serial mixing imply that the air and oxygen are mixed into a container before it enters the inspiration valve. The mixing of the air is done by two gas mixing valves whereas the inspiration valve controls the flow of gas to the patient. Since the gas is mixed in a tank this type of ventilator will be refereed to as a tank based ventilator for the remainder of the thesis.

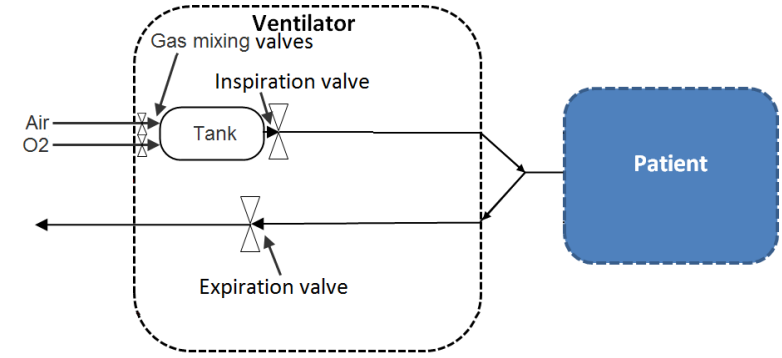

(a) Working principle of serial mixing with a tank based ventilator.

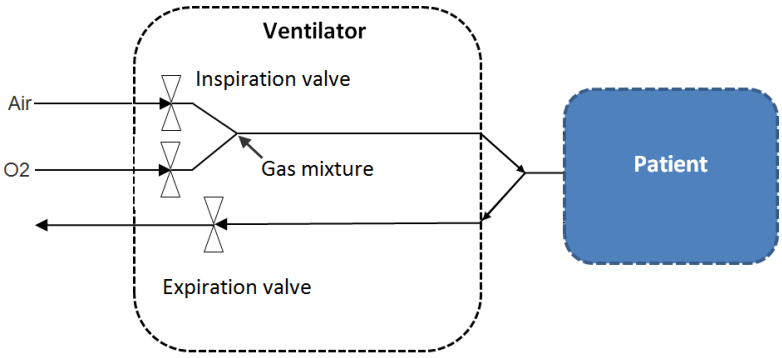

(b) The working principle of parallel mixing that is used in Servo-i.

Figure 5: Two gas mixing principles.

Companies that utilises this ventilator technology include Dräger (VN500), Hamilton (G5) and Viasys (Avea) [14].

For parallel mixing - used in Servo-i - gases are mixed directly after it exits the inspiration valves. In this case the gas mix and flow control is achieved by the same valves. Competitors using parallel mixing ventilators include Dräger (Evita) and GE (Carestation) [14].

Design Consequences of Gas Mixing Approaches

The pressurised gases supplied to these ventilators originate from two possible sources. Most hospitals - in Sweden for example - have built in pressurised gas lines. These gas lines should have a nominal pressure of 4 Bar according to standard *7396-1 Medical Gas Pipelines System Part 1* [13]. This standard also states that the ventilators should be certified to handle pressures up to 10 Bar without endangering the patient. Many other hospitals around the world use compressors in order to create the pressures needed by the ventilators. The compressor Servo-i uses today normally operates with a pressure of 3.5-4.5

Bar [46].

In the case of a parallel mixing ventilator there are two different approaches for coping with varying inlet pressure. Servo-i uses high performance inspiration valves that are certified to operate with a big pressure range of 2-6.5 Bar [16] as well as being able to handle fault cases of up to 10 Bar.

From a design perspective the low inlet pressure (2 Bar) determines the valve size and consequently the stroke length of the valve in order to deliver required maximum flows. The highest inlet pressure (10 Bar) on the other hand determines the maximum forces needed by the valve actuator. The consequence of designing for this large pressure range is that a larger more expensive valve actuator is needed. Further elaboration on the interaction between valve sizes, stroke lengths and actuator forces is covered in *Chapter 3 - Valve Seat Design* and *Chapteter 4 - Valve Actuator*. Another difficulty with an uncontrollable pressure range is that the valve gain - from control signal to desired valve flow - changes depending on the inlet pressure. This poses difficulties to the robustness of the control strategy used for the valve.

The other approach for parallel mixing ventilators is to have pressure regulating valves before the inspiration valves. These valves would ensure that the inspiration valves have a set and relatively low pressure at their inlet. For these ventilators there would be two more valves added to the ventilator in Figure 5b.

For a tank based - serial mixing - ventilator the problems of high pressure range is handled by the gas mixing valves. These valves will regulate the pressure in the tank to a set pressure. They do not have the same high dynamic flow demands since they are not responsible for controlling the flow of gas to the patient. In this case the inspiration valve is working with a controllable inlet pressure. Primarily, this enables optimization of the actuator force and stroke length. Another benefit with a controllable inlet pressure, is being able to adjust the pressure to different patient groups. For example it could be set to 1 Bar to handle an adult patient or be set at 0.25 Bar to handle an infant patient.

The sensor signals that control the inspiration valves are flow and pressure. The control signals used for the inner control loop, depend on the ventilator principle that is used. For parallel mixing ventilators, the flow through the valves has to be controlled in the inner most control loop, this in order to be able to set the desired gas concentration (see Figure 5a). For the serial mixing ventilators the inner loop could be controlled by either flow or pressure. This is due to the fact that the gas concentration is already set before the gas reaches the inspiration valve (see Figure 5b).

1.1.5 Incentives for the Development of New Valves

The main aim of this thesis was to develop a new inspiration valve and a new expiration valve. According to the requirements from Maquet, these valves would be adapted to meet the requirements of a tank based - serial mixing - ventilator. Since the inspiration valve is right next to the tank, the design of the inspiration valve is closely related to the tank concept. The development of a new expiration valve on the other hand is more related to possible improvements that could be made to the existing expiration valve as well as and the whole expiration assembly.

A secondary aim of the thesis was to implement a tank based ventilator using the newly developed valves. In order to limit the scope of the thesis the gas mixing valves would not be included in this ventilator. An illustration which indicate the aspects of the ventilator - that are included in the thesis - are seen in Figure 6.

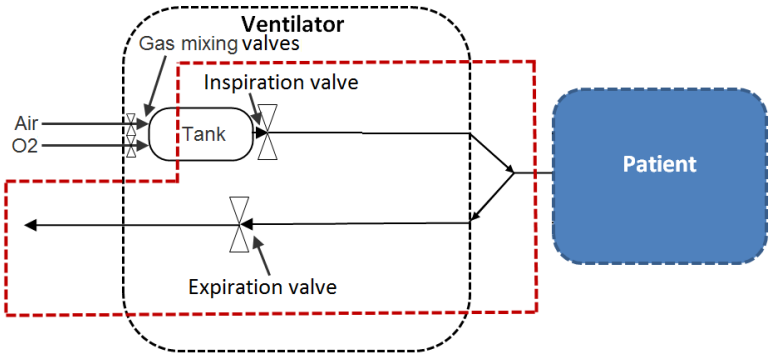

Figure 6: The areas of the tank based ventilator to be implemented in this thesis.

This thesis will not elaborate on all the benefits and drawbacks of a tank based ventilator. Instead it will focus on the implications that a tank based ventilator would have on a inspiration valve. A comprehensive investigation into the entire tank based ventilator is instead presented in Carl Troili's research report *Tankar om Tankar* [22].

Even though the tank based ventilator does not affect the expiration valve, there are a lot of improvements that could be made compared to the current design in Servo-i. These improvements are investigated in this thesis.

Improvements Possible to the Inspiration Valve

As covered in *Design Consequences of Gas Mixing Approaches* above, the inspiration valve have different working conditions on a tank based ventilator compared to a parallel mixing ventilator. The assumption is that these differ-

ent conditions will result in the inspiration valves being smaller, less expensive and be easier to control compared to the ones used on the Servo-i.

Fulfilling the requirements given by Maquet (see *1.3 Requirements*) would be a first step in proving the assumed benefits of using a serial mixing ventilator.

Improvements Possible to the Expiration Valve

The expiration valve in the current ventilator was originally designed to be driven by a solenoid that could deliver high forces with a short stroke. Hence the diameter of the expiration valve seat was made relatively big. Due to a last minute design change the actuator was changed to a voice coil that has a long stroke and handles lower forces. Since the valve seat design required high forces, the voice coil got big and expensive.

By reducing the size of the expiratory valve, the needed forces are lower; hence a smaller and lower-cost actuator is needed. The solution today is a cassette assembly that consist of a water trap, flow sensor, valve and a check valve. This assembly has a separate check valve that prevents air re-breath of exhaled air. By combining valve and check valve in one design the number of parts is reduced and enables to a lower production cost and size. There will also be possible to use active opening with that means the valve can be opened by the actuator. Consequently you have control over the membranes position.

The regulations of the hygiene say that you need to clean the expiration valve after each patient. In the current system you need to wash a big cassette that hold all the parts of the expiration valve. Cassette need to be replace every year and is expensive because of integrated electronics.

A smaller and lower-cost design of the cassette would make it possible to replace it and get rid of the wash process that take time and also is expensive. The response against single use are mostly than is not environment-friendly but the process to sterilize is power consuming and not friendly at all. With compact design the amount of material to be thrown away can be kept low.

1.2 Purpose

The main purpose with this thesis was to get, theoretical as well as practical insights into benefits and drawbacks of a new type of inspiration valve as well as expiration valve.

Implementing a ventilator on the basis of the two valves would also give insights into the concept of a tank based ventilator.

1.3 Requirements

Since the main aim with the thesis was to develop new valves, most of the requirements cover the inspiration and expiration vales separately. These requirements can be found in reference [16] and [17] and a summary of these requirements are given in bullet form below.

Inspiration Valve

- Be able to deliver flow rates of 120 and 180 lpm at 0.5 and 1 Bar respectively.
- Be able to adjust the flow between 0.5 and 180 lpm.
- A flow change of 0 to 180 lpm should take less than 20 ms.
- The valve actuator should be a Voice Coil Motor (VCM)
- Without power the flow should not be more than 0.5 lpm at 0.5 Bar.
- The power consumption shall be less than 5 W when flow is 0.5 lpm at 1 Bar.
- The flow shall be less than 0.04 lpm at 1 Bar for at least 1 s.
- The peak power consumption shall no exceed 20 W.
- The Ferromagnetic material in the valve should be 50% of that in the current ventilator.

Expiration Valve

- When active have same pressure drop as Servo-i.
- Inactive valve should have a pressure drop less than 3 hPa at a flow 30 lpm.
- The valve actuator should be a Voice Coil Motor (VCM)
- Reverse flows above 0.5 lpm shall be blocked even with no power.
- Flow shall be adjustable from 0.5 lpm to 180 lpm.
- Power consumption shall be less than 5 W.
- Peak power less than 15 W.
- It shall be possible to reduce flow to less than 20 ml/min at 50 hPa for 10 seconds.

- Cost of assembly less than 500 SEK.
- Easily detach of expiration assembly.
- The Ferromagnetic material in the valve should be 50% of that in the current ventilator.

The requirements on the integrated valves, i.e. the prototype ventilator was to achieve similar performance to that of Servo-i, when used in pressure control mode. This is the mode used when a desired pressure profile is desired in the patient lung. These pressure profiles are to be achieved on four different test lung configurations.

1.4 Delimitations

The major delimitation in this thesis have been showed in Figure 6. This shows which aspects of the tank based ventilator that have not been investigated.

The focus on the practical implementation of the prototype has been to prove functionality rather than optimizing performance.

1.5 Methodology

The basic framework for how the thesis was to be implemented were given by Maquet. This framework (shown below) also gives a good view of the general tasks that were to be performed during this thesis.

The method framework

- Theoretical analysis of valves.
- Simulation of flow and pressure drop of valves in SolidWorks Flow Simulation.
- Manufacture valves in Maquets workshop.
- Measuring of pressure drop, flow and force with Mecmesin.
- The development a VCM with the help of an external partner.
- Implement ventilator control algorithms in MATLAB Simulink which are to be executed on DSpace.
- Verify requirements.

The development work of the ventilator prototype were in large parts a cooperative effort, with an individual focus on each valve. Linus Kemmler focused on the expiration valve whereas Per Bergqvist focused on the inspiration valve.

Linus Kemmler also worked on developing a VCM for a future version on the tank based concept.

Per Bergqvist also worked on developing a model for the gas chain.

2 Theory

This part describes the theoretical knowledge that was deemed necessary to be enable to realize this Master Thesis. This section gives the basic understanding of how this works in theory.

2.1 Modelling Analogies

By using analogies, one is able to describe diverse fields of engineering by the same principals. Hence one can describe fluid domain, mechanical domain and electrical domain problems using equations for fundamental components such as resistors, capacitors and inductors [10]. In this thesis Bond Graphs [11] are used when systems have been modelled. This is a graphical representation of dynamic systems where the product of the system variables - referred to as effort and flow - are the physical energy of the system. The system variables as well as the component equations for the corresponding domain are described in Table 1. The systems described in Table 1 also describes the main physical

System	**Effort**	**Flow**	**Resistor Equation**	**Capacitor Equation**	**Inductor Equation**
Electrical	Voltage	Current	$U = R \cdot i$	$i = C\frac{dU}{dt}$	$U = L\frac{di}{dt}$
Mechanical	Force	Velocity	$v = \frac{1}{d} \cdot F$	$F = m\frac{dv}{dt}$	$v = \frac{1}{K}\frac{dF}{dt}$
Fluid	Pressure	Flow Rate	$p = R_f \cdot Q$	$Q = C_f\frac{dp}{dt}$	$p = L_f\frac{dQ}{dt}$

Table 1: Analogies between engineering domains

domains in which a ventilator work. The electrical characteristics of the VCM result in a movement of the mechanical valve which in turn results in an effect on the gas in the fluid system.

2.2 Valve Seats

This section gives an overview on the valve types that were of interest for this master thesis project.

2.2.1 Membrane Valve Seats

Membrane valve is also called a diaphragm valve seat, we will use the name membrane valve in this report. This type of valve seat uses a flexible di-

aphragm or membrane to control the flow. Valve appearance can be seen in Figure 7 where shown in open and closed mode.

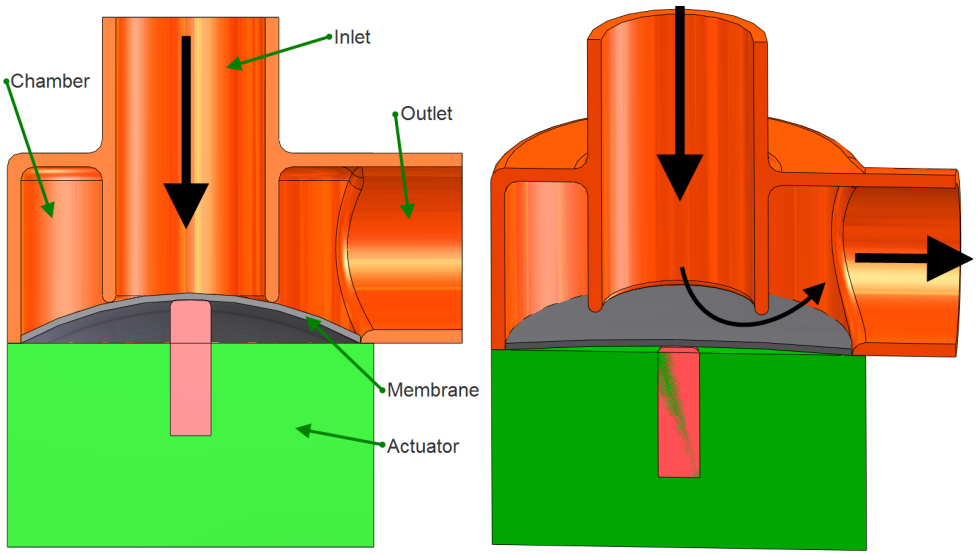

(a) Closed (b) Open

Figure 7: An example of a Membrane Valve.

The main part of the valve seat is also declared. The end of the inlet is the part that is pressed against the membrane to control the flow, this area is important for the characteristics of the valve seat. As seen in Figure 7 the actuator is not exposed to the fluid due to the sealing membrane. For the ventilator application, the fluids can in some cases consist of high fractions of oxygen, which causes combustion hazards. Having the actuator separated from this environment puts more regulatory constraints on the actuator. This is one of the benefits of the membrane valve seat. This type of valve seat is commonly used in medical applications [9].

2.2.2 Globe Valve Seats

The principal of a globe valve seat is seen in Figure 8. In this case the valve plug surface seals the valve. In contrast to the membrane valve, this valve has an exposed actuator. Even though this puts harsher requirements on the actuator these problems are believed to be solvable for this application. For example, by using actuators with lower maximum power consumptions, the regulatory requirements are also lower. Since one of the aims with this thesis is to lower the power consumption of the actuators, compared with the actuators used today, the safety requirement on this aspect will be lower.

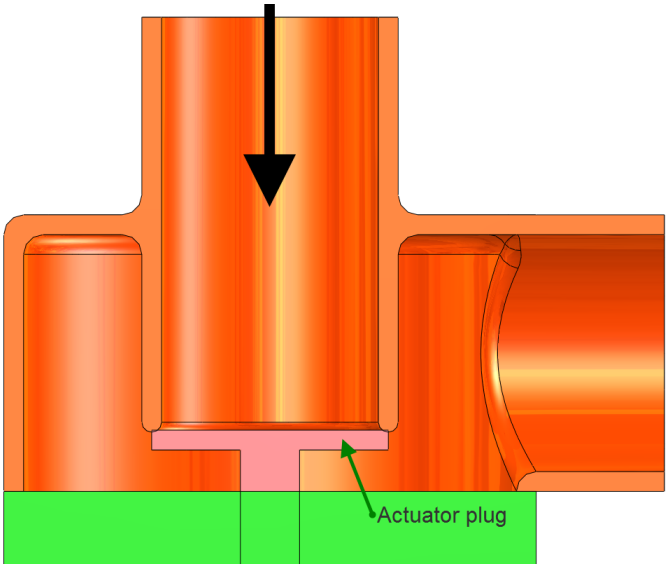

Figure 8: An example of a Globe Valve.

Under certain circumstances the pressure in the ventilator valve chamber fluctuates. In the worst case this makes the valve oscillate which would be unacceptable for a ventilator. Having a membrane increases the surface on which the valve pressure is acting. Instead by having only a valve plug this surface is minimized. Hence globe valves are less affected by valve chamber pressure fluctuations. Generally the globe valve is also good for flow rate control.

2.3 Valve Actuators

Voice coil are common used in loudspeaker but can also be used as actuator a example can be seen in Figure 9. The basic principle of a voice coil is a permanent magnet and a coil that are place in the magnetic field. By applying current in the coil this generates a force that what to move the coil which can be described with Lorenz force law equation (1). Where B is the magnetic flux density, i is the current flowing through the wire and l_w is the length of the wire.

$$F = Bil_w \tag{1}$$

The limitation of coil movement is to where the flux field is strong or present. Given equation (1) force can be described as proportional to current. This gives that VCM have no limit in position precision[34], this will only be limited by the driver of the VCM. Friction can be a problem at small movements but can be reduce with different suspension. This makes it perfect for position control with small stroke length. A basic voice coil assembly can be found

Figure 9: A voice coil where the coil is removed from the magnet.

in Figure 10a. The characteristics of the voice coil are mainly defined by the flux field in the air gap. The coil will move up and down in gap depending on how much current is applied and direction of current. A model of the electric circuit of the VCM is shown in Figure 10b. The power consumed by the VCM is given by $P = i^2/R$ with R is resistance is the coil winding. In turn R is given by $R = (\rho \cdot l_w)/A$ where ρ is the resistivity for the cable and A is the cross sectional area.

2.3.1 Linearity of a Voice Coil Motor

If the force needs to be linear over a long stroke it is desirably to design the voice coil for this purpose. This can be accomplished in two ways either by making an overhung or underhung coil. A overhung coil is a coil that is significantly longer than the gap height seen Figure 10c. With this design you don't use the part of the coil that's not placed in the gap height. But this part still consumes energy. Underhung is the other way around, here you need a big permanent magnet instead to get a strong flux field in the air gap.

2.3.2 Modelling the Voice Coil Motor

The mechanical part of the VCM - with the valve setup in consideration - is described in Figure 11. The spring force acting on the system is F_s whereas the damping force is F_d. The explanation into why a spring is added to the valve is given in Section 3.1.8. The damping force is caused mainly by the sliding bearing in the VCM. Except the spring and damper, other forces acting on the system are F_g, F_{VCM} and F_{ex}. F_g being the force of gravity on the moving mass. F_{VCM} is the force created by the VCM and F_{ex} represents external forces. The external forces

$$F_{ex} = F_p$$

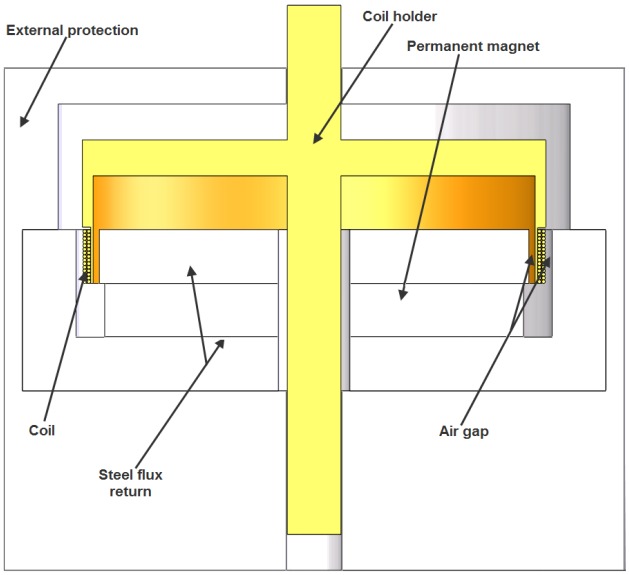

(a) Different parts of a voice coil assembly.

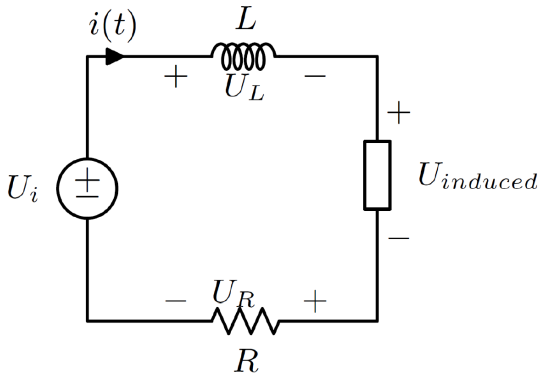

(b) A model of the electrical circuit of a voice coil.

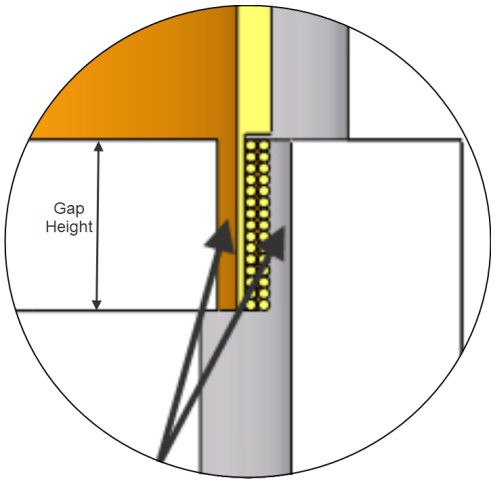

(c) Enlargement of air gaps in voice coil.

Figure 10: Basic of mechanical and electronic of a voice coil.

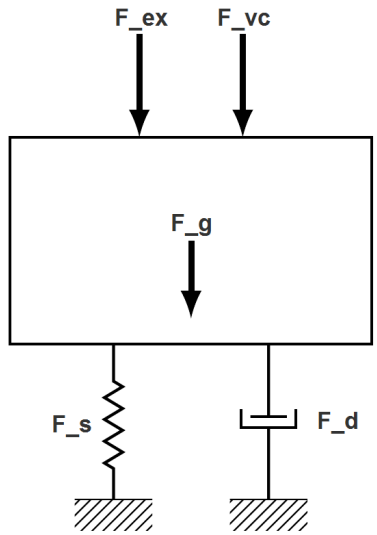

Figure 11: The mechanical mass, spring and damper system.

Are in this case only made up by the forces due to the gas pressure F_p. The easiest way to model F_p is to assume that the inlet pressure to the valve is acting on a surface the same size as the valve inlet, i.e

$$F_p = A_{inlet} \cdot p_{inlet}$$

The model of the combined electrical and mechanical system of the voltage controlled VCM were implemented using the Bond Graph shown in Appendix K. From this Bond Graph a state space model were developed as described in Appendix K. If one only considers the voltage as input to the system, the corresponding Laplace transfer function, from voltage $U(s)$ to position $Y(s)$ is

$$\frac{Y(s)}{U(s)} = \frac{K_F}{mLs^3 + (mR + dL)\, s^2 + (K_F K_b + kL + dR)\, s + kR}$$

VCM Modelling Discussion

The main purpose with this model has been to gain general understanding of the valve as opposed to be using it to find an optimized control system. It has been of importance when drawing conclusions on how - for example - the bandwidth of the system is affected when different voice coils are considered.

2.4 Gas and Lung Modelling

The gas chain is a vital part of the ventilator system and the properties of the gas are important in order to understand how the gas behaves in the system. This section is aimed at describing the reasoning behind the gas chain modelling approach used in this thesis.

2.4.1 Gas Standard

The Ideal Gas Law in (2) is a good approximation of the state of a gas. It describes the relations between the pressure p, the volume V, the number of moles n, the gas constant R and the temperature.

$$p \cdot V = n \cdot R \cdot T \tag{2}$$

This law indicates that one state of the gas is highly dependant on the other states. Hence when stating volume it is of importance to know at which temperature and pressure the volume is expressed. A gas standard gives a standardized way of expressing in which state the gas is expressed. The gas standard ATPD - Ambient Temperature Pressure Dry has been uses throughout in this thesis. This means that the volume is given at the ambient temperature and pressure and that the gas has 0 % relative humidity.

2.4.2 The Aim of Gas and Lung Modelling

In Section 2.3.2 *Modelling the Voice Coil Motor* the external forces acting on the valve were described as

$$F_{ex} = F_p$$

with a simple estimation of the force from the gas pressure being

$$F_p = A_{inlet} \cdot p_{inlet} \tag{3}$$

In static conditions this estimate were found quite accurate in Section 3.1.7. With that said there are conditions when the pressure in the valve chamber (see Figure 7) has a big impact on the valve. This is not captured by (3) since p_{inlet} is the constant pressure at the inlet to the valve. The most prominent example of when the estimate in (3) is flawed is when there are standing waves present in the gas chain.

A pressure anti-node present at the valve chamber might cause the valve to become unstable without a robust controller. In order to create a robust controller it is therefore of importance to develop a gas chain model that can capture behaviors such as standing waves.

2.4.3 Lumped Based Modeling Approach

In many modelling cases it is straight forward and intuitive to use lumped models on the system of interest. As described in Section 2.3, the physical mass-spring-damper system is described as a lumped model without considering any other modelling approach.

When modelling a gas the lumped modelling approach is not as obvious. Therefore investigations into lumped based modelling approaches were conducted. In the book Sound modelling: source-based approaches [32], Federico Avanzini gives a good general description on how to model acoustics with a source based approach. According to Avanzini a source based model should be used when the important thing to study, is the interactions that have generated the acoustic signal, rather than the acoustic signal itself. This is the case for the gas chain since the possible sound generated is not of interest in order to ventilate the patient. One consequence of using a source based approach is that those modelling parameters have physical interpretation like mass and pressure e.t.c.

Avanzini states that the source based modelling is generally grouped into two major categories, lumped and distributed systems. A distributed model is good at describing systems which propagate along both time and space. These are able to describe one dimensional resonator such as strings, as well as three dimensional resonators such as rooms. Mathematically these systems are described by the use of Partial Differential Equations (PDE).

The lumped model is more limited when the systems extension in space is to be described. For the physical spring-mass-damper system, the velocity is assumed to be the same for the entire mass, this is often a valid assumption. For a gas on the other hand, the flow and pressure may vary greatly along the length of a tube for example. A way to include special dependence is to introduce lumped elements that are coupled, also refereed to as lumped model synthesis. A basic example of a lumped model with modal synthesis is seen in Figure 12.

As described in Modelling Analogies 2.1, the mechanical system in Figure 12 might just as well describe a fluid system. In this case the mechanical system gives an intuitive description into the assumed behavior of the gas.

2.4.4 Lumped Model Parameters for Fluids

As stated the parameters in source based models all have physical interpretation. A good description and explanation into the reasoning behind the equivalent parameters in the fluid lumped models are given in [10]. Since the

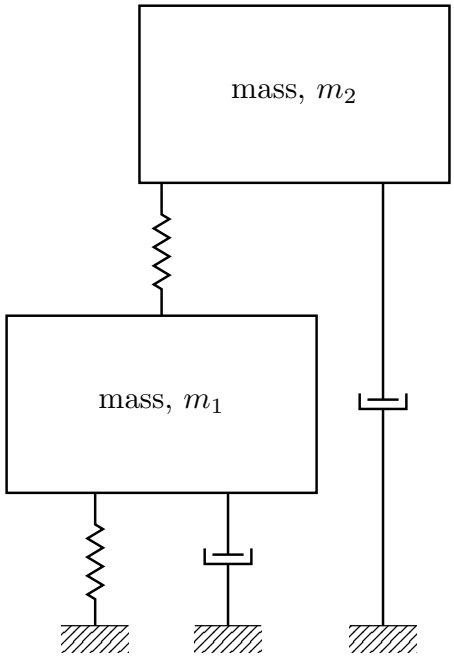

Figure 12: The principle for the lumped model with modal synthesis.

fluid resistance is given by

$$R_f = \frac{\Delta p}{Q} \tag{4}$$

it is easy to measure the fluid resistance. For a given flow Q there will be a pressure drop Δp which gives the fluid resistance R_f. According to [10] the fluid resistance for a gas or fluid, at laminar flow - through a cylinder - is directly proportional to the viscosity ν, the length of the airway l on the tube and reversely proportional to the radius by the power of 4 as

$$R_f = \frac{128\nu l}{\pi D^4}$$

It should be noted that dealing with fluids often include non-linearities. Most fluid resistors are non-linear [10] and one of the causes for non-linearity are turbulent flow. The measured resistance will therefore be different for different flows Q. The fluid capacitance can be described as an air charged accumulator with

$$C_f = \frac{Q}{\Delta \dot{p}} = \frac{\Delta V}{\Delta p} \tag{5}$$

where the integrated flow Q is a change in volume ΔV. C_f could therefore be determined by inserting a known amount of volume into the object to be investigated. By measuring the resulting change in pressure, C_f could be determined. In theory the parameter C_f for a cylindrical reservoir are described as

$$C_f = \frac{A}{\rho g} \tag{6}$$

where A is the area of the cylinder, ρ is the density of the fluid and g is the constant of gravity. The fluid inertia which is described by

$$L_f = \frac{\Delta p}{\dot{Q}} = \frac{\int \Delta p}{Q} \tag{7}$$

Although this also could be measure it is not as straight forward as in the case of the fluid resistance and capacitance. In this thesis the inductance have only been used when modelling cylindrical tubes and hence one could use

$$L_f = \frac{\rho l}{A} \tag{8}$$

to determine the inertia of the gas. Here l is the length of the tube section.

2.4.5 Lumped Model Parameters for the Lung

A common lumped approach to describe the lung is as a low pass RC-filter [9]. In medical terms the equivalent to capacitance in the lung is called compliance and the resistance is often refereed to as airway resistance. An example of a one adult category lung is

$$R_f = 5 \cdot 10^5 \left[\frac{Pa \cdot s}{m^3}\right] \quad C_f = 5 \cdot 10^{-7} \left[\frac{m^3}{Pa}\right]$$

which results in an equivalent time constant of

$$\tau = R_f C_f = 0.25s$$

This gives an indication of the time it takes to change the pressure of the lung, when a flow change is introduced to the lung. The lung compliance, which is depicted in Figure 13 is non-linear, depending on the pressure and volume present in the lung. From (5) one sees that the compliance is constant when the relationship between the volume change and pressure change is constant, i.e. where the line in Figure 13 is straight. From a medical point of view, the desired zone of ventilation is the linear compliance zone indicated in Figure 13.

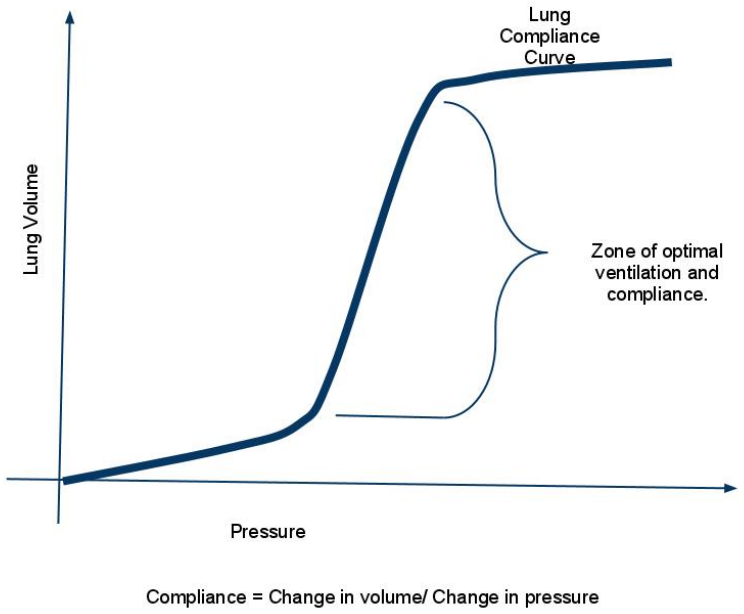

Figure 13: The compliance of the lung [29].

2.4.6 Modelling the Gas Chain

The electrical circuit in Figure 14 is a model that describes one way of modelling a part of the gas chain. This model is limited to the inspiration valve, one tube and a lung. The aim of this section is to describe why modal synthesis is needed for some aspects of gas chain model. Therefore this model is made as simple as possible, while still capturing the general behavior of this part of the gas chain.

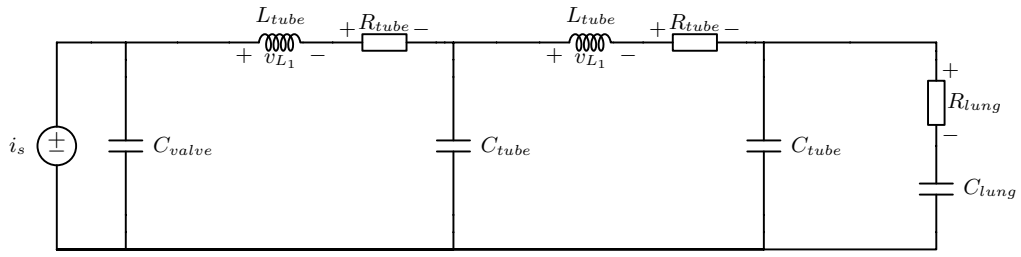

Figure 14: A basic model of a part of the gas chain.

Tube Section

The two tube sections depicted in Figure 14 represent the same system as in Figure 12. Each tube section is made up by one RLC-link, hence there are two tube sections in the model in Figure 14. The two tube sections are a linear combination of the outputs of two second order oscillators, each of which represents one mode of oscillation. According to Jon Price in Acoustic Waveguides [31], this can give a good representation of system behavior if each oscillator describe a section that is much shorter than the wavelength of the sound at the frequency of interest. In order to understand why each second order oscillator need to be shorter than the wavelength at that frequency, one need to revisit the theory of standing waves. This is done in Section 2.4.6 below.

Valve

Assuming that the valve inlet - in Figure 14 - can be modelled as a flow(current) source, this can not be directly in series with a tube section. The current through a inductor cannot change instantly whereas a current(flow) source can. Therefore a capacitor is set parallel to the current(flow) source. The value of the valve capacitance C_{valve} can be determined by the measurements described in Section 2.4.4. One could for example also add a resistor in series with this capacitance, which would correspond to the resistance of the valve chamber.

Standing Waves

Figure 15 show the two first tones of standing waves with a set flow at the left and a set pressure at the right. In analogy with the model in Figure 14 the set flow comes from the flow(current) source and the relatively set pressure comes from the low pass RC-filter of the lung. A linear model can only depict linear relationships between the state variables. The longest linearization possible, for a sine- or cosine function is 1/4 of its wavelength. Capturing the behavior for the 1/4 wavelength case will therefore require the flow and pressure at a minimum of two nodes. This means that the tube sections need to be able to describe two pressure states and two flow states. The tube sections in Figure 14 have two flow states and two pressure states and it would therefore be able to describe the 1/4 wavelength case. By adding a number of tube sections (second order oscillators) the model would get more pressure and flow states in the tubes. By adding the number of states the sinusoidal function could be more accurately depicted. The 3/4 wavelength case have four nodes, meaning that at least four pressure states and four flow states are needed to describe this oscillation. The model in Figure 14 only have three elements in which the flow is described. Hence one more tube section could be added in order to capture the 3/4 wavelength case. The wavelength λ for the gas in the 1/4

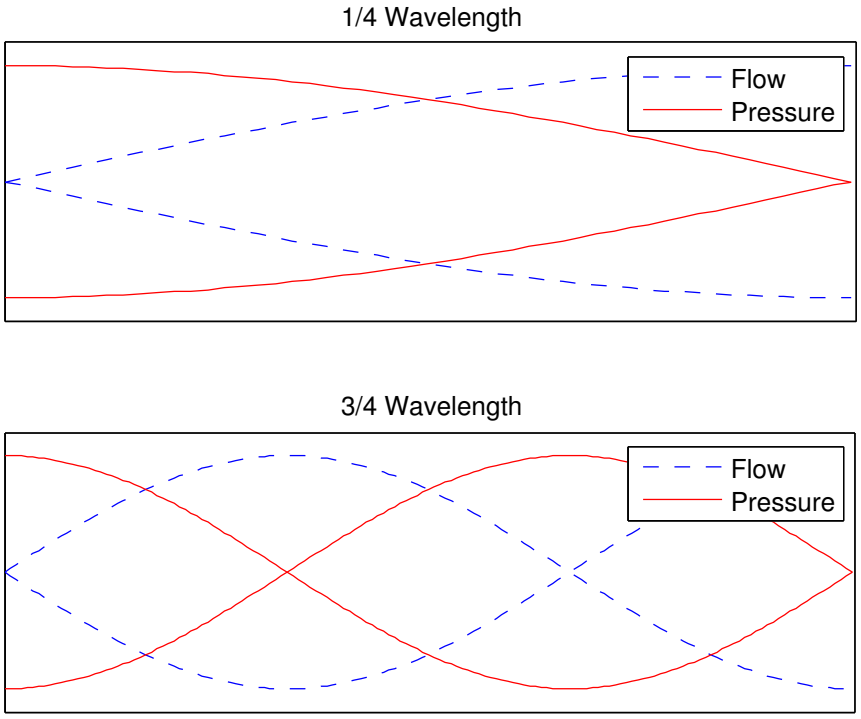

Figure 15: The standing waves with 1/4 and 3/4 of the wavelength. A flow source at the left and a set pressure at the right.

wavelength case is given by the length L of the tube as

$$\lambda = 4 \cdot L$$

The corresponding frequency f are given by γ and the speed that the medium travels

$$f = \frac{v_{sound}}{\lambda} = \frac{v_{sound}}{4L}$$

Assuming that the medium is air ($v_{sound} = 343$ m/s) and that the length of the tube is 1.5 m the corresponding standing wave frequency would be

$$f_{1/4} = 57\text{Hz} \quad f_{3/4} = 170\text{Hz}$$

2.4.7 Gas Chain Modelling Discussion

In accordance with the modelling theory in the previous section, a Simulink model of the gas chain was developed. This model was integrated with a Simulink model of the inspiration valve and corresponding VCM. By doing this the pressure at the valve chamber - given by the gas chain model - could

be fed back to the model of the valve. Also a model of an expiration tube as well as an basic model of the expiration valve were added. Assuming that the model is valid, it would be valuable when designing a controller for the valves. In the scope of this thesis there was not enough time to verify this model. Hence the explanation into the implemented model has been put in Appendix I. This study could serve as groundwork for any future research into this area.

2.5 Simulation

Simulation has been an important part in this project to get a better understanding of how things behave with different forms, shape, size and more. We were given some programs to use for different areas and problems. This part describes the basics about how the program works and how it solves the given problem.

2.5.1 Fluid Dynamics

To simulate fluid dynamics we chose to work in SolidWorks 2009 Flow Simulation which uses Computational fluid dynamics(CFD) that is a process to solve fluid problems [33]. Which use Navier-Strokes equations and Finite Volume Method to solve fluid dynamic problems. The basic step for simulation is:

- Define type of analysis - Type of material, fluids and physical features.
- Boundary conditions - Define inlet and outlet conditions velocity, pressure etc.
- Define goal of analysis - Pressure, velocity etc. at all points in the model.
- Mesh - Dived the model in to small pieces that are called cells.
- Analysis and result - Result can be show in many different forms 3D-profile, plots etc.

In Figure 16 a basic simulation model is shown where an inlet flow of 180 lpm and the environment pressure is defined as boundary conditions.

2.5.2 Finite Element Analysis

To simulate a Finite Element Analysis(FEA) problem we have used SolidWorks Simulation. The program uses two different solvers depending on problem (Direct Sparse or FFEPlus). Where Direct Sparse is mostly used for simpler program and FFEPlus for problems with more than 50 000 degrees of freedom [23].

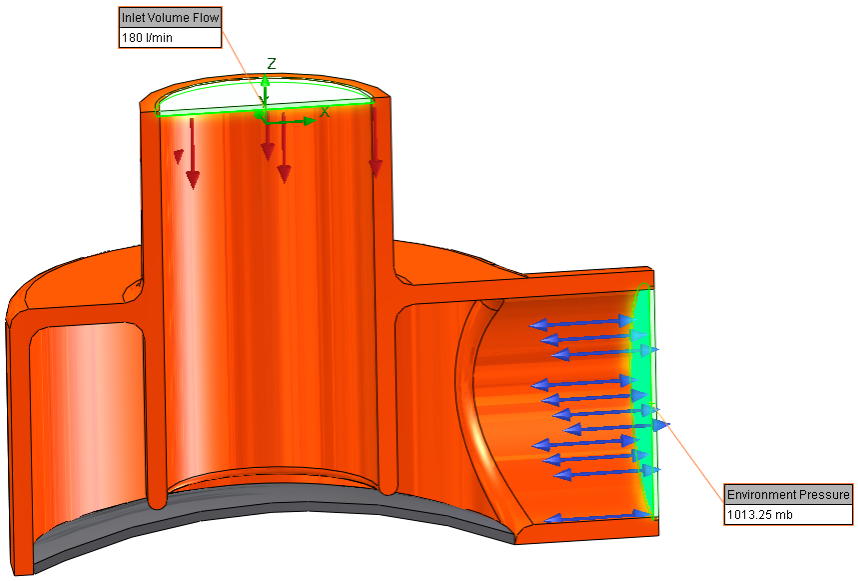

Figure 16: The basic model when performing simulations in SolidWorks.

2.5.3 Finite Element Method Magnetics

Finite Element Method Magnetics (FEMM) is an open source software that provides FEMM analyse of 2D magnetic problems or axis symmetric problem [28]. FEA is perform through these order of steps:

- Define geometry to simulate.
- Apply material to geometry.
- Create Boundary Conditions.
- Select problem characteristics.
- Generate Mesh and run FEA.
- Show result.

This program can be executed with MATLAB script for batch testing.

2.6 Tools

Short description of the tools we have used.

2.6.1 Matlab/Simulink

In this project we have used MATLAB 2011a developed by MathWorks. This is a program for numerical and technical calculations, which have better preference than traditional program languages for this type of calculation[24]. MATLAB have a built in graphical modelling and simulation environment called Simulink. This can be used to develop embedded system models. You build up your models from block libraries, where you can control and generate signals.

2.6.2 DSpace

DSpace is a real-time system that execute c code generated from MATLAB/Simulink. We have used a DSpace system with model name MicroAutoBox 1401/1501. This system allows several input and output types we have only used analogue ports.

2.6.3 Bode 100 Analyser

The Bode 100 from Omicron Lab is a device that can be used to determine the Bode response of a system. The device outputs a range of selected frequencies to the input of the system to be analyzed. In the case of the VCM, the Bode 100 outputs the input voltage to the VCM. At the same time one measured signal from the system is read.

3 Valve Seat Design

This section is aimed at describing the design process of the valve seats for both the inspiration and expiration valve. Most of the nomenclature used in this section are described in Figure 7a in Section 2.2.

In order to develop a valve that fulfils the requirements of the valve it was important to get some insight into how different designs of the valve affect the flow dynamics of the valve. Initially this meant revisiting general fluid dynamics and thermodynamics knowledge. But most of the insight was given from *SolidWorks*[27]. With an add-on *Flow Simuation* it's possible to simulate flow dynamic problems with Computational Fluid Dynamics(CFD).

All simulations were preformed with gas standard ATPD.

3.1 Inspiration Valve

The inspiration valve simulations used different pressures at the valve inlet and valve outlet as boundary conditions. Varying the valve gap then resulted in different flows. Given high pressure drops - up to 1000 mBar through the valve - there were difficulties simulating flows less than 40 lpm i.e. small valve gaps. There were no investigations made into why these simulations failed but it seemed as if the valve gaps used for those simulations could have been the cause of the simulations either crashing or resulting in unreasonable results. Those simulations required a valve gap less than 0.25 mm and it seemed as if the mesh - used to calculate the fluid behaviour - could not be made small enough to have a fine mesh over that gap. All inspirational valve flow simulations were therefore aimed at investigating the behaviour of big flows through the valve. The main design criteria of these simulations was to develop valves that would fulfil the flow versus pressure requirements that were posed on the inspiration valve.

It was also of importance to look at the forces that would be put on the valve. Creating a valve that requires less force might enable the valve actuator to be more cost and space effective as well as reducing its power consumption.

3.1.1 Valve Type Evaluation

As described the most promising valve types for the inspiration valve were membrane valves and globe valves. Therefore the valve design process started out with a basic design that could be made into a membrane valve or a globe valve. A cross section of this basic design in a membrane valve configuration is shown in Figure 17.

In Figure 17 the membrane is made up by the whole bottom surface of the valve chamber. This design is principally the most similar to the one Maquet

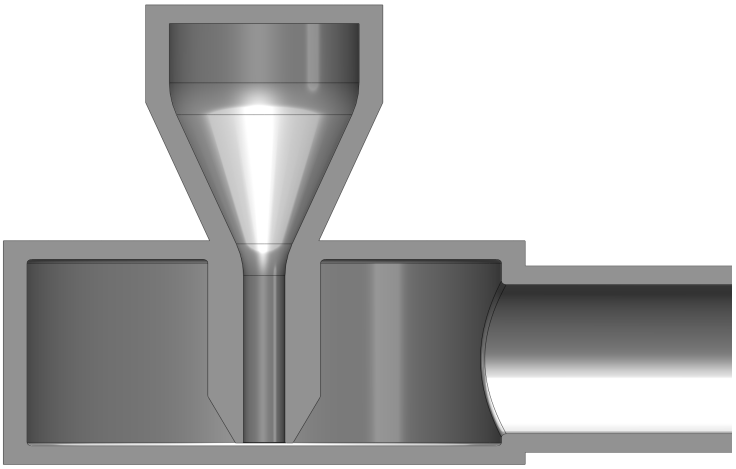

Figure 17: The basic design chosen to be used as a reference to be optimized upon.

use in their ventilators today. This design was compared to the three other designs shown in Figure 18 below. These designs are also described in detail below. The globe design was the only valve type to be tested that did not have a membrane.

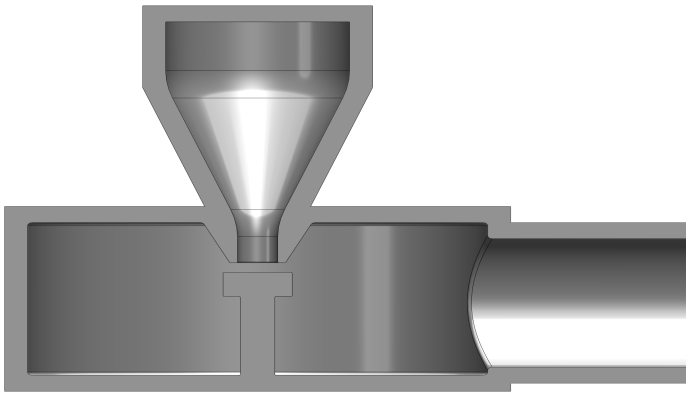

(a) Globe design. The actuator is exposed to the same pressure as the valve chamber.

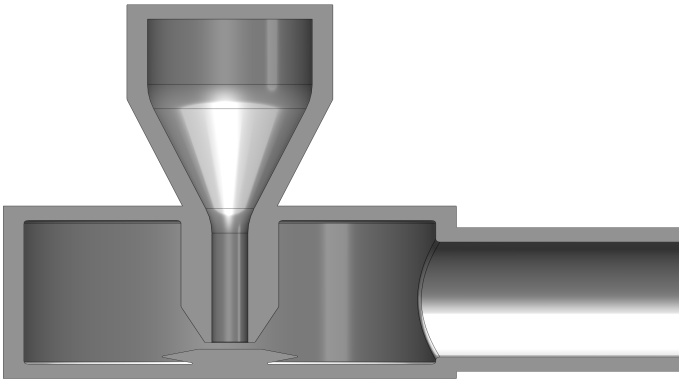

(b) Folded membrane design 1.

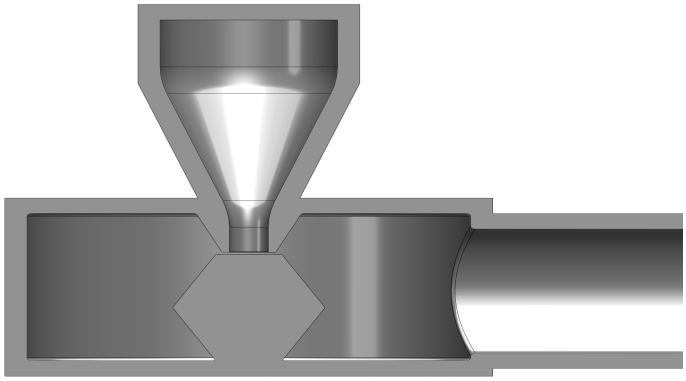

(c) Folded membrane design 2. Compared with design 1 this design enables a outlet positioned lower than the inlet.

Figure 18: Three different membrane designs to be compared with the Standard Membrane Design.

Simulation Conditions

The 4 designs were simulated with a pressure drop, from inlet to outlet, of 1000 mBar and the resulting flow was calculated for a valve with a inlet diameter of 3.5 mm. The results of the simulations are showed in Figure 19.

Each configuration was simulated at four different gaps, 0.3, 0.6, 0.9 and 1.2 mm. At each simulation the force acting on the membrane surface and the flows through the valves were logged.

As seen in Figure 19a the flow through the valves are quite similar at the same gaps. Therefore the flow resistance of the valves can be said to be roughly the same for all valve configurations. Also noted from the simulations are that all valves fulfil a requirement of at least 180 lpm at a pressure drop of 1000 mBar. This is done at a valve gap of just over 0.9 mm.

Standard Membrane Design

The membrane used in the standard membrane design, seen in Figure 17, would in reality be made up by a flat membrane fabric. This membrane is straight forward to design and manufacture. The downside is that it's large surface area result in larger forces placed on the actuator. This can be seen in Figure 19b where the standard membrane design require much higher forces compared with other designs. For example, at an inlet gap of 1.2 mm, the standard membrane design requires more than two times the force needed by the other membrane designs.

Globe design

The valve design in Figure 18a is a globe valve with actuator being exposed to the same pressure as is present in the valve chamber. Hence there will not be a membrane that separates the air from the inlet and the air in and around the actuator. This design also has a small surface area compared with the standard membrane design and as seen in Figure 19 both the forces and flows are comparable with the folded membrane designs.

Folded Membrane Designs

The folded membrane design, seen in Figure 18b and Figure 18c is something in between the standard membrane design and globe design. Similarly to the standard membrane design the folded membrane design offers separation between the fluid and the actuator but at the same time it requires about as much forces as a globe design, which seen in Figure 19.

The membrane surfaces for the folded membrane design are defined in Figure 20. By simulating the forces on all membrane surfaces one could determine that the sum of the forces acting on the angled - or folded - parts of the

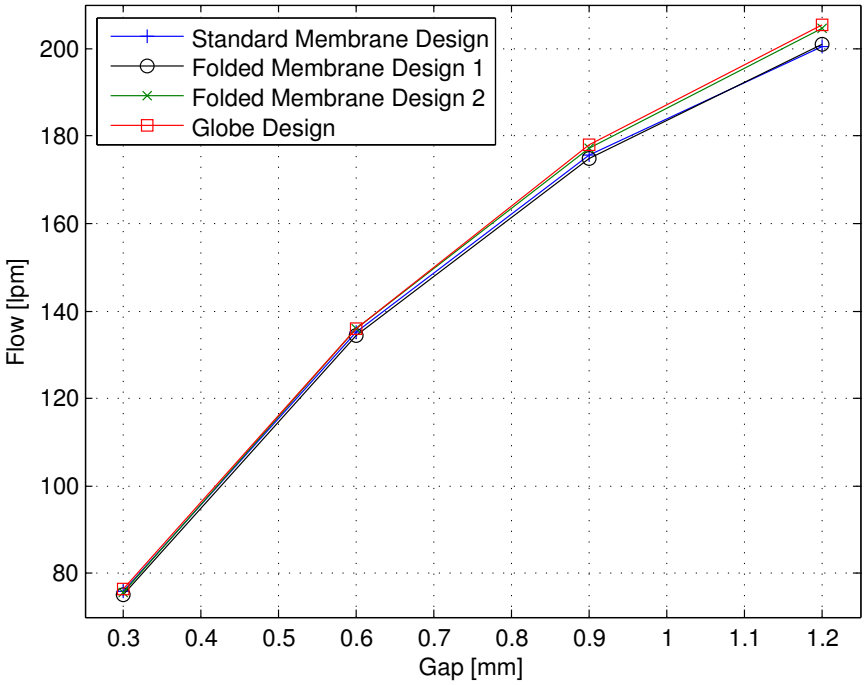

(a) The flows through the valves at a pressure drop of 1000 mBar.

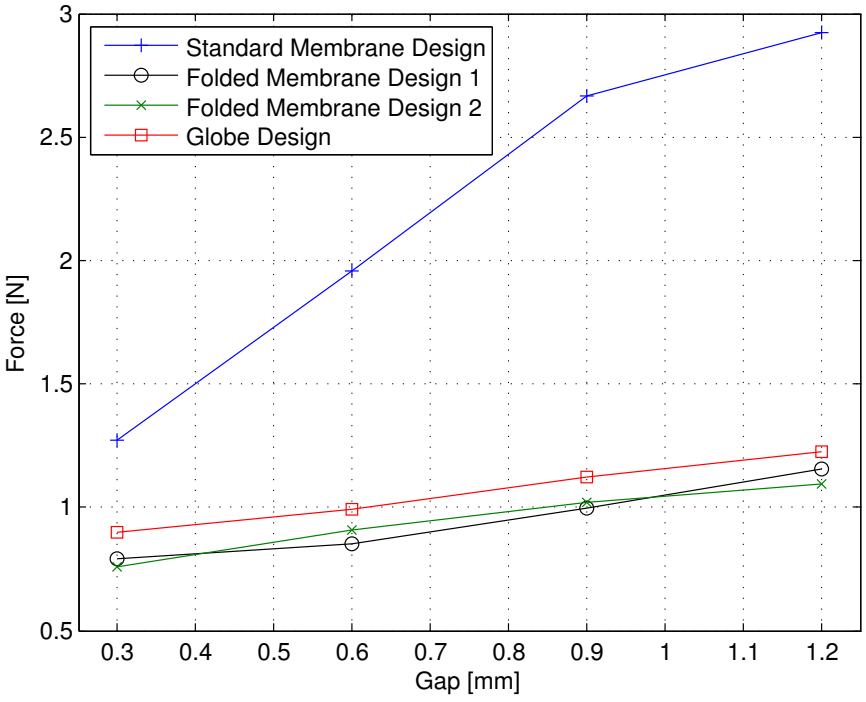

(b) The forces put on the valves at a pressure drop of 1000 mBar

Figure 19: A comparison of the flow through and force on the different valve seats.

membrane were close to zero. The only major force acting on the membrane is therefore much smaller in comparison to the standard membrane design, explaining the results in Figure 19.

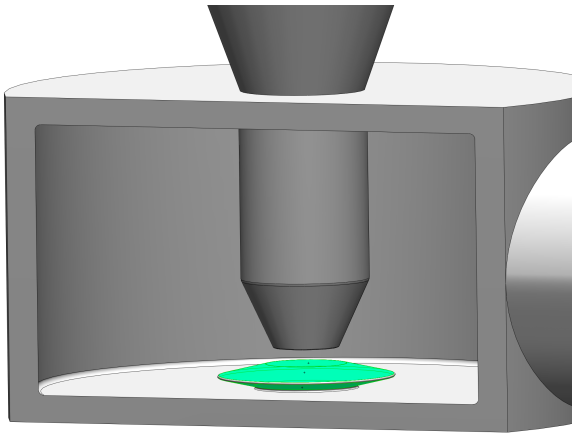

Figure 20: Angled membrane design 1. The highlighted surfaces illustrate the folded membrane.

The main difference between the folded membrane design 1 and 2 is that design 2 allows for an outlet to be positioned differently. This did result in an decreased resistance for design 2 compared to design 1, as seen in Figure 19 but the differences are still very small. A drawback with these Folded membrane designs is that they would require a custom membrane to be developed.

Valve Type Conclusions

Combining the fact that the globe design performed similarly to the folded membrane designs and that the globe design is simpler to implement it was deemed the best design. Since it was possible to implement the standard membrane design and the globe valve with the same valve seat, just by adding a membrane, a decision was made to try to optimize some of the basic dimensions on the valve seat for both of these designs.

3.1.2 Chamber Height Evaluation

Different valve chamber heights were simulated in order to get an idea of the effect this has on the resistance of the valve and the forces put on the membrane. Two examples of configurations can be seen in Figure 21.

Simulation Conditions

The simulations were conducted with a pressure drop of 1000 mBar over the valve, the inlet diameter was set to 3.5 mm and the gaps tested were 0.3 and

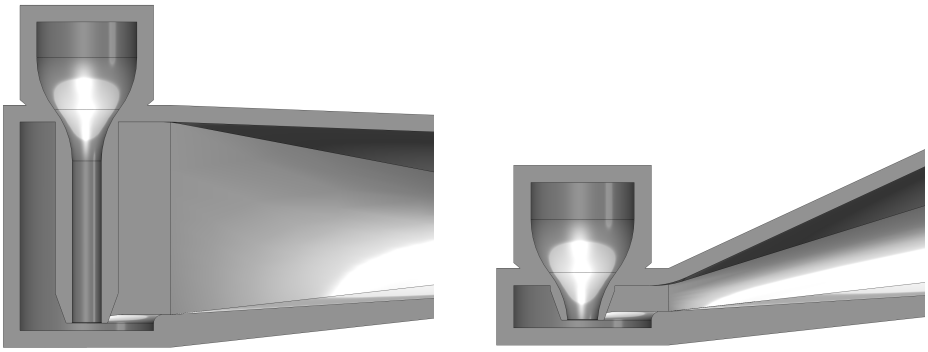

(a) A valve chamber height of 24 mm. (b) A valve chamber height of 4 mm.

Figure 21: The tallest and shortest valve chamber configurations.

0.9 mm. The simulation results are shown in Figure 22.

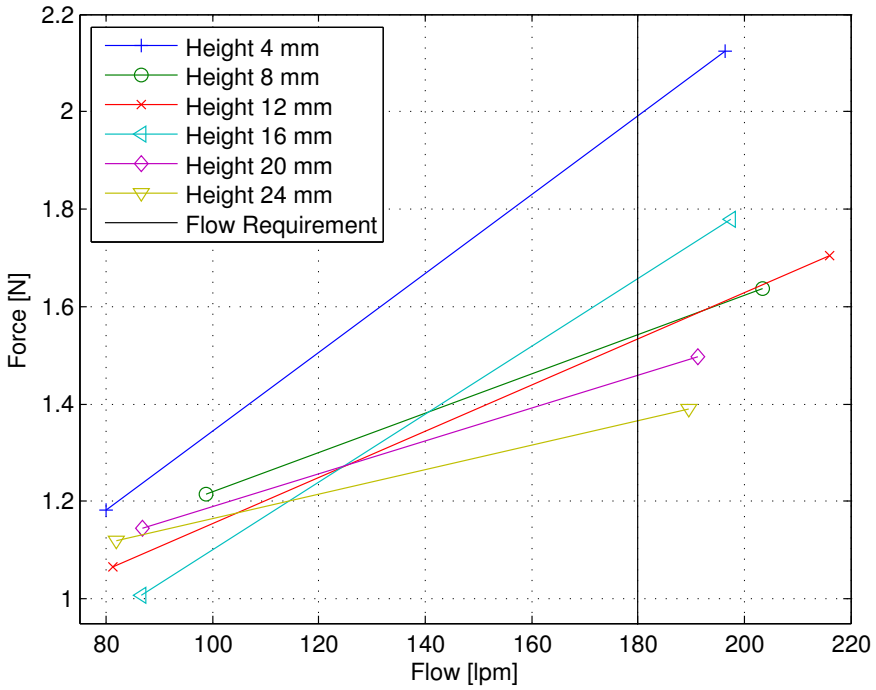

Figure 22: Graphs corresponding to different valve chamber heights.

Chamber Height Conclusions

According to the simulations, the shortest chamber height results in the highest forces at both gaps. The tallest chamber height results in relatively low

forces for the small gap and the lowest forces at the big gap. At the same time the results in between are quite erratic with the configuration Height 16 requiring more force than Height 8 and Height 12. The flows are also greater for Height 8 and 12. Higher flows are assumed to increase the forces put on the actuator but this is not the case here.

One explanation for the results might be that the chamber height is turn affects two other valve parameters. The first affected parameter is the length of the inlet, as seen in Figure 21 the length of the inlet is increased with a taller chamber height. A longer inlet causes an increase in the valve resistance. The second parameter is the size of the valve outlet which can be made larger for configurations with taller chamber height. This should in theory, give a reduction of the valve resistance by some magnitude.

Of course it is also important to question the validity of the simulations at all times and the best way to determine this would be to build valves with different chamber heights. Important is also to note that the requirement of 180 lpm at 1000 mBar pressure drop, is satisfied for all height configurations. This can be seen by the line indicating 180 lpm in Figure 22.

These simulations were deemed not reliable enough to solely base any design decision on. Instead the height to be used was also based from the dimension of the outlet diameter. The prototype outlet was to be connected to a 22 mm tube and therefore similar dimensions were deemed suitable for the outlet diameter and the valve height. The chamber height finally chosen was 20 mm.

3.1.3 Inlet Diameter Evaluation

The valve inlet is one of the narrowest channels in the valve, hence the inlet diameter has a big impact on the resistance of the valve.

Simulation Conditions

The valve inlet diameter simulations were made with a pressure drop of 500 mBar over the valve and the flow requirement corresponding to this pressure drop is 120 lpm. Results are described in Figure 23a, showing gap-flow relation and Figure 23b showing the gap-force graph.

Inlet Diameter Conclusions

As seen in Figure 23a configurations with inlet diameters 2.5 mm and 3.0 mm did not fulfil requirements. They were therefore rejected. Of the configurations left to consider, the configuration with inlet diameter 3.5 mm required the least amount of force as seen in Figure 23b. 3.5 mm was therefore considered the best suited dimension for the inlet diameter of the developed prototype.

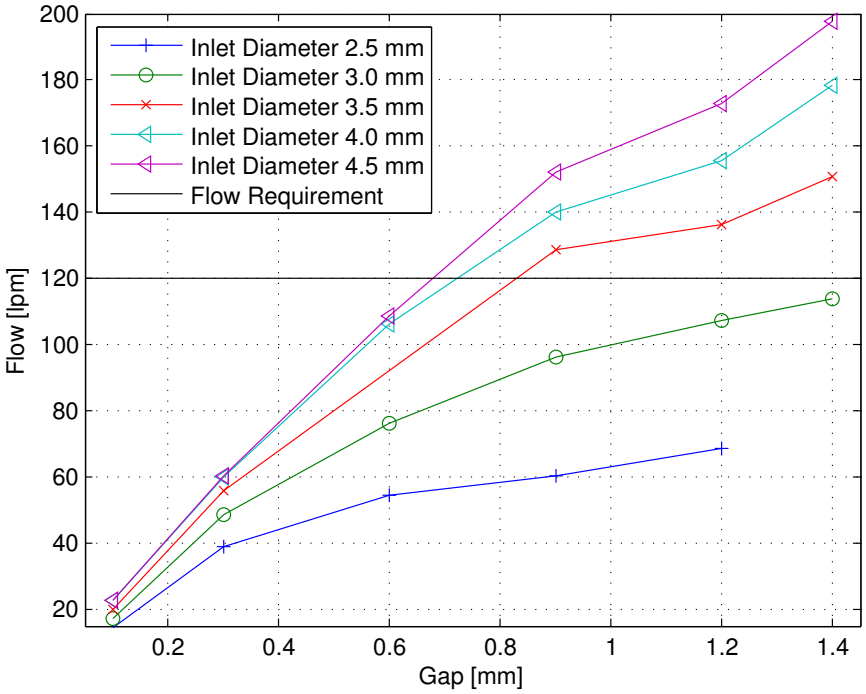

(a) Graph describing the gap-flow behaviour.

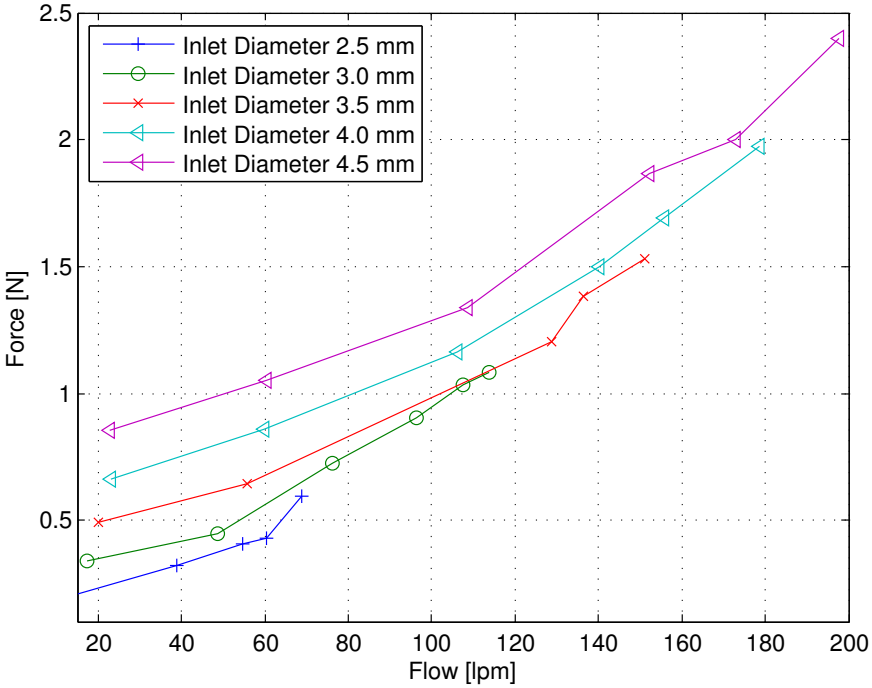

(b) Graph describing the flow-force behaviour.

Figure 23: Graps comaparing different inlet diameters.

3.1.4 Chamber Diameter Evaluation

The diameter of the valve chamber determines the membrane surface area for the Standard membrane design. Therefore it has a big impact on the force that the membrane puts on the actuator. Simulations investigating the effect of alternating valve chamber diameters were therefore mainly preformed with the Standard membrane design in mind. Still, these simulations were also made in order to see how the general valve resistance would be affected by the valve chamber diameter.

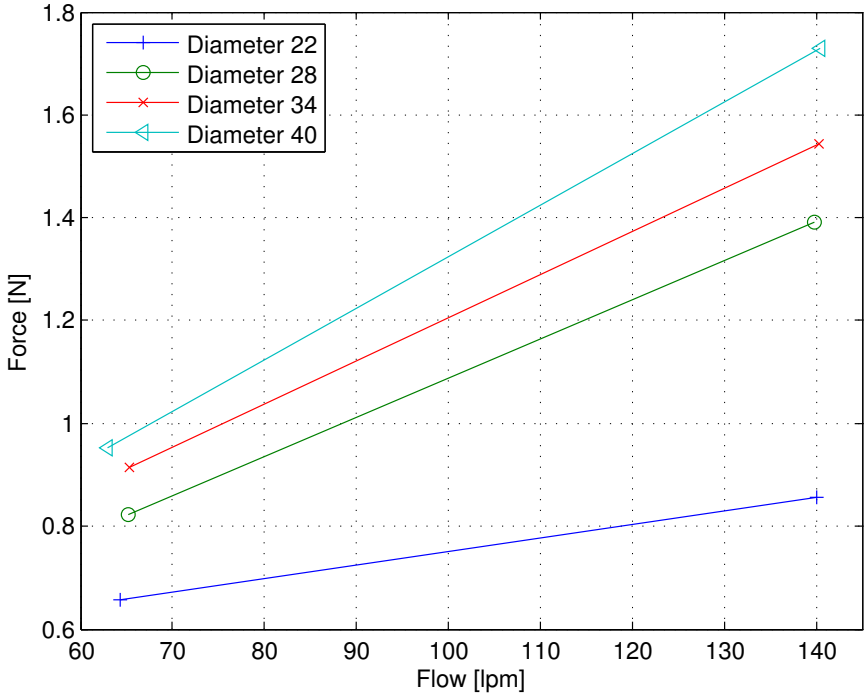

Figure 24: Graph showing the flow to force relation for different valve chamber diameters.

Simulation Conditions

The simulations that were made with a variable valve chamber diameter were set to have a pressure drop of 1000 mBar across the valve. Each different valve chamber diameter was simulated at two different gaps 0.3 and 0.9 mm. The results of simulations are shown in Figure 24. These simulations were made with an inlet diameter of 3.0 mm, hence increasing the general resistance of the valve compared to a 3.5 mm inlet. This had less importance since the aim of these simulations been to get insight into how a changed chamber diameter impacts the flow through and forces on the valve.

Chamber Diameter Conclusions

As for the resistance among the valve configurations in Figure 24 there are no major differences since a gap of 0.3 mm result in roughly 65 lpm for all configurations. More important is that - as believed - the forces on the actuator can be decreased greatly by decreasing the valve chamber diameter.

Considering the dimensions chosen for the prototype the decision was made to try two different chamber diameters. One configuration would be based on the force benefits of a smaller diameter valve chamber. The downside with this is the fact that the membrane surface has a smaller area on which to stretch freely. Therefore one valve prototype would be made with as small chamber diameter as possible, limited only by the dimensions of the valve inlet. The other configuration would be a somewhat safer choice based on the valve proportions of Maquets existing inspiration valves. That means that the chamber diameter has roughly the same dimension as the valve height. The final dimension chosen were 11 mm and 16 mm chamber diameter.

3.1.5 Prototype Designs

This section gives a descriptions into the prototypes that were developed. The measurements made on these prototypes were compared with its corresponding simulations.

Given the reasoning in the previous section there were 4 valve configuration prototypes to be built and tested

- Wide w. Membrane - Membrane Valve with wide chamber diameter
- Narrow w. Membrane - Membrane Valve with narrow chamber diameter
- Wide w.o Membrane - Globe Valve with wide chamber diameter
- Narrow w.o Membrane - Globe Valve with narrow chamber diameter

One of the membrane valve configurations Wide w. Membrane, is seen mounted to a VCM in Figure 25. This configuration can be changed to the other version of the membrane valve - Narrow w. Membrane - by replacing the parts named Chamber Outlet and the Membrane attachment plate - with a smaller diameter version.

By removing the membrane and replacing the actuator plug, the membrane valves become globe valves, refereed to as Wide/Narrow w.o Membrane. The actuator plug is also replaced since the configurations without membrane has got a membrane canvas glued to its top side. In this way the sealing of the valve is still done with a membrane surface.

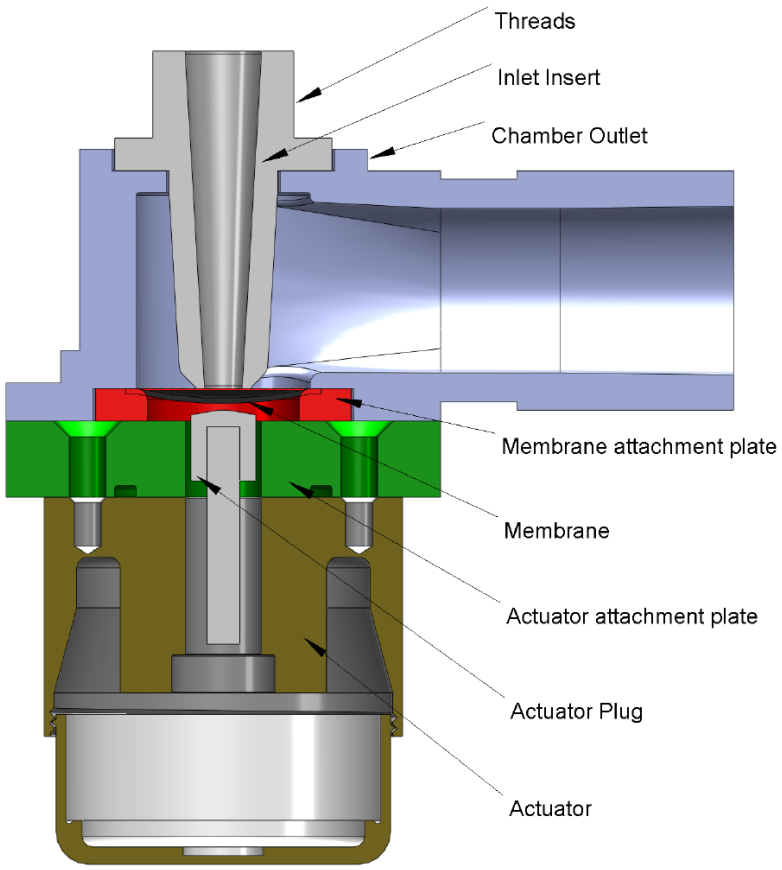

Figure 25: The configuration Wide w. Membrane with a valve chamber diameter of 16 mm is shown named valve components.

3.1.6 Prototype Manufacturing

With the exception of the actuator, all parts in Figure 25 were made in the Maquet workshop.

Ideally the Inlet Insert and Chamber Outlet would have been made in one piece with the use of a 3D-printer. This was not possible since the Inlet Inserts section needs smoother surfaces than the 3D-printer at Maquet can produce. Hence the Inlet Insert was made of brass and were produced in a lathe whereas the Chamber Outlet could be made using the 3D-printer. These parts were then joined by epoxy adhesive.

The Inlet insert is threaded, this in order for it to fastened to the tank as seen in Figure 26.

The membrane used is the same textured material that Maquet is using in their current inspiration valves. The materials used for the Membrane attachment

plates, the Actuator attachment plates and the Actuator plug was not critical in respect of their functionality. The Membrane attachment plates and the Actuator attachment plates were made of steel whereas the Actuator plug was made of brass.

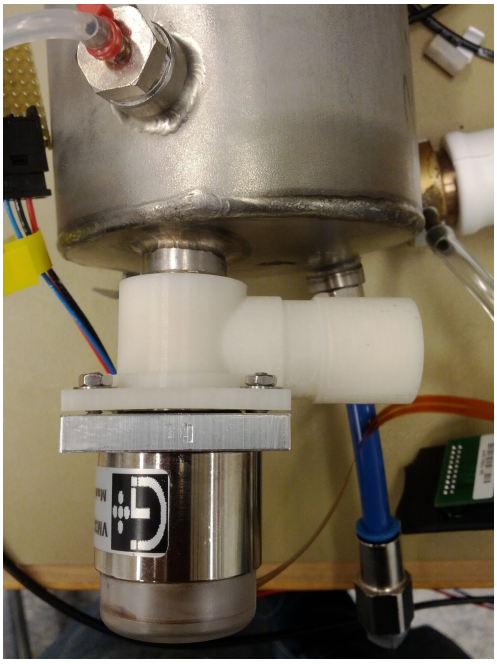

Figure 26: The valve prototype connected to the tank and actuator.

3.1.7 Simulation Verification

In order to compare measured and simulated valves, two tests were preformed. In the first test the inlet pressure was swept from 100 mBar to 1000mBar with the gap being constant. In the second test the gaps were swept whereas the inlet pressure was constant. For both tests the valve flow and the force needed to keep the valve in place were logged.

In Figure 27 the two solid lines show the simulated valve configurations whereas the dashed line show the measured test results from one valve configuration. For the simulated valves, the configurations Simulated Wide w. Membrane and Simulated Narrow w. Membrane were the configurations with the highest and lowest flow resistance. The measured results for all valve configurations had very similar flow results, hence all result are lumped into Measured Valves in Figure 27.

As seen the simulated valves generally have less resistance than the real valves. Also while there are some noticeable differences between the resistances of the

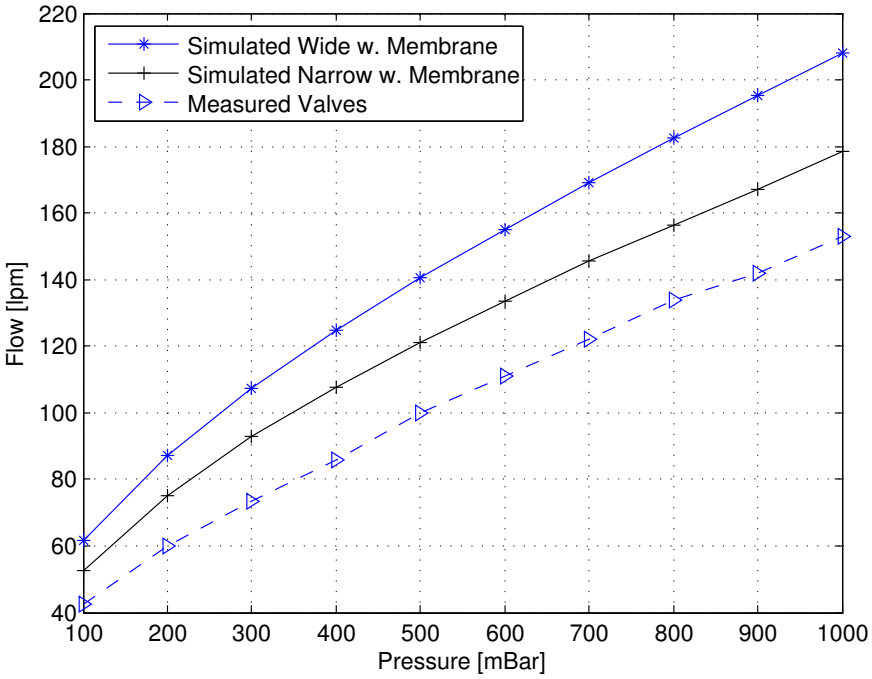

Figure 27: The resulting flow for 10 different inlet pressures at a gap of 0.9 mm.

simulated valves there are relatively small differences between all the measured valves.

For the same test setup as in Figure 27, the forces needed to keep the valve in place were simulated and measured. In these test the simulated forces resembled the measured results more closely. The difference between simulated and measured results for one configuration are shown in Figure 28. Although forces differ between configurations, the general differences between simulated and measured forces are roughly the same for all valve configurations.

A common estimate for the forces on the valve is the product of the inlet pressure and the inlet area, i.e. the estimated effective area on with the inlet pressure is acting is much less than the entire membrane area. At a inlet pressure of 1000 mBar the estimate is

$$F = p_{inlet} \cdot A_{inlet} = 0.96\,\mathrm{N} \tag{9}$$

This estimate is just 0.2 N less than the the measured results at 1000 mBar in Figure 28. Although this proved to be a decent estimate it is about 20 % off. From simulation results one could see that the acting area of the pressure

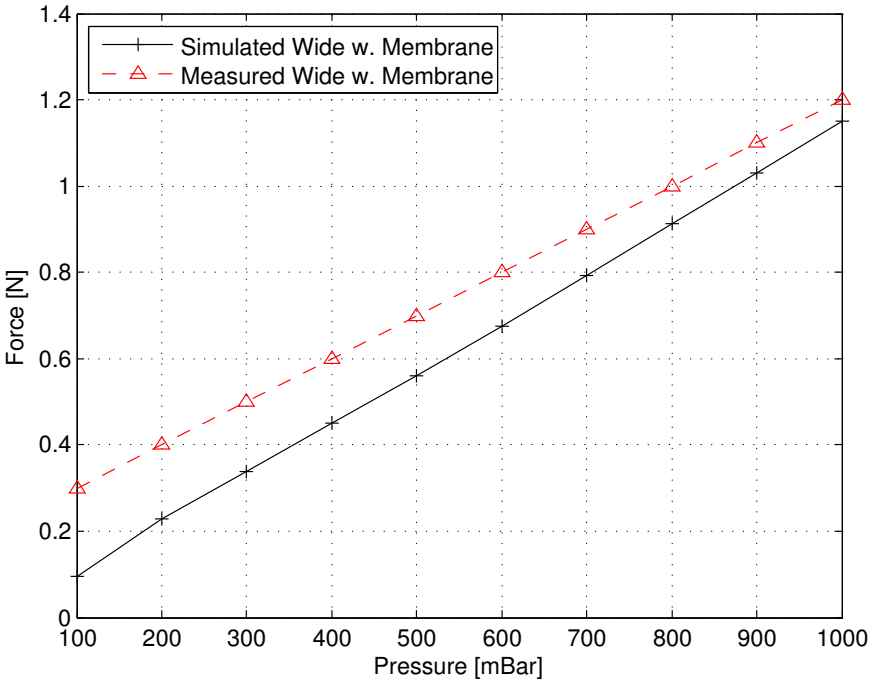

Figure 28: The resulting force on the actuator for 10 different inlet pressures at a gap of 0.9 mm.

was quite the same as A_{inlet}. The estimate error is therefore believed to stem from the fact that the pressure acting on the membrane is higher than p_{inlet}. This in turn is believed to be caused by the kinetic energy of the flowing gas. The membrane is changing the direction of flowing gas. This results in the membrane and actuator having to produce a force that counteracts the force created by the flowing gas.

For the second comparison test, the inlet pressure was held at 1000 mBar and the gap was swept from 0 to 1.8 mm. The flow characteristics is seen in Figure 29. Since the measured flows are lower than the simulated flows in Figure 29, the flow resistance is generally higher for the measured valves compared to the simulated valves. Also the difference in flow resistance between simulated configurations, were much higher than the actual measured difference between different configurations. The Most important thing to be seen in Figure 29 is that all the measured valves fulfil the flow requirement of 180 lpm at a pressure drop of 1000 mBar.

Figure 30 shows the gap force relation in this test. The measured globe valve configurations had similar gap to force relation and were therefore lumped together. Again the measured force is higher than the simulated force. Due to difficulties with simulating high pressure drops for small valve gaps the

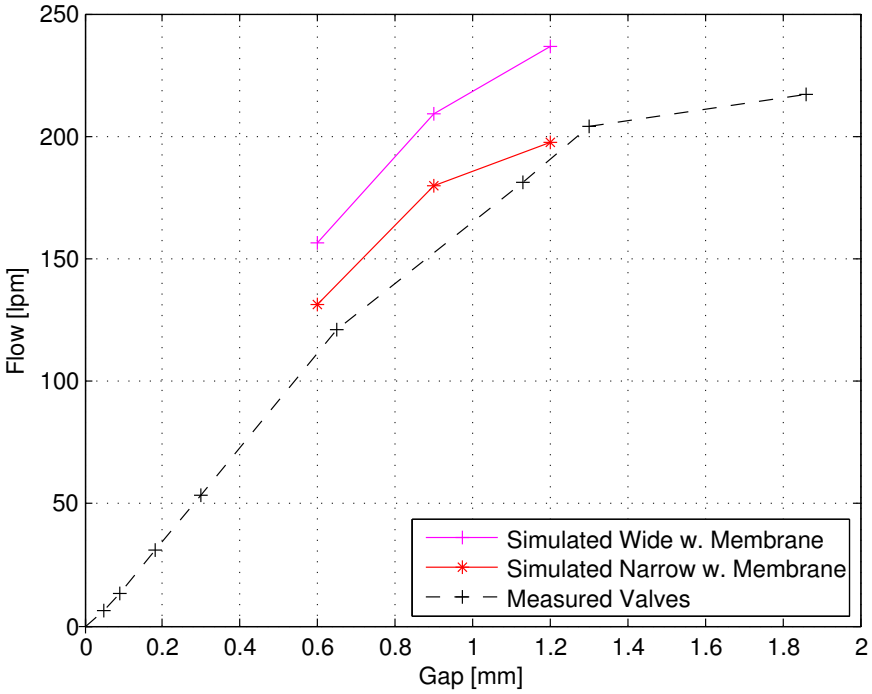

Figure 29: The gap-flow relationship for two measured and simulated configurations.

smallest simulated gap was 0.6 mm. It can be noted that the estimation of 0.96 N, for all valve gaps is a acceptable estimate.

One can also note the behaviour of the measured configurations at gaps $>$ 0.1 mm and gaps $<$ 1.2 mm. At gaps around 0.1 mm the membrane surface comes in contact with the inlet and the valve flow is around 10-15 lpm for all configurations. In order to reduce the flow to zero the force on the valves has to be increased by around 100 %. As seen the forces needed to close the valves completely are the same for all configurations. This makes sense since the same type of membrane material is used for all prototype configurations. In order to get a tight seal these membranes need to be compressed by the same amount of force in order to get a tight seal.

The difference in behaviour at gaps larger than 1.2 mm depends on the membrane. At gaps $>$ 1.2 mm the membrane runs out of slack, therefore it starts to stretch and absorbs more and more force. In contrast, the configuration without membrane continues to require more force as the gap increases.

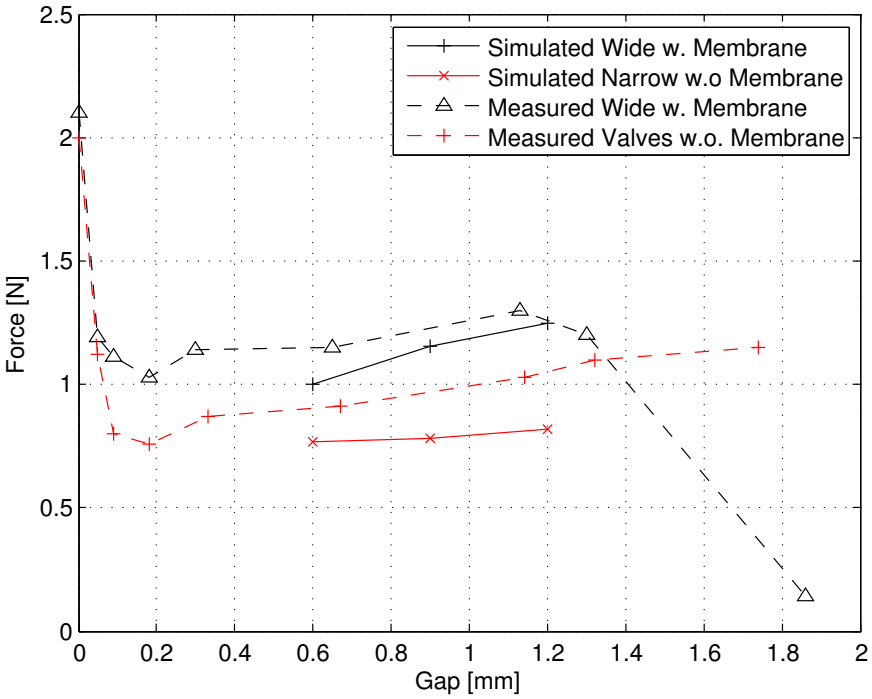

Figure 30: The gap-force relationship for two measured and simulated configurations.

Simulation Discussion

Regarding the simulated flow results it is obvious that it results in too low flow resistance, still it captures the general behaviour of the real valves. All measured configurations show very similar flow resistance whereas the simulated configurations showed more diverse results. This would indicate that the real flow resistance is dominated by one factor that is the same for all valve configurations. As indicated in Section 3.1.3 the valve inlet diameter has the greatest impacts on the flow resistance and it is likely that this is an even more dominating factor for the real configurations.

However, this does not explain the big difference in flow resistance between all simulated and measured configurations. One possible factor for this might be the material roughness selected for the simulations. This parameter was set to the equivalent of relatively fine plastic. For the prototypes the valve chamber and outlet is made of rough 3D-printed plastic and the membrane has a quite rough rubber surface. Therefore one might assume that this parameter should have been increased.

The simulated forces are closer to reality than the flow resistance. Compared to the estimate in (9) the simulations are not that much better. Still simulated

force estimates is good at indicating if an alternate design would increase or decrease the forces needed by an actuator.

3.1.8 Adding Pre Tension to the Valve

One valve requirement addresses the fault condition of having a loss of power to the valve. Specifically the valve is not supposed to leak more than 0.5 lpm for an inlet pressure of 500 mBar. One way of solving this problem is to add a pre tensioned spring to the valve.

Given a pre tensioned spring, the forces needed by a valve actuator is dependant on the amount of pre tension and the size of the spring force constant. Increasing the spring forces will result in the forces needed by an actuator being dominated by the spring. Figure 31 shows how the force curve changes by adding a spring to the globe valve configurations. As described earlier there was no difference in the force characteristics between the two globe valve configurations. It should be noted that the values of the forces shown in Figure 31 are absolute. Given that "Force needed: valve w.o. spring" is defined in the positive direction, the "Spring force" is also positive whereas "Force needed: valve w. spring" is negative. The valve with a spring has to work against the spring it in order to open the valve gap.

Looking at Figure 31 one get an idea of how the inspiration valve is to be controlled by achieving a force balance. Applying a certain amount of actuator force, the valve will eventually result in the actuator positioned at a certain gap. The size of the gap and the inlet pressure will then determine the flow let through the valve.

At an inlet pressure of 500 mBar all valve configurations needs around 1 N to have a leakage of around 0.5 lpm, hence fulfilling the leakage requirement. The spring used in Figure 31 and for all prototype configurations, have a pre tension of 1.9 N and a spring constant of 2 N/mm. The benefit by having a larger than needed spring force is that the spring force will be the dominating factor whereas the non-linear "Force needed: valve w.o. spring" will have less impact on the resulting force balance. This is even more prominent for the membrane valve configurations described in the next section (3.1.9). With that said, the choice of spring could be further optimized if it would turn out that the forces needed in Figure 31 are to big for a particular choice of VCM.

3.1.9 Screening Valve Prototypes

Originally the one of the membrane configurations - Narrow w. Membrane - did not meet the flow requirement of 180 lpm for a inlet pressure of 1000 mBar. In order to fulfil the requirement, the membrane attachment plate were replaced with the one used for the wide valve chamber configurations (seen in Figure 25). This membrane attachment plate has a wider inner diameter

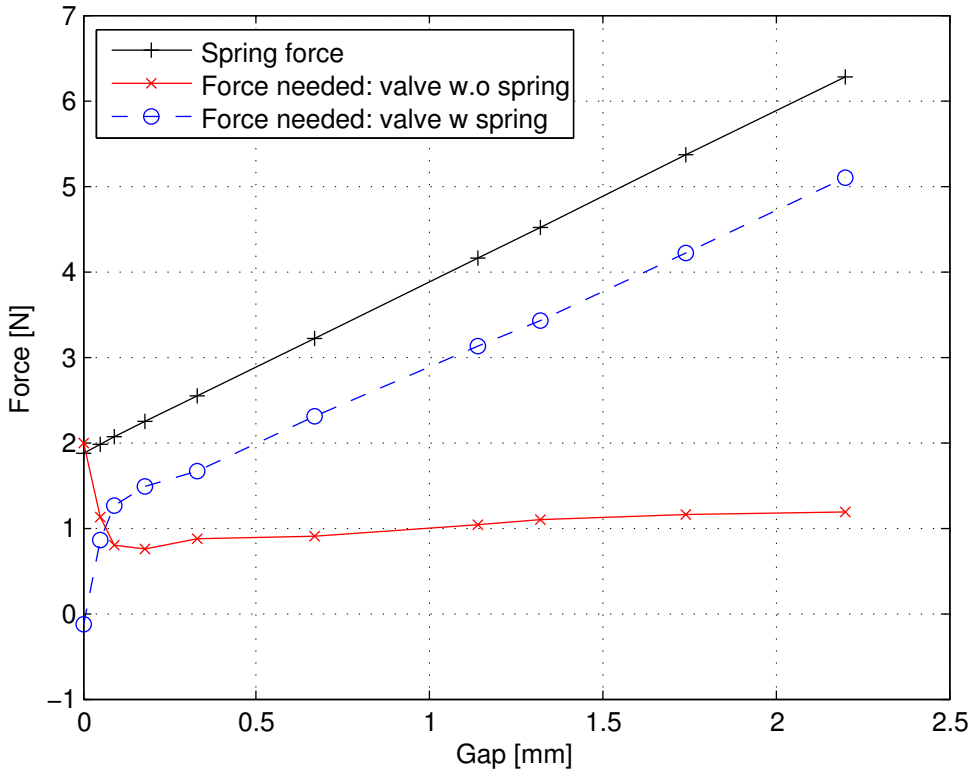

Figure 31: The forces required by an actuator when a spring is added to the valve configurations without membranes.

meaning that the membrane surface area increased. This in turn eliminated one of the original purposes of having a narrow valve chamber. Also, this new attachment plate gave Narrow w. Membrane the undesirable force balance curve seen in Figure 32a above. The force balance curve for Narrow w. Membrane is undesirable since the applied force could result in different gaps. It is possible to remove this effect by increasing the spring constant but this would lead to unnecessarily high forces needed by the actuator. Wide w. Membrane in Figure 32b on the other hand, has a desirable force balance curve. This is most easily recognized by the fact that no force that can result in more than one gap.

The two globe valves had similar and desirable static flow and force performance. It was believed that these valves would have similar dynamic flow behaviour. Therefore dynamic test were only done on the Wide w.o membrane, i.e the globe valve with a wide valve seat.

The force curves of the membrane valve were different compared to the globe valves. Wide w. Membrane had desirable static behaviour whereas Narrow w.

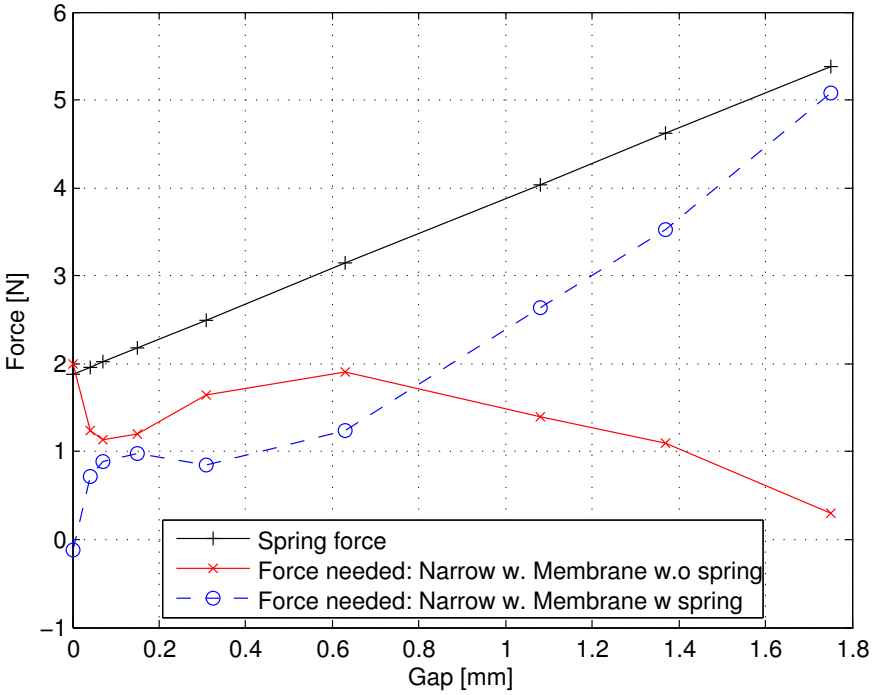

(a) The gap to force relation for Narrow w. Membrane.

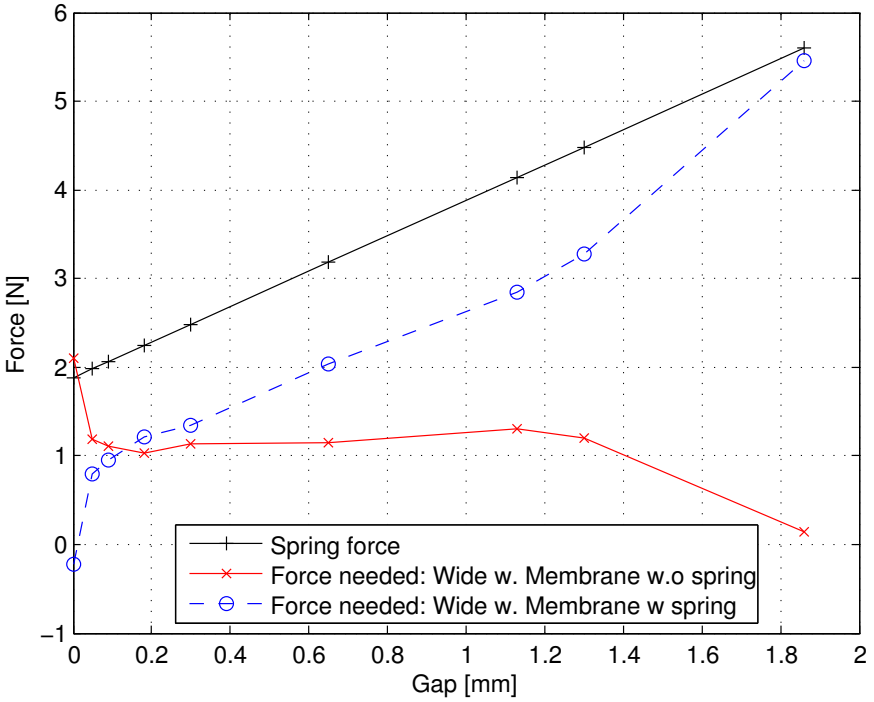

(b) The gap to force relation for Wide w. Membrane.

Figure 32: The force consequences of adding a spring to the membrane valves

membrane had not. Wide w. Membrane - the membrane valve with a wide valve seat - was chosen to make dynamic testing on.

3.2 Expiration Valve

The aim of a new expiration cassette is to have the same performance as the Servo-i expiration cassette. In Figure 33 the current expiration cassette is shown. The overall goal is to make a smaller cassette.

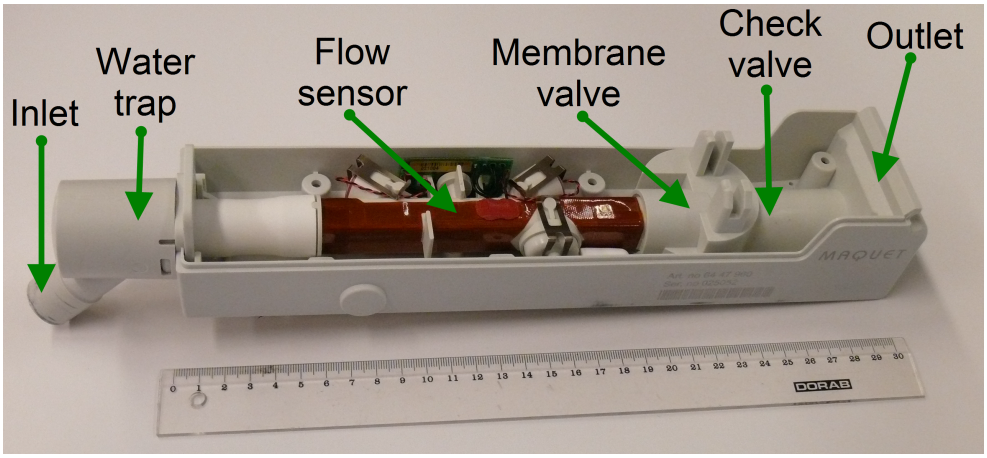

Figure 33: Servo-i expiration cassette.

3.2.1 Current Solution

The current expiration cassette assembly consists of four different parts: water trap, flow sensor, membrane valve and check valve. Arrangement of the parts can be seen in Figure 33.

Each part contributes to the maximum allowed pressure drop for the expiration cassette. Drawbacks with current solution are number of parts that contribute to the total ΔP and a big membrane valve seat which require an actuator with high force.

The demands on maximum allowed ΔP is different depending on if the ventilator is active or passive. Active means that the ventilator is running and passive means that the ventilator have lost power and have no possibility to control the actuator. Demands are lower with a passive ventilator which is something that Maquet don't take advantage of in their current expiration cassette. This gives the consequence that the pressure drop is the same in both active and passive mode. Here there is an opportunity to reduce the pressure drop by help moving the membrane in active mode. This is possible because of the force that is required to move the membrane give a large pressure drop compared to pressure drop arise by the area change in the valve. This will make it possible to have smaller area without get high pressure drop.

Size of the expiration cassette is big and the external measurements are 300x60x60 mm. This part also holds electronics which makes it expensive to manufacture.

Improvements of Current Solution

Given a new proposal of the expiration cassette assembly where you move the flow sensor after the membrane valve, there may be a possibility to remove or combine parts which allow a higher ΔP of each part. The new proposal can be seen in Figure 34 where the arrows represent the flow direction. This gives the possibility to have a smaller valve seat resulting in lower force demands on the actuator. There is proposed to use the flow sensor from Flow-i that have less ΔP than current used flow sensor. Or have a new transducer based flow sensor. Combining parts will result in a smaller expiration cassette and by removing the transducers this will give the opportunity to have a disposable cassette.

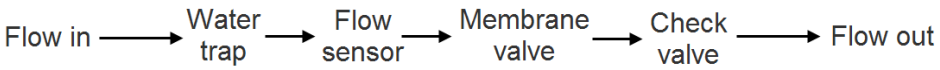

Figure 34: New proposal for expiration cassette assembly.

Measurements performed on the existing expiration cassette show that the pressure drop is between 0.9 and 11 hPa with a flow from 30 to 180 lpm see Figure 35 with result (see Appendix A for test set up). To get an understanding of how much each part in the cassette assembly contribute to total ΔP. Measurements from an existing test [21] were used to get an approximately division between the parts, result from this approximation are found in Table 2.

Table 2: Division of pressure drops between parts in Servo-i expiration cassette at 60 lpm.

	Water trap	Flow sensor	Membrane valve	Check valve	Total
Pressure drop	0.76	0.36	0.43	0.58	2.13
hPa	36%	17%	20%	27%	100%

Result shows that the water trap and the check valve stands for more than 60% of the total pressure drop. This makes it interesting to investigate the potential in combining different parts of the cassette to give the opportunity to have a smaller valve seat and be enable to use a smaller and lower cost actuator.

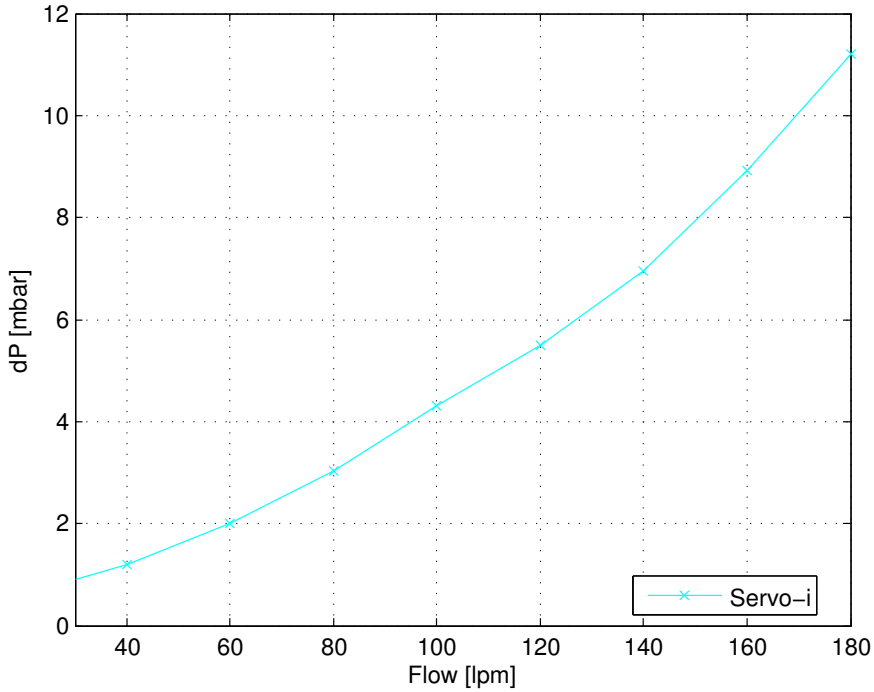

Figure 35: Servo-i expiration cassette assembly.

3.2.2 Valve Inlet Diameter Analyze

The overall goal is to reduce the force that is required by the actuator. Force is depending on the valve seat diameter but with a too small diameter the pressure drop gets too large.

Investigation were performed with two different models.

The first model is found in Figure 36 with an inlet diameter that can vary between 11 and 18 mm. The outlet is the area on the external cylinder. The model is called *Variable outlet* since that external diameter will very with two times the inlet diameter. The bottom plate represent the membrane, that is placed a quarter of the inlet diameter from the valve seat which is the edge of the inlet cylinder.

The second model has a fixed outlet diameter to fit the required flow sensor. The outlet is located on the left side on the model seen in Figure 37. The rest of the design is identical to the first design.

These two models were used in simulations with different inlet diameters. Boundary condition where set with an inlet flow of 180 lpm with ATPD standard and outlet at atmospheric pressure. Result in a graph with ΔP compared to diameters shown in Figure 38.

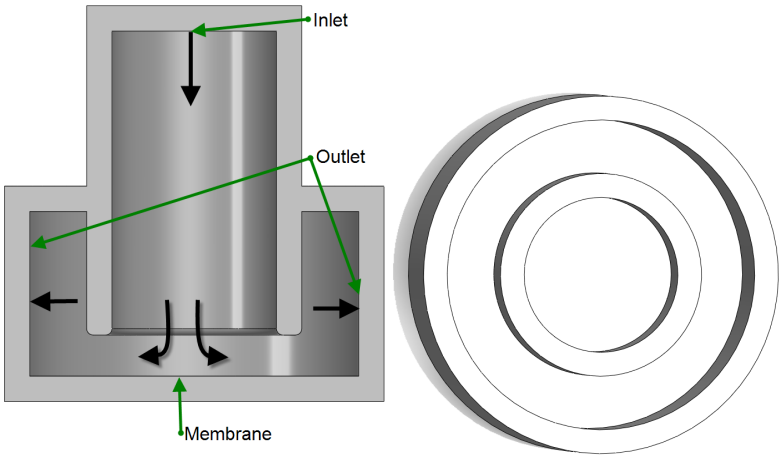

(a) Side cut (b) Top cut

Figure 36: Variable outlet.

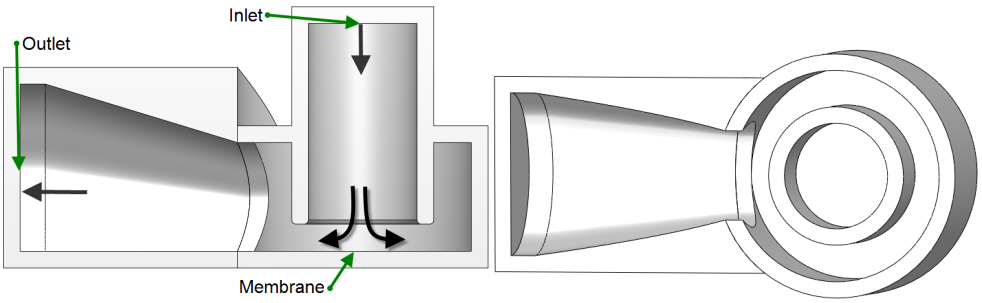

(a) Side cut (b) Top cut

Figure 37: Fix outlet.

As describe different parts contribute different amount. In an optimal case we have a cassette with only the valve and flow sensor. This means that the valve can stand for 83% of the total pressure drop. The simulation results indicated that it should be possible to have an inlet diameter down to around 12 mm. Conclusion will be to investigate this more with a complete cassette assembly and use three different inlets 12, 13.5 and 15 mm. That will be an interesting span to investigate further.

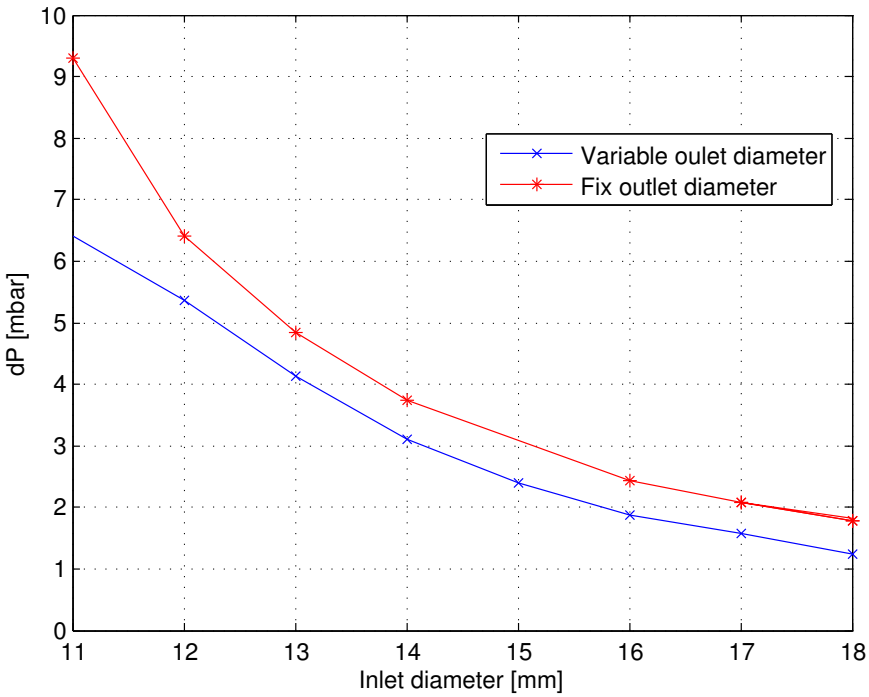

Figure 38: Inlet diameter compared to pressure drop.

3.2.3 Water Trap Analysis

The water removes water droplets for the air flow. Water might short circuit the ultra sound transducer used in the flow sensor. In the current assembly the flow sensor is placed before the membrane valve. Therefore the water trap must be a separate part in the current assembly. In the new cassette the flow sensor is placed after the membrane valve. This gives a possibility to use the membrane or the valve design as water trap instead. Results from this will be important to the final appearance of the valve design that going to be manufactured and tested.

Membrane as Water Trap

The first approach is to have the membrane as water trap. Because of the change in flow direction at the membrane all water droplets will hit and stick to the membrane. This have been proven with simulation and the result from this is found in Figure 39. This design will be named uTurn in the rest of the report.

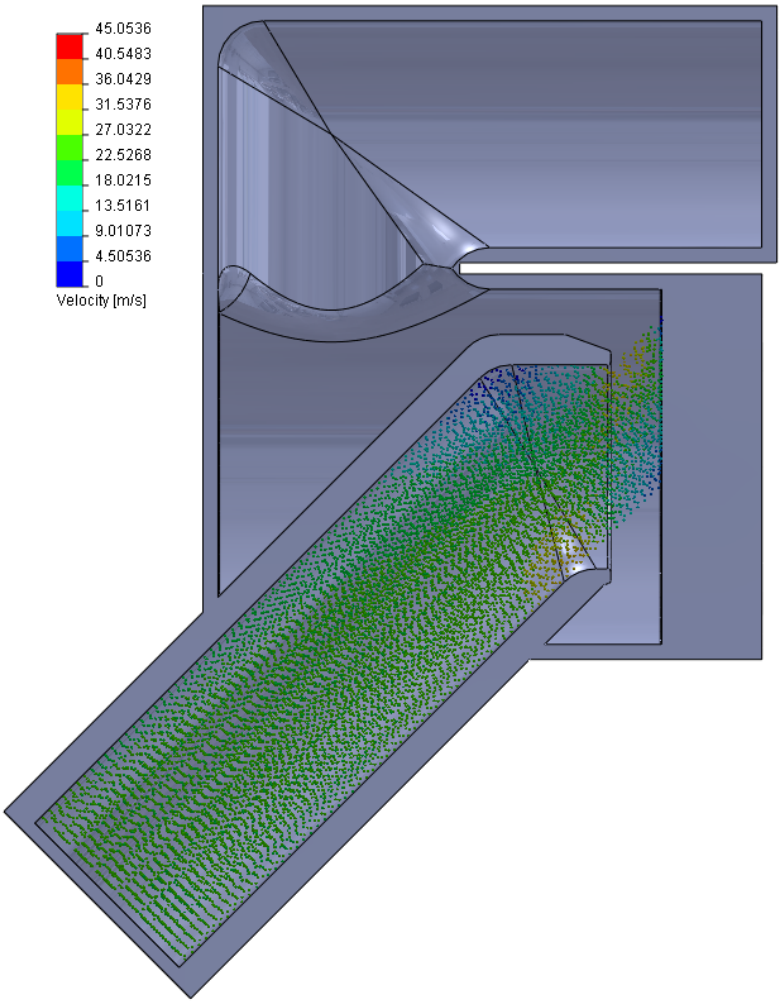

Figure 39: Simulation of 200 water droplets with surfaces type absorption.

Vortex Water Trap

If the membrane is not sufficient as water trap some extra part that's helps to remove the droplets is required. The idea is to create a vortex after the membrane that will throw the droplets to the sides where they will stick. This has been realized with a design with a chamber formed as a half cylinder. Simulations shows that this desired performances is realized and this can be seen in Figure 40. This design will be named *Flow* from here.

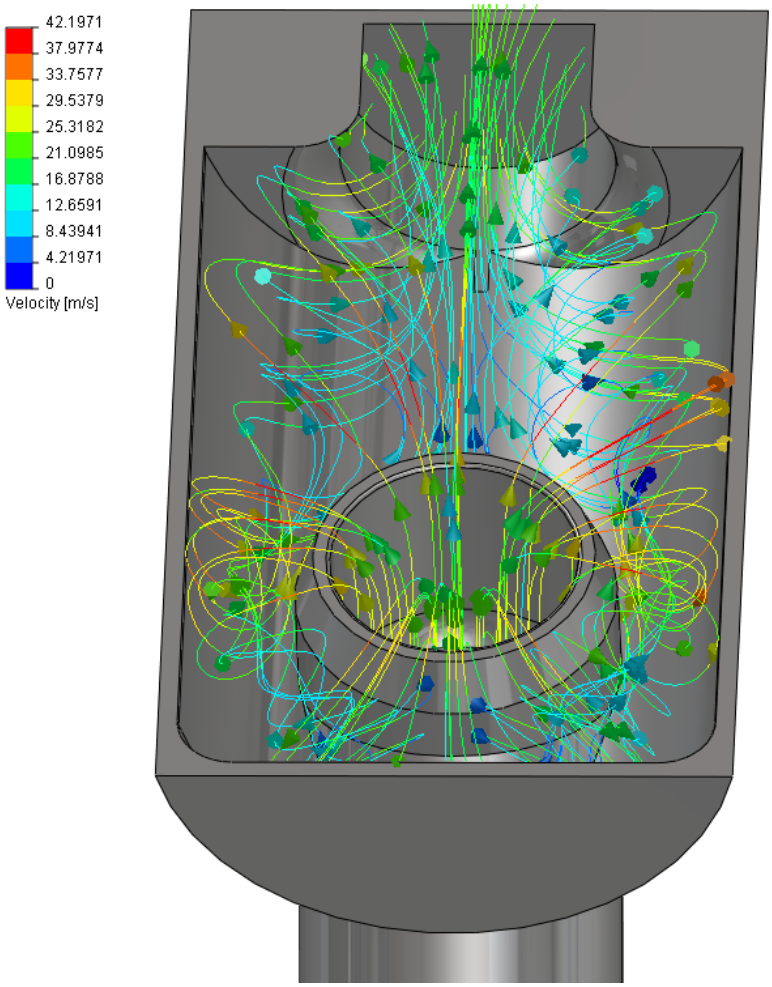

Figure 40: Whirls in design Flow.

3.2.4 Analysis of Inlet Diameter on Flow and uTurn

This section will be a study of the two designs performance in three different tests.

- The pressure drop with a flow of 180 lpm.
- Pressure difference of 10 mBar. (In this case the pressure difference refer to the pressure difference between the inlet and outlet pressure.)
- Pressure difference of 120 mBar.

In Figure 41 the designs is show also how the gas flow velocity is distributed.

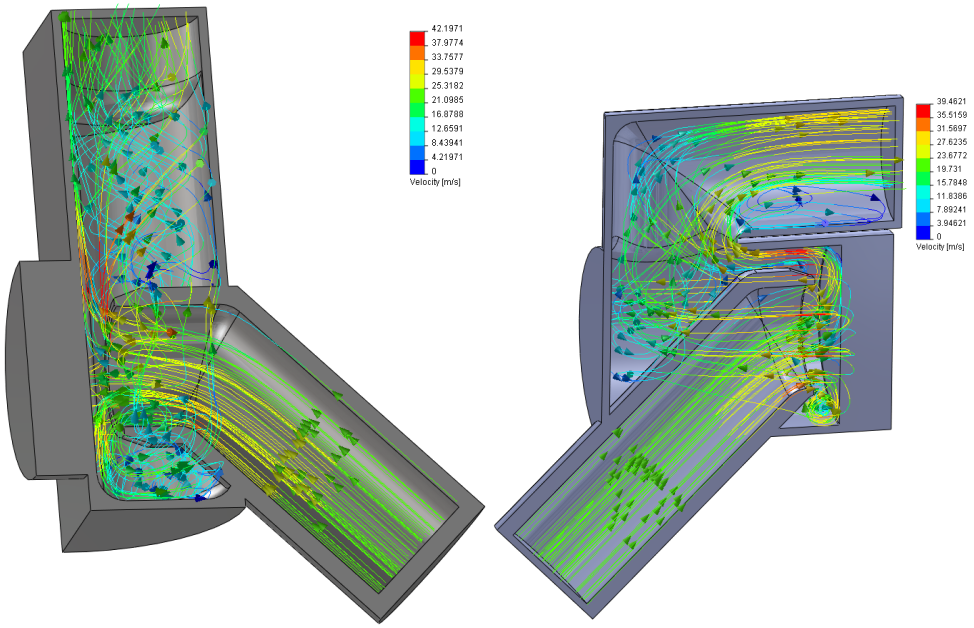

(a) Flow through valve design Flow. (b) Flow through valve design uTurn.

Figure 41: Appearance of the two different designs with flow velocity characteristics.

Pressure Drop Analysis

Result from this analyze shows that both given design with all inlet diameter meet the set demands of maximum ΔP. This result is show in Figure 42. As seen with an inlet of 12 mm maximum allowed Δ relativity close. (If there any error in simulation probably cause problem with final prototype.)

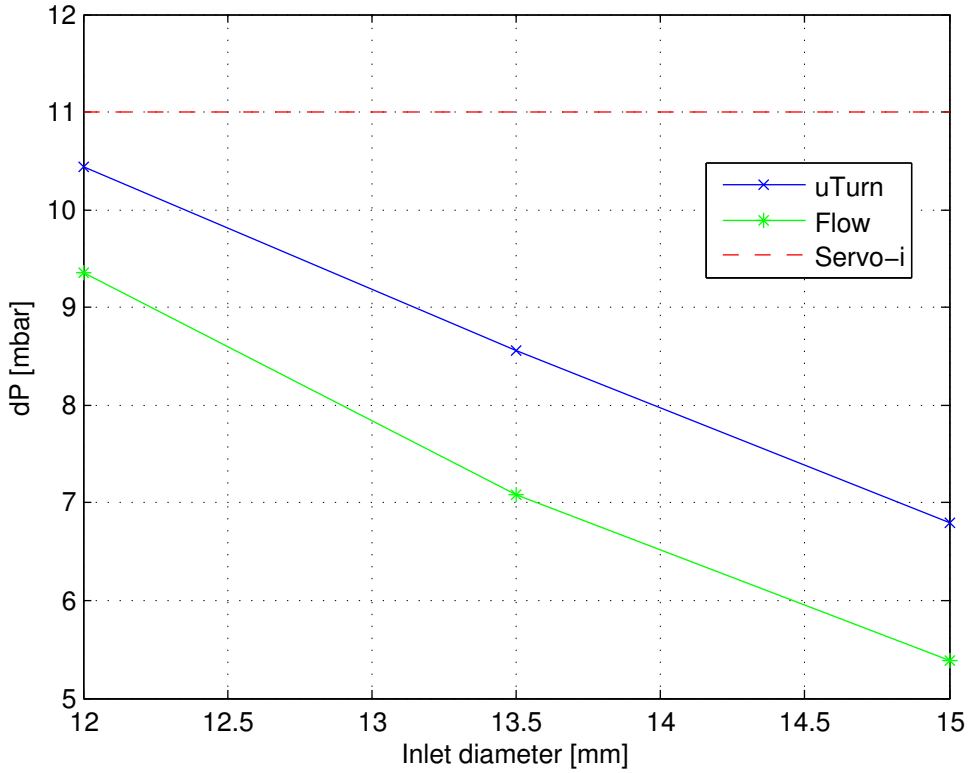

Figure 42: Flow and uTurn with Flow of 180 lpm to Atmosphere Pressure.

Pressure Difference of 10 mBar Analysis

This study is to assure that the valve is enable to deliver the required flow of 180 lpm with a pressure difference of 10 mBar. Without open the valve more than a fourth of the inlet diameter. With an inlet of 12 mm we find that it just manage to deliver the required flows, result is presented in Figure 43. This inlet is too small to use in a final prototype.

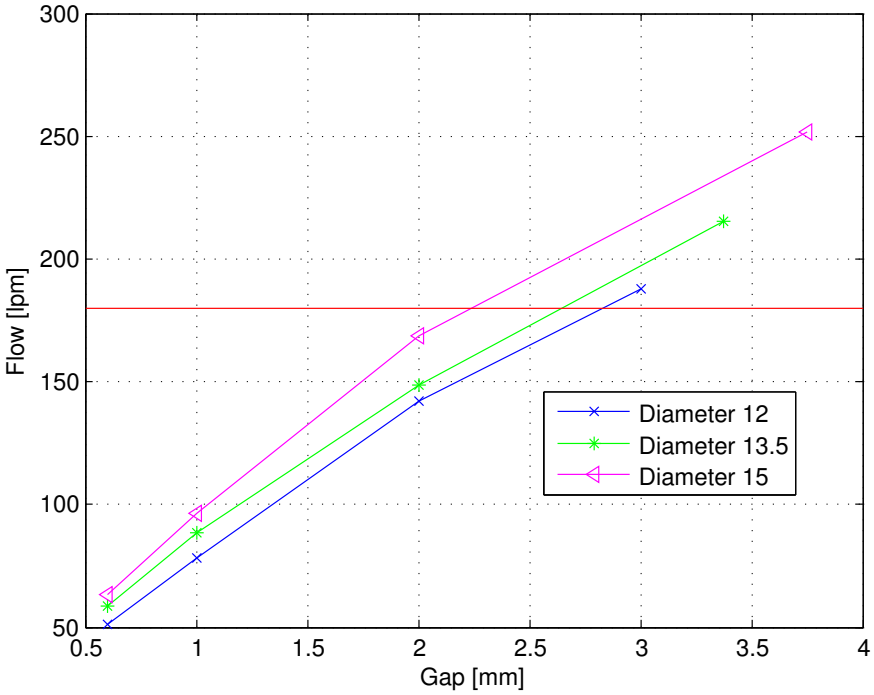

(a) Flow: ΔP of 10 mBar with variable gap.

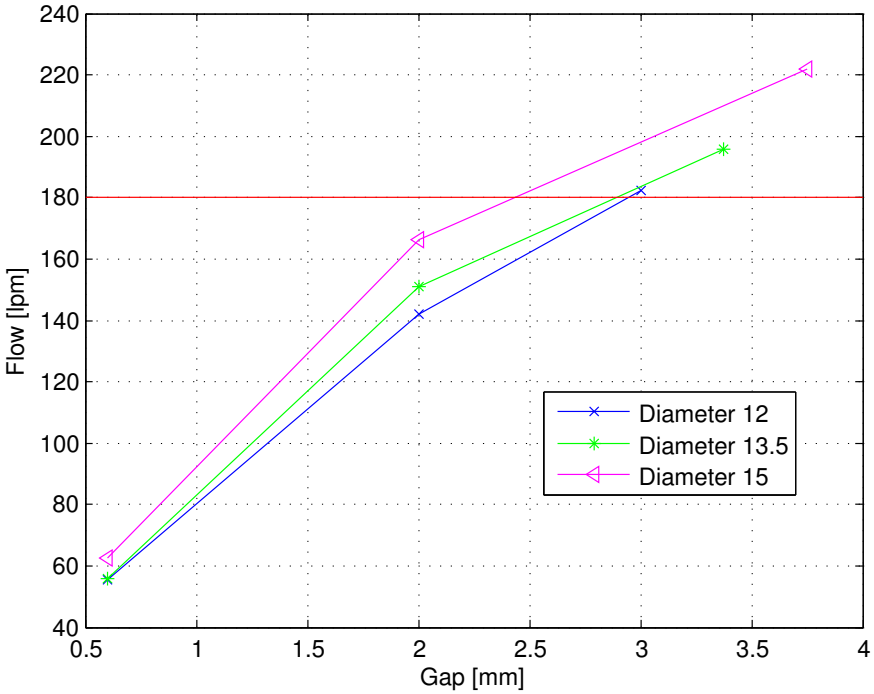

(b) uTurn: ΔP of 10 mBar with variable gap.

Figure 43: Simulation Results with a Pressure Difference of 10 mBar.

Pressure Difference of 120 mBar Analyze

This part will give a hint of the maximum forces that can be expect by the actuator. This is executed by measuring the pressure acting on the surface that is described as the membrane. By changing the gap we will get different flow throw the valve as show in Figure 44. All forces are in a range that see ms acceptable. Compare this with the force created by the pressure before the membrane, gives a result that seems probable. Where the result differ 5 % for Flow and 10 % for uTurn.

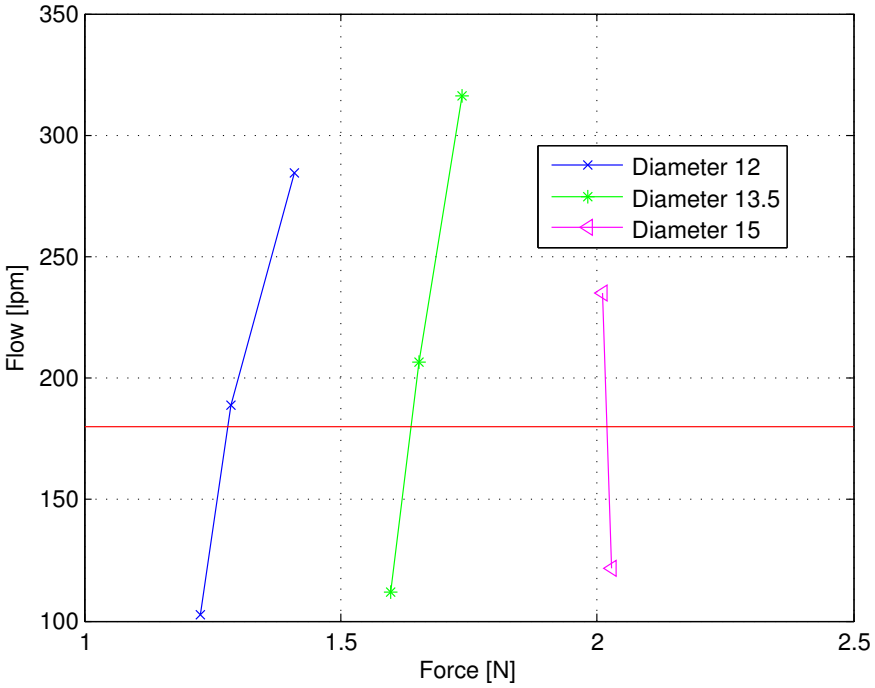

(a) Flow: ΔP of 120 mBar with variable gap.

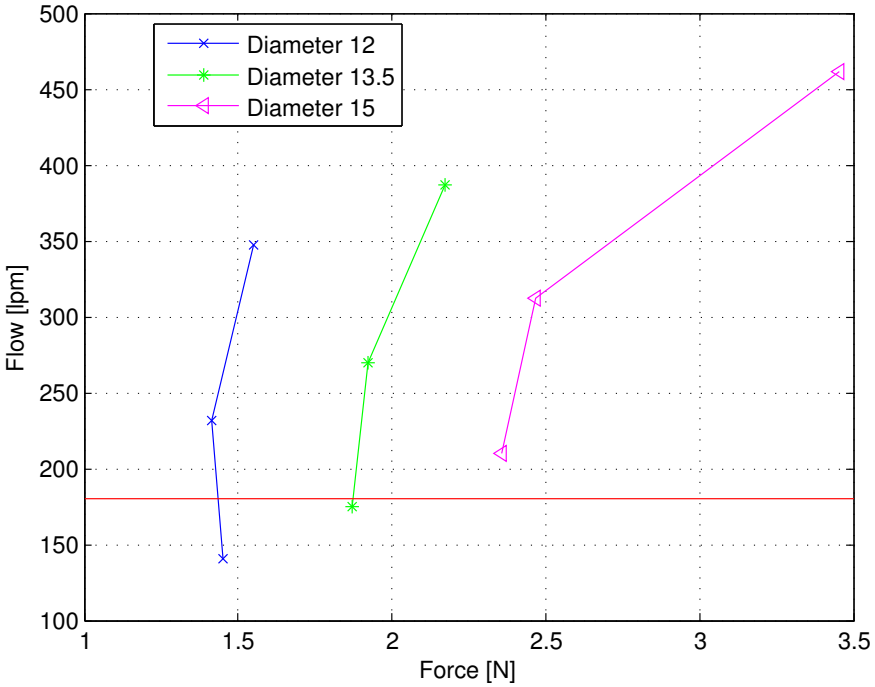

(b) uTurn: ΔP of 120 mBar with variable gap.

Figure 44: Simulation Results with a Pressure Difference of 120 mBar.

3.2.5 Check Valve

A thing that has not been taken into account in simulation is the pressure drop created by the check valve in inactive mode. By measuring the spring constant for the chosen membrane we get the force needed to open the valve. This measurement was performed with Mecmesin. The maximum force that is needed is around 0.1 N depending on gap as seen in Figure 45 and the appearance of membrane is shown in Figure 46.

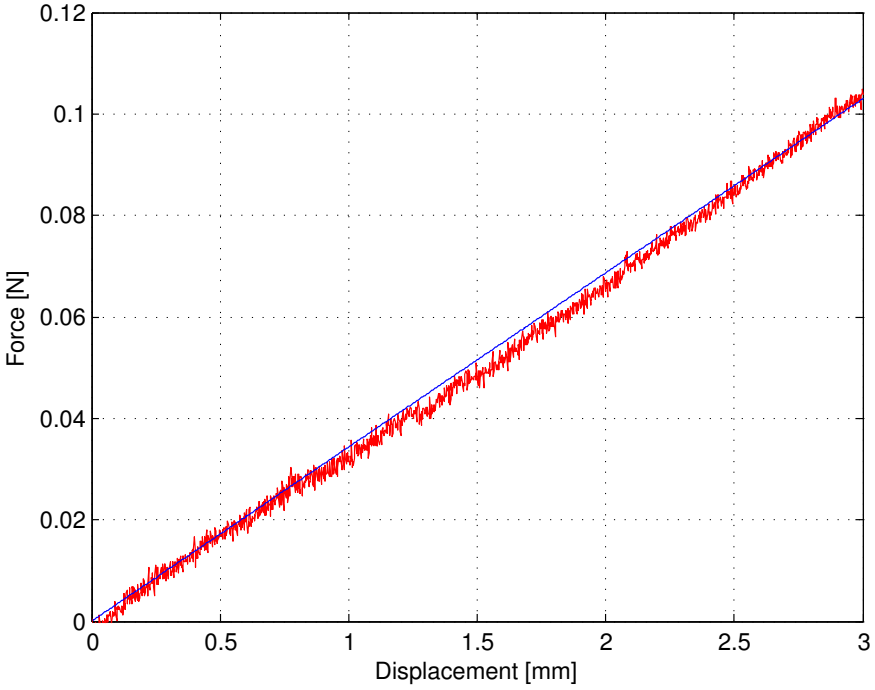

Figure 45: Spring constant for Expiration membrane.

3.2.6 Prototype Manufacturing

To evaluate the design further the next step will be to manufacture two of the designs. When deciding an inlet diameter for the final prototype all simulations have been taken into account. A compromise between ΔP and the force on the membrane will be an inlet diameter of 14 mm. This is a half of current valve and should give an understanding of the benefits/drawbacks with using a smaller inlet diameter.

To make the designs more suitable for manufacturing the inlet has no 45°bend before the membrane. Final design has also been made to fit with actuator GeePlus VM3334. The valve and actuator attachment can be seen in Figure 47. The prototypes have been manufactured with 3D printing, to get a pro-

Figure 46: Picture of membrane.

totype fast. Surface of printed prototype gets relative rough, but it will be good enough for testing, but not suitable for a final product.

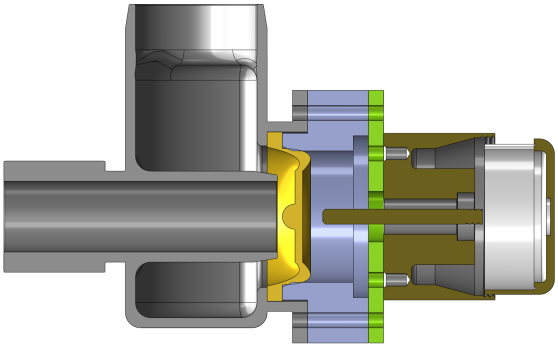

(a) Flow: Cross section.

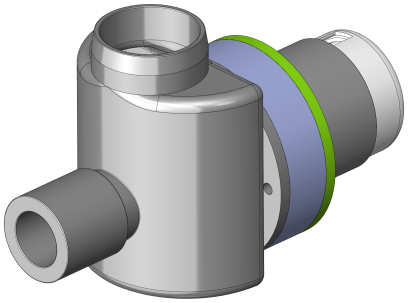

(b) Flow: Apperence.

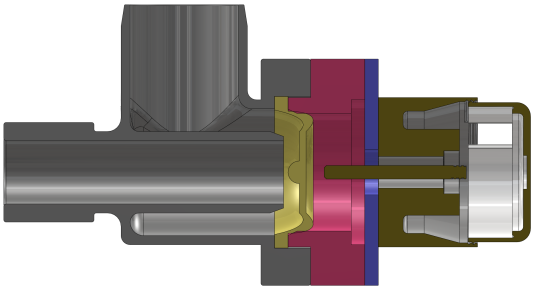

(c) uTurn: Cross section.

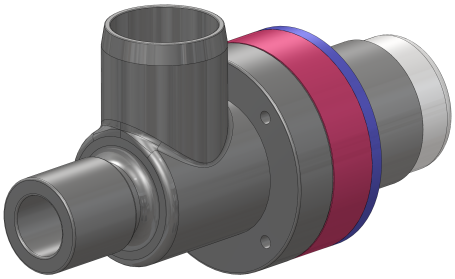

(d) uTurn: Apperence.

Figure 47: Final designs with actuator.

3.2.7 Prototype Testing.

The tests that have been performed on the prototype valves have been divided in to three category's active, inactive and leakage test. The leak test is performed with an inactive valve and a pressure difference of 20, 30, 60 and 120 mbar. The goal is to find the maximum force that is needed to keep the flow between 0 and 0.5 lpm.

Inactive means that pressure itself moves the membrane and active where actuator helps to move the membrane. Inactive measurements will help to evaluate what's happens when ventilator lose power. Those test where preformed at 30, 60, 120 and 180 lpm and ΔP and force as output. Gap varied from 0 to 3 mm. Test data can be found in Appendix B and C. How the test set-up where made can be seen in Appendix A. A special holder was manufactured to hold valve when tests were executed.

Pressure Drop

The result in Figure 48 shows that both designs have a lower ΔP than Servo-i which is requirements [17]. The result that is used here is with an active valve. Here we also see that there is a big difference between simulation and prototype test. This is not any surprise when the simulation has almost perfect surfaces and the prototype have a rough surface. But as seen the curves follow the same shape as the simulation and the difference between the two designs are small both in simulation and prototype test. There is a big difference of the setup in real compared to simulation test. The simulation of atmospheric pressure is defined as the surface that is located in the end of the valve. In the prototype testing the pressure drop for the gas when it's enter surrounding air is included.

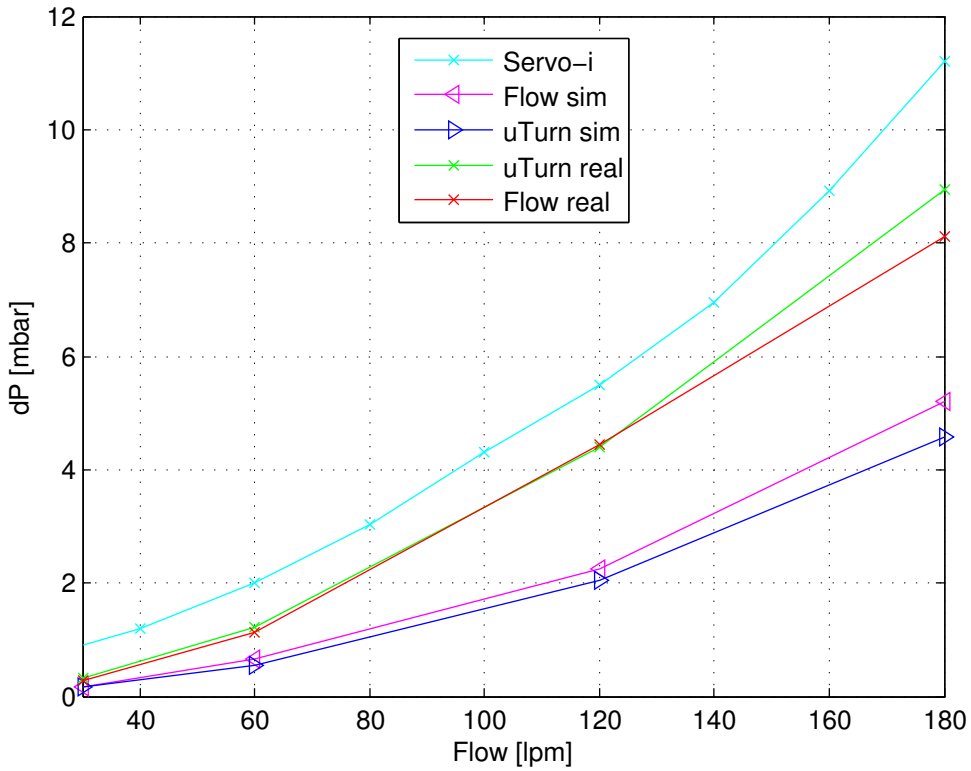

Figure 48: Compare simulation, prototype and Servo-i.

Active and Passive Test

Test result show in Figure 49 is a comparison of active and passive valve at a flow of 30 lpm. According to the Swedish standard the ΔP need to be less than 6 cmH20 $\approx$ 6 hPa when the ventilator have lost power [12]. Given that expiration cassette can stand for half of this. Conclusion from this is that uTurn gives best result and Flow is just above the limit. This difference should not be taken too seriously because of the small difference and were measurements error easy can influence the result. To remember that the design are exactly the same from inlet to the valve seat that is after this the designs differ. With a better valve seat surface and a material with better surface this can give clearer and better result. There also a leak test performed in chapter 5 System Integration, where we use an actuator instead of solid measurement equipment. Hence they don not meet the requirements in this aspect.

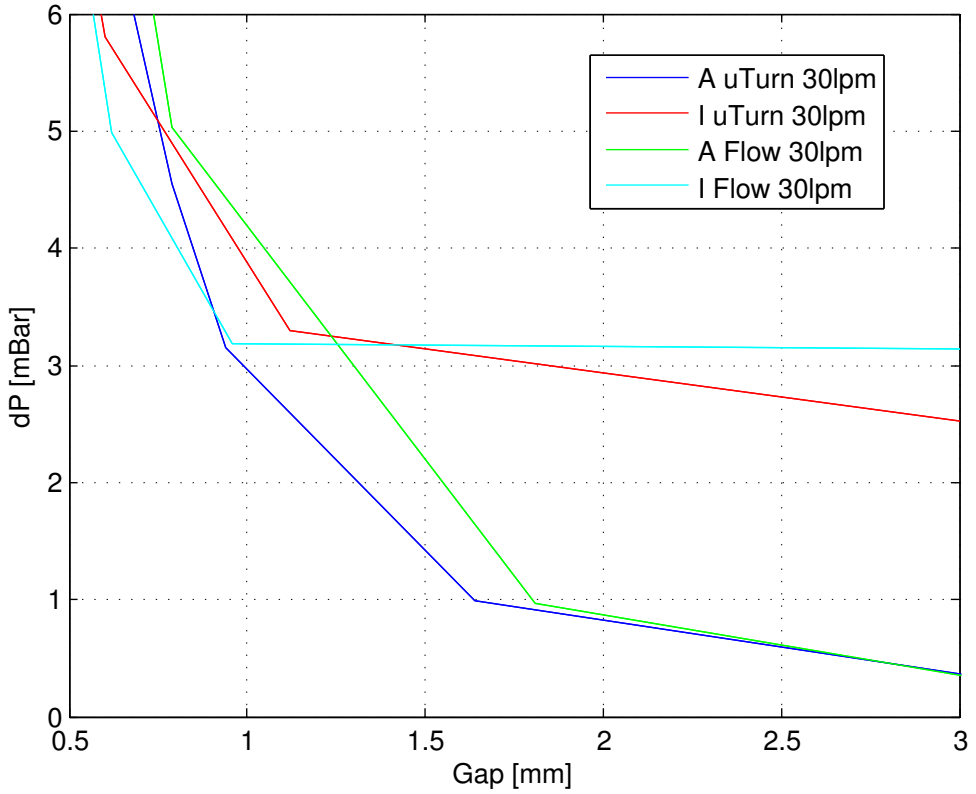

Figure 49: Comparison of active(A) and passive(I) valve.

Leak Test

The final test is the leak test where there is a requirement on maximum consumed power with a ΔP of 120 mBar and flow less than 0.5 lpm shall not exceed 5 W. In chapter 4. *Valve Actuator* it will be described more about how to optimize to get lower power consumption. Hence we get that maximum force with a leak of 0.5 lpm is 4 N for Flow and 2.5 N for uTurn. There is a big difference between the results of each design. A cause for this may be that it was hard to center rod. Hence gives problem when you want to close the valve complete.

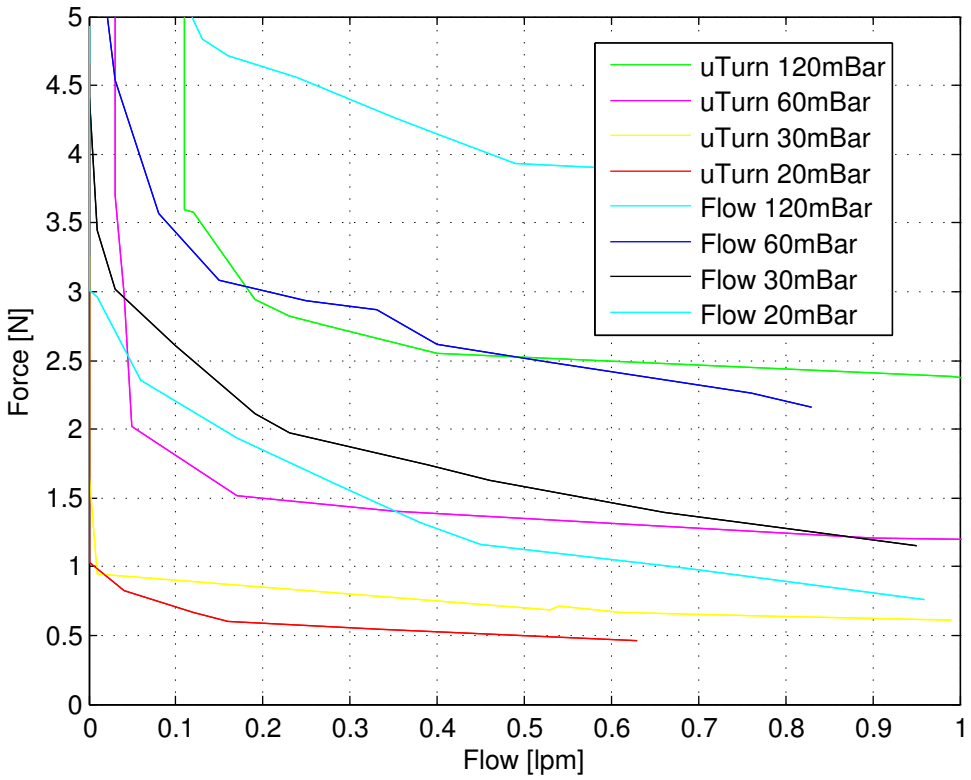

Figure 50: Leak test.

3.2.8 Discussion

Conclusion is that overall Flow shows to have better performance than uTurn. The difference is not big and by optimizing in design and manufacture method this can probably be improved. Because of the complexity in Flows design, uTurn is much more suitable for manufacturing. Therefore this should be the best choice to use in a final product. One problem that not has been discussed is the importance of have the membrane centered with the valve seat. To use

a flexible attachment between membrane and actuator will be recommended to handle tolerance errors. To handle problems with to high ΔP when lose of power. There can be different ways to solve this, like have a membrane with lower stiffness or adjusting the zero point of the membrane. Where the chosen zero point was predefined because of use of already existing membrane.

4 Valve Actuator

This chapter describes how the actuator and all essential parts will be designed. To be used as base for a deeper investigation of required parts. Where the design base include a basic investigation in bearings, axis, spoke wheel and wire from coil to connector. The spoke wheel is the part that connects coil winding with the axis. This will be confirmed and further developed by the external part.

There has also been an investigation of an alternative method for the actuator suspension. Where use a bearing called flexure that has close to zero friction is used. This investigation can be found in Appendix H.

4.1 Voice Coil Design

The demands of the actuators are heavily dependent on the characteristics of the valve. Given the valve designs in Chapter 3. *Valve Seat Design* it is possible to determinate the requirements for the actuator.

The goal has been to investigate the possibilities to make a optimized voice coil for the determinate demands. This to develop a voice coil that has low power consumption, small moving mass, low cost and low ferromagnetic volume.

The result from this will be a base in a discussion with an external partner. The partner will investigate and optimize this more by simulate and manufacturing a few different prototypes.

This part will be focus on making a voice coil to fit both valves. In *M Appendix - Optimization for Inspiration- and Expiration Actuator* their is investigation of two different actuators.

4.1.1 Simulation Model

Design of the actuator have been performed with a magnetic FEM program called FEMM[30]. A flexible model was created where main measurements could be changed. This model can be seen in Figure 51. Their is also possible to change type of coil wire, number of coil windings, windings layers and type of material for all parts.

4.1.2 Valve Actuator Demands

The continues force characteristics can be seen in Figure 52. The biggest difference between the two valves is that expiration require a longer stroke. The highest force demands is located at the same stroke length for both actuators. Expiration valve is operating most of the time in short stroke area. The force

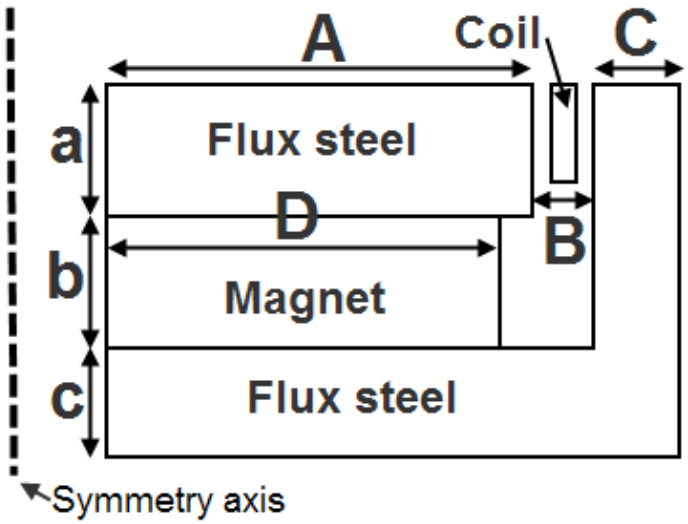

Figure 51: Voice coil model used for simulations where model is symmetric around the axis.

demands is low when the valve is open more than 1 mm that can be used when design the voice coil.

With a duty cycle of 10% as seen in Figure 52 the peak forces for both valve seats have the same magnitude. This is true if the tank before the inspiration valve is empty, meaning there is atmospheric pressure in the tank. In normal case when there is 1 Bar in the tank the force demands is lower.

4.1.3 Simulation of Actuator

First step is to draw a model of the voice coil and define materials. To be enable to perform calculations a mesh is generated. This shown in Figure 54 were selected material is shown also.

Calculating the FEM problem gives a flux density plot seen in Figure 55. The coil is place in the flux gap as defined in figure.

The flux density is plotted in Figure 56 this is measured in the middle of the flux gap from bottom of the gap upto one coil length up from were it's placed in Figure 55. Field is strongest over a distance of 3.5 mm with roughly 1 Tesla.

By defining the current over the coil and moving the coil in flux gap the force characteristics could be determined. Two different simulation were made with 1 and 1.5 A over the coil. Result is shown in Figure 57 and 58.

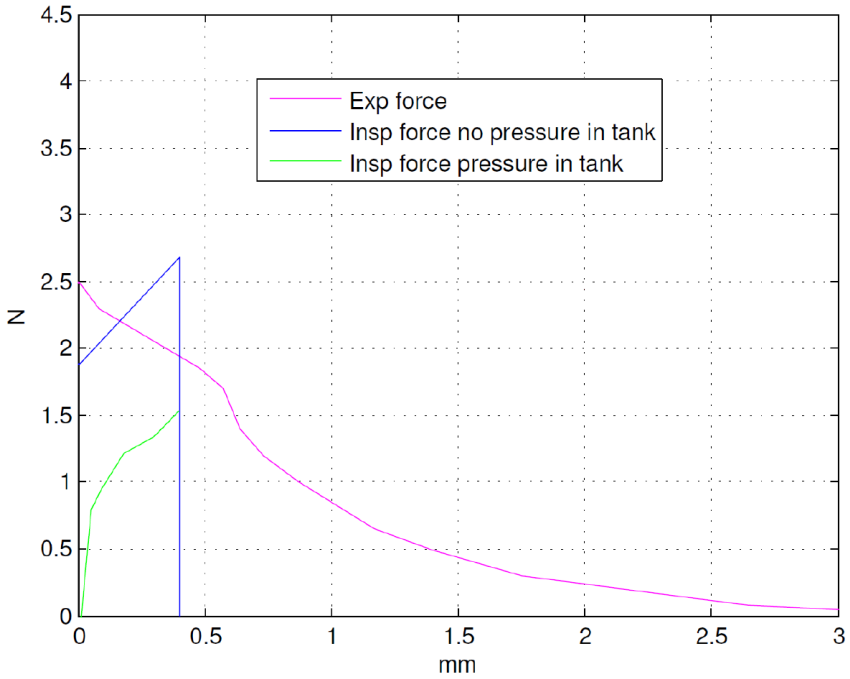

Figure 52: Force characteristics of the different valves with constant drive.

By determine the resistance of the coil the power consumption were defined. The result is summarized in Table 3a and the used materials is listed in Table 3b.

Ampere	1.0	1.5
Power	1.6	3.7
Resistance	1.6	1.6

(a) Voice coil diffrerent test result.

Name	Material
Magnet	NdFeB 52
Steel	Steel 1018
Coil	Copper, Ø = 0.2m
	Windings = 20
	Layers = 2

(b) Voice coil materials.

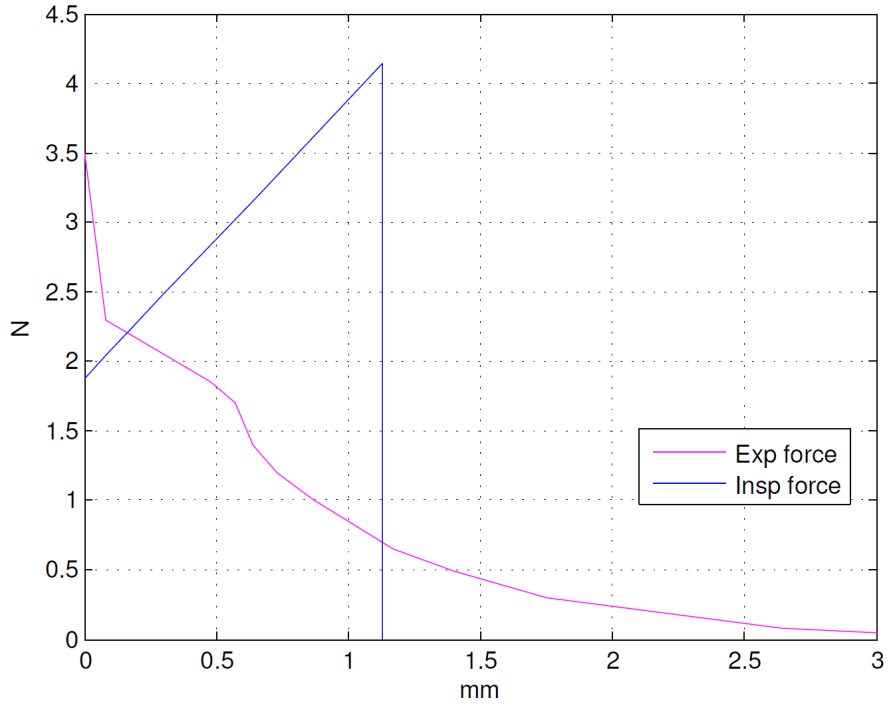

Figure 53: Force characteristics of the different valves with 10 % duty cycle.

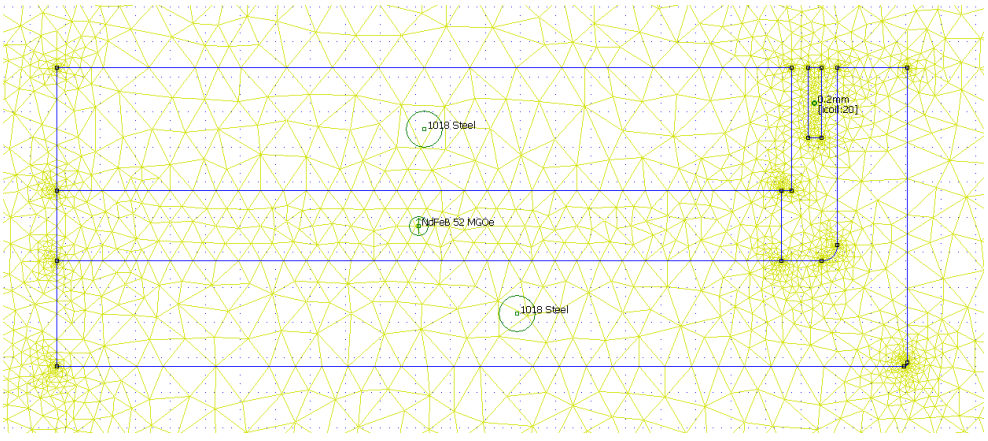

Figure 54: Voice coil model with generated mesh.

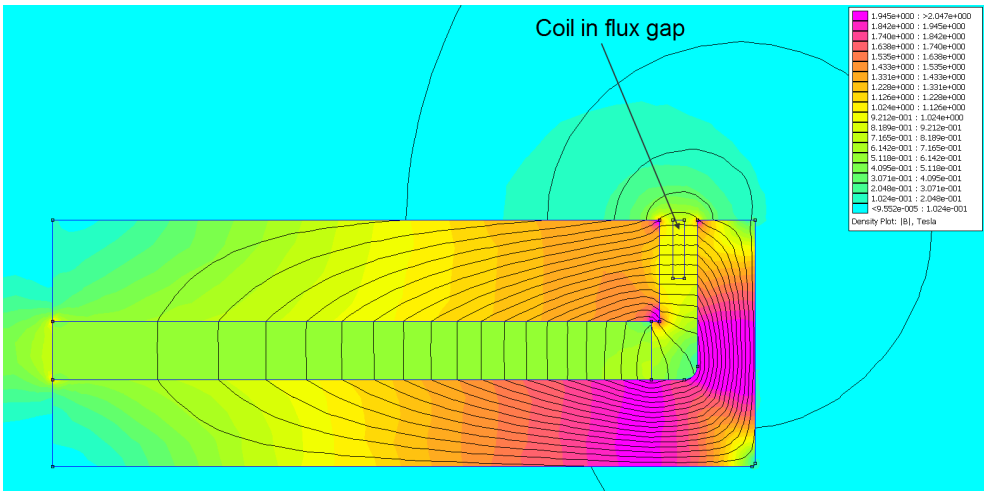

Figure 55: Voice coil model with flux density plot.

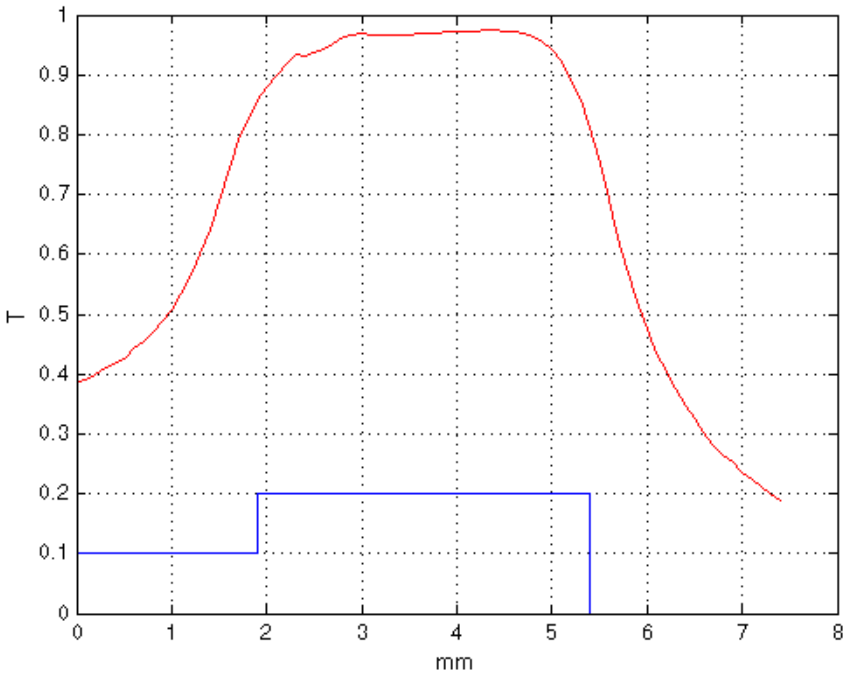

Figure 56: Flux density middle of the flux gap were the red line is the flux strength and blue is the form of the voice coil.

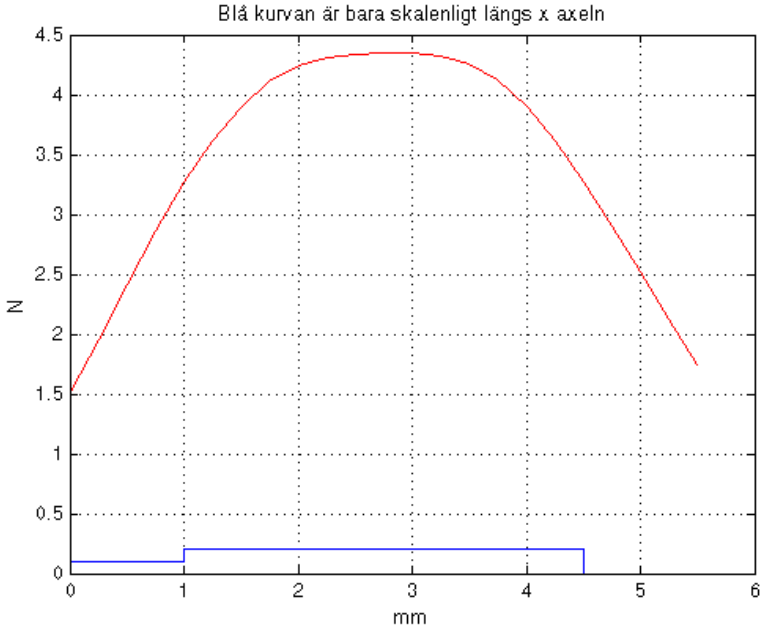

Figure 57: Force characteristics with 1.0 A over the coil.

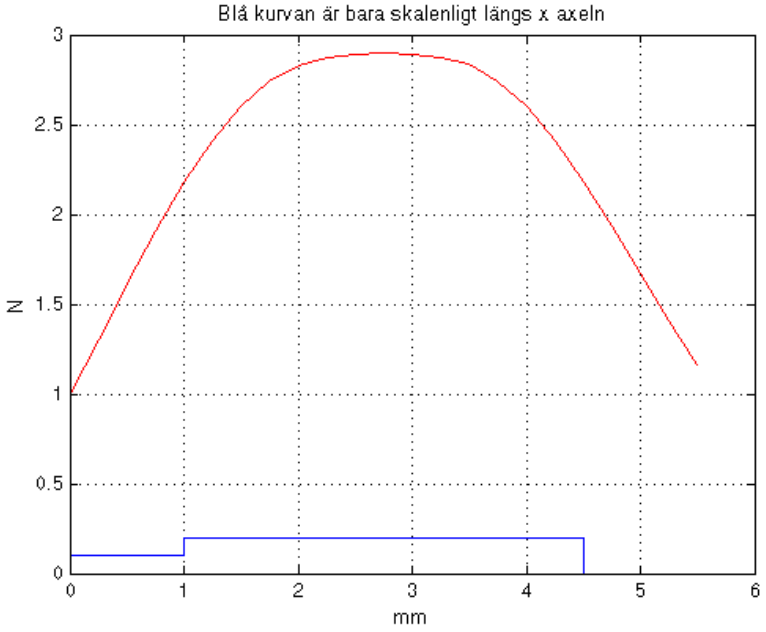

Figure 58: Force characteristics with 1.5 A over the coil.

4.2 Main Parts for Voice Coil Assembly

Model of how the Voice coil assembly could be is show in Figure 59. Following part will describe how to design the different parts with basic requirements.

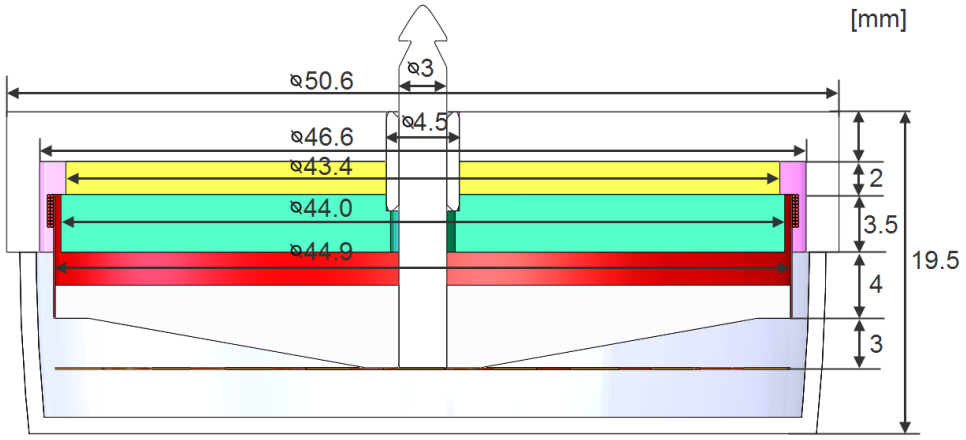

Figure 59: Voice Coil Assembly.

4.2.1 Spoke Wheel

This part is very important hence connection between the axis and coil need to be very accurate to have as small air gap as possible. The requirements of design of spoke wheel are:

- Stand temperatures up to 120 ℃.
- Sustain forces of 10 N in axis direction.
- Sustain force in radial direction of 1 N.
- Weight less than 3 gram.
- The rotation forces is minimal.
- Distance between axis and coil has precision of tenths of a millimetre.

By making the spokes thick we get high strength in the axial direction and thin in the other direction because of the low force demands. This resulting in a spoke wheel as seen in Figure 60.

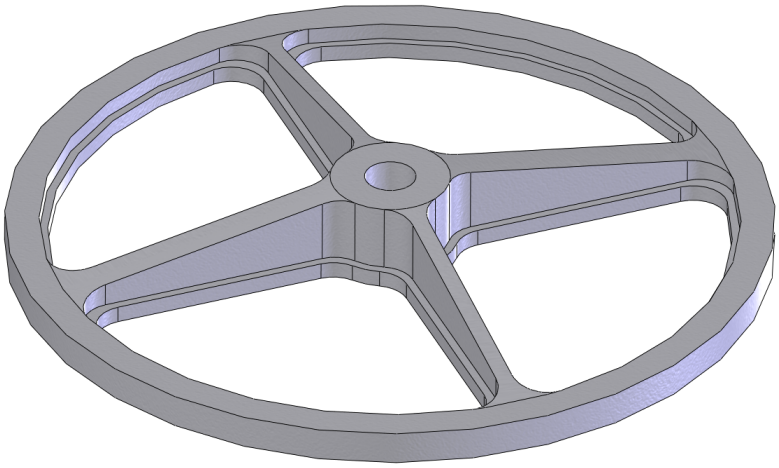

Figure 60: Spoke wheel proposal.

4.2.2 Plain Bearing

There has been an investigation if it suitable to use flexure as bearing that can be found in Appendix H. Flexure is a type of bearing that bending a material to be enabled to have a movement. They have advantage like low or zero friction and long life time. The investigation shows that they are not suitable for this application do to need for a flexure with low spring constant.

Instead a plain bearing with three layer of steel mantle, sinter bronze and PTFE were selected [45] a picture of the plain bearing can be found in Figure 61. This has a temperature range of -200 to 280℃ and a friction coefficient of 0.03-0.20μ.

4.2.3 Axis

The material that has been selected id stainless steel that is a bad conductor. To make the coil assembly as light as possible the axis will be made hollow and still have high strength.

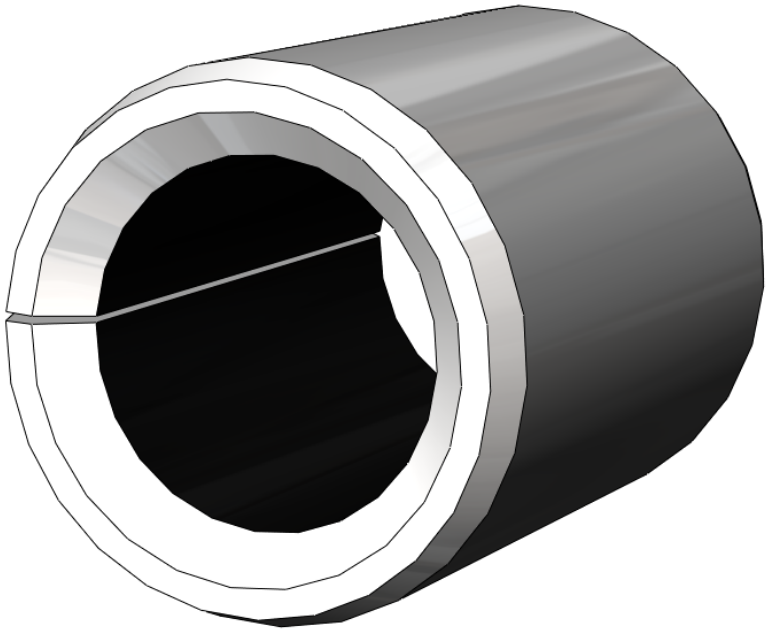

Figure 61: Plain bearing used in voice coil.

4.3 Discussion

There are two main reasons to making this optimization first lower power consumption and second reduce moving mass to get a faster control. The power consumption has from the executed simulations shown that there will be no problem to have so low power consumption as specified. With help from the external expertise this can be verified and manufactured and perform tests on the final actuator. Since the actuator is smaller the need of ferromagnetic volume mass is lowered of what is used in current actuator. Therefore there should be no problem with reducing this to half of what is used in current solution. With the used test actuator from GEEplus that have been used we fulfill all given requirements. There is more interesting to know hove much better it will get.

The placement of the force peak for respective valve could have been place better, curves are seen in Figure 53. This would allow a shorter optimal force stroke. That had given a actuator that where even more effective.

4.4 Test Actuator

Because of the long process to develop and manufacture the actuator this was not finished in the Master Thesis project time. To be enabling to realize a respiration process and perform certain tests a stock actuator was chosen. The

choice where a VM3334 from GeePlus [36], characteristics of that actuator is a better than what is required but should work fine to perform the tests.

Both the inspiration valve and the expiration valve prototypes have been run with the VM3334. The performance of this VCM is linear and has a stroke of 4 mm and is able to produce up to 5 N in continuous drive. Even though the valves at rare occasions need up to 5 N this is under short period. This actuator therefore has more performance than an optimized actuator would have.

Both actuator is regulated with a Maxim MAX9736A [42] Class D voltage amplifier.

4.5 Dynamic Properties Analysis

With the use of Bode 100 Analyser the bode response of the inspiration valve and test actuator were investigated. The frequency response to be determined was VCM voltage input to flow output. Since the ultimate task of a valve is to generate flow these are key input and output signals of a valve.

For these tests there were two aspects of the input voltage that could be varied, the input bias voltage as well as the amplitude of sinusoidal voltage input. A certain choice of these parameters corresponds to a certain flow oscillation at low frequencies (around 1 Hz). When the sinusoidal input signal is increased the frequency response - corresponding to that input - is generated.

Figure 62 show the non-linear force to flow relationship for the membrane type inspiration valve. The same types of non-linear behaviour apply for the globe type inspiration valve. This result in the fact that the frequency response will be alter depending on the flow oscillation. This was also verified during frequency response tests.

Doing a full investigation of the frequency response for all kinds of flow oscillations were not a focus in this thesis. Instead one of the main aims of the frequency analysis was to find if there were any differences between the globe valve and the membrane valve flow performance. Figure 63 and Figure 64 shows the gain and phase of the frequency responses corresponding to flow changes of 35-70 lpm. In this range the force to flow relationship is relatively linear as seen in Figure 62.

As seen in Figure 63 and 64 the two valves behave relatively similar with a bandwidth of around 100 Hz. These similarities were found for several different frequency response tests. Hence, no flow performance difference could be detected between the two inspiration valves. One note is that the globe valve generate a lot more high frequency sound (»100 Hz) during these tests.

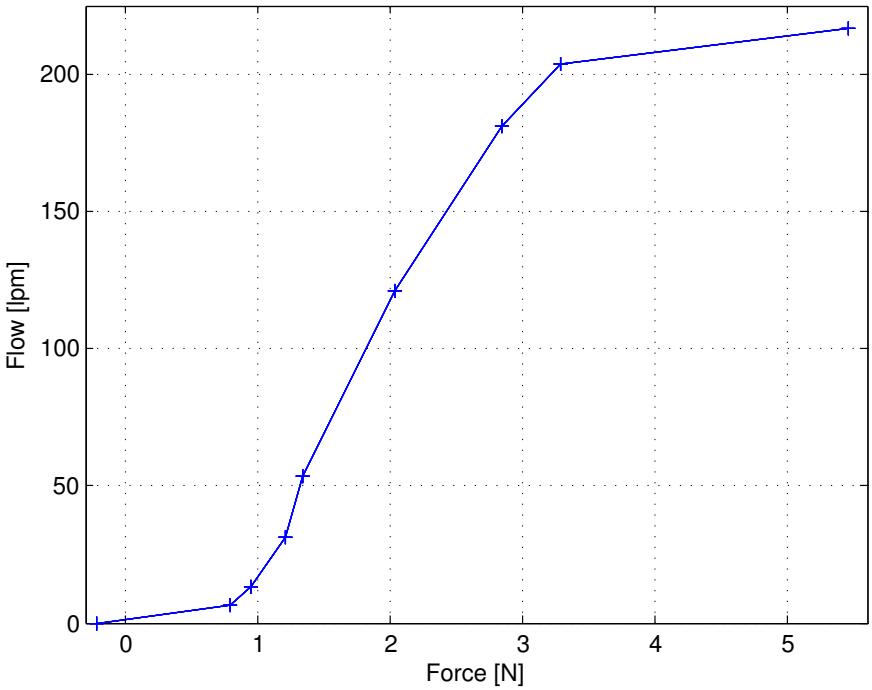

Figure 62: The non-linear force to flow behaviour of the membrane inspiration valve.

Another thing that should be noted for these tests is that the bandwidth of the valves decreased when smaller flow changes (around $+/-5$ lpm) were introduced. This behaviour might be caused by the valves but it might also be caused by the device used to measure the flow for these tests. This device uses a net that the gas passes through and the resulting pressure drop is then measured over the net. This net might have contributed to the fact that a smaller flow oscillation was not detected at high frequency flow oscillations. This should be investigated before any further conclusions are drawn.

Another aim with the frequency analysis was to analyze the test actuator and its bandwidth. It would have been interesting to be able to analyze the frequency response of the actuator itself. This could have been done by measuring the velocity and position of the actuator with an encoder. In that case it would have been possible to compare the actuators performance with the actuator-valve performance.

The VCM-model described in Section 2.3.2 contain the main parameters that govern the main dynamic properties of the VCM. The damping constant d is the one parameter that is unknown in the VCM-model. This parameter could be determined by the use on an encoder. How to do this is further elaborated in *Minimization of Modeling Error of the Linear Motion System with Voice*

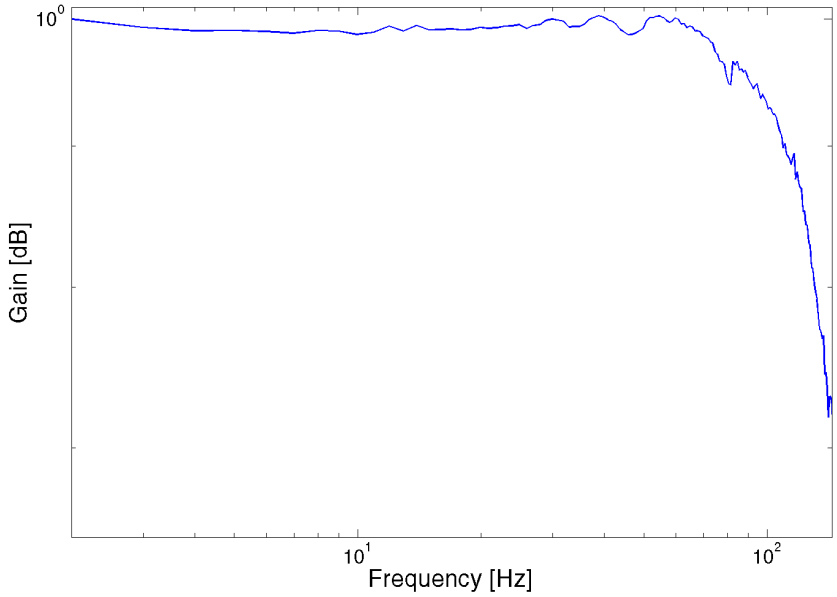

(a) Gain of the globe valve.

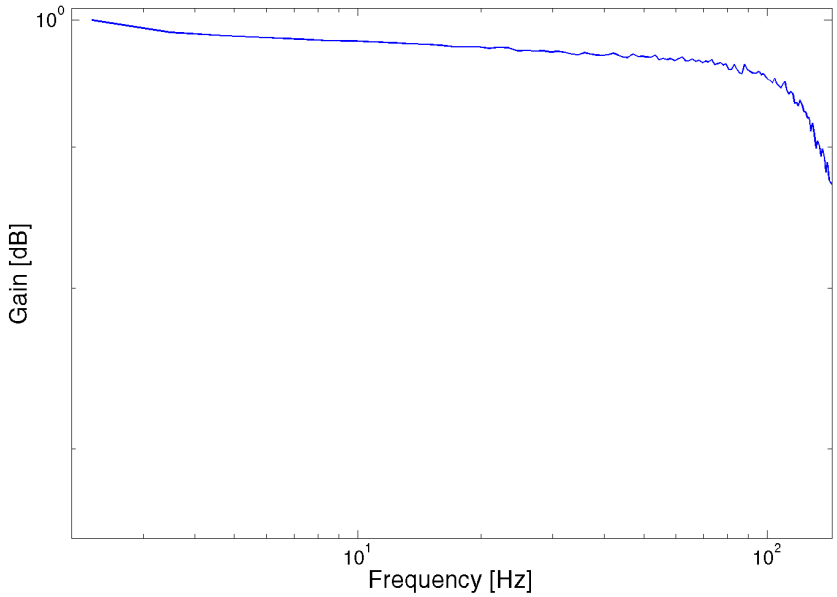

(b) Gain of the membrane valve.

Figure 63: The frequency gain response of the inspiration globe valve and membrane valve. The gain at low frequencies corresponds to a flow signal of 35-70 lpm.

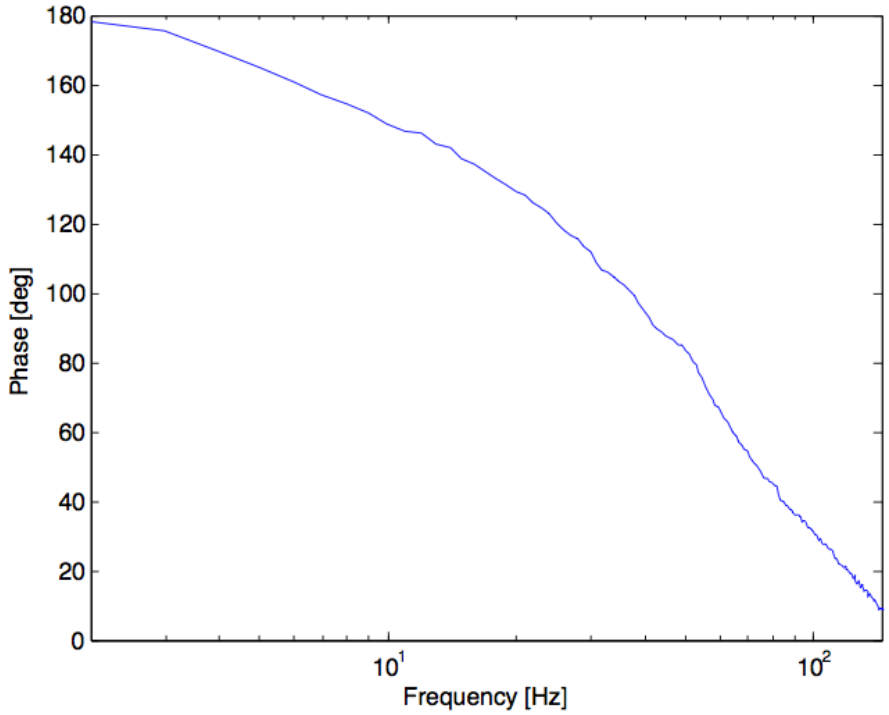

(a) Phase of the globe valve.

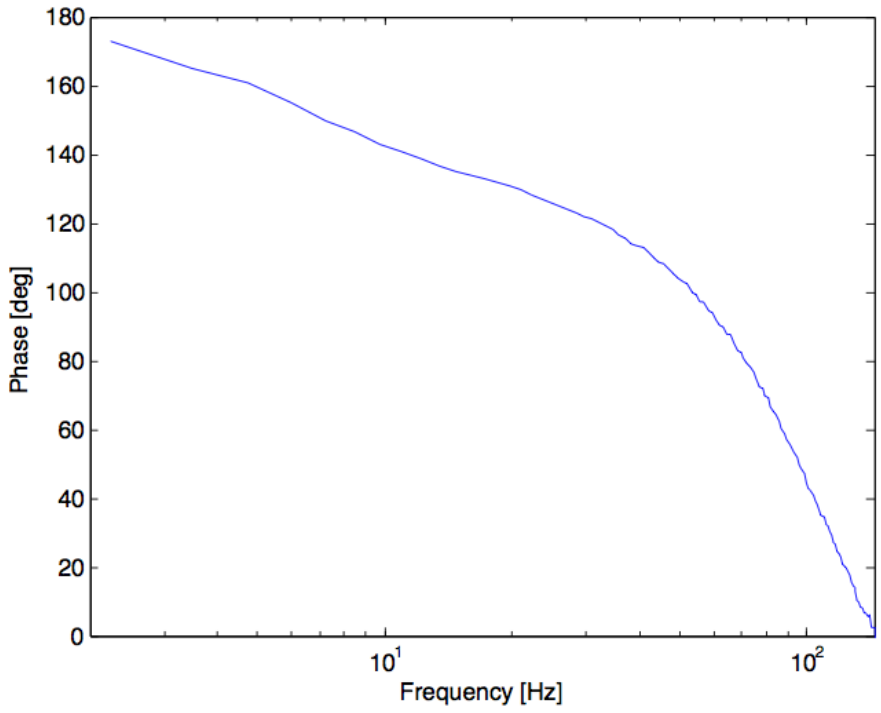

(b) Phase of the membrane valve.

Figure 64: The frequency phase response of the inspiration globe valve and membrane valve.

Coil Actuator [8].

A wide range of different damping constant values gives a model with an bandwidth of around 100 Hz. The bandwidth of the model is around 100 Hz as long as the damping constant d has a value of less than 1 N/(m/s). As seen below, for values $d < 1$ the damping constant has got a limited effect on the actuator model.

$$d = 1.000\,[\text{N/(m/s)}] \Rightarrow \omega_{BW} = 97\,[\text{Hz}]$$
$$d = 0.001\,[\text{N/(m/s)}] \Rightarrow \omega_{BW} = 102\,[\text{Hz}]$$

Just by feeling of the moving mass and the quality of the bearings, it is deemed most likely that $d < 1$. Even though this is a crude assumption this is in a sense verified by the fact that the $\omega_{BW} \simeq 100$ in Figure 63. Given this assumption about the damping constant it is assumed that the test actuator has got a bandwidth of around 100 Hz.

Given this value of the damping constant, the spring constant and the moving mass of the VCM could be optimized in order to achieve an ever greater bandwidth. An increase - from the current spring constant of 2 [N/m] - gives the following change on bandwidth to the model

$$k = 2\,[\text{N/m}] \Rightarrow \omega_{BW} = 102\,[\text{Hz}]$$
$$k = 4\,[\text{N/m}] \Rightarrow \omega_{BW} = 147\,[\text{Hz}]$$

An decrease - from the current moving mass of 0.014 [kg] - gives the following change on bandwidth to the model

$$m = 0.0140\,[\text{N/m}] \Rightarrow \omega_{BW} = 102\,[\text{Hz}]$$
$$m = 0.0075\,[\text{N/m}] \Rightarrow \omega_{BW} = 134\,[\text{Hz}]$$

Looking at the second order spring damper system, the natural frequency ω_n is given by

$$\omega_n = \sqrt{\frac{k}{m}}$$

Even though the bandwidth and the natural frequency is not the same thing it is seen that the same type of cause and affects apply to the bandwidth of

VCM. This in turn, implies that the mechanical properties have a dominating affect on the dynamic behaviors of the VCM.

Given that an increase of the bandwidth would be needed, a further analysis of the optimal values of the moving mass and spring constant should be done. The only downside with decreasing the moving mass is that it might result in a more expensive VCM. The downside with increasing the spring constant is that the maximum forces needed by the VCM increase.

5 System Integration

In order to build a demonstrator of a tank based - serial mixing - ventilator, the inspiration valve and expiration valve had to be integrated. Because of the advantages with the resolution and speed of pressure sensors compared to flow sensors, only pressure control was implemented in this thesis. It is possible to introduce volume control in the future by adding flow sensors.

This section is aimed at describing the ventilator system, with the corresponding control strategy, as well as the describing the performance of this system.

5.1 System

The control system has been implemented in MATLAB/Simulink and executed with DSpace. This part describes how the ventilator system is design. An overview of the implemented ventilator system is show in Figure 65. Besides the different components, this gives a view of how the gas is travelling through the system.

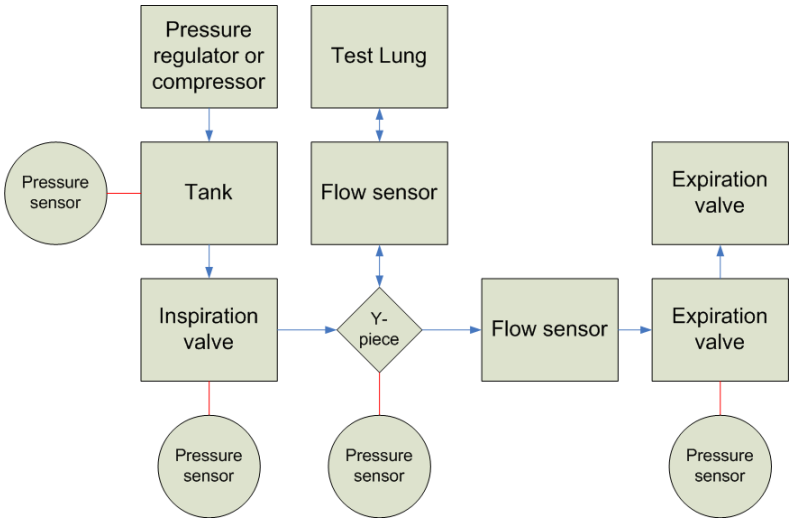

Figure 65: An overview of the test system, were arrows represent the gas flow. The blue arrows represent air flow whereas the red lines represent pressure measurement points.

Below is a list describing the different parts of the ventilation system and in Figure 66 the prototype is shown.

- Pressure regulator: To keep a constant pressure in the tank.
- Tank: Tank of approximately 2 liters.
- Inspiration valve: The developed valve in the thesis.
- Pressure sensor: PC1781, from Servo-i system [40].
- Tube: 1.5 meter Hytrel tube [16].
- Pressure sensor: PC1781, pressure in y-piece [40].
- Volume/flow sensor: measure the delivered volume to lung [44].
- Test Lung: [43].
- Tube: 1.5 meter Hytrel tube [17].
- Flow sensor: [37].
- Pressure sensor: PC1781, from Servo-i system [40].
- Expiration valve: The developed valve in the thesis.
- Flow restrictor:

A more detailed description of the sensor can be found in Appendix G. Analogue in and out signals are controlled with a DSpace system named MicroAutoBox 1401/1501. The connection between components and DSpace is described in Appendix D. In *Appendix L* there is a concept of how a future ventilators appearance.

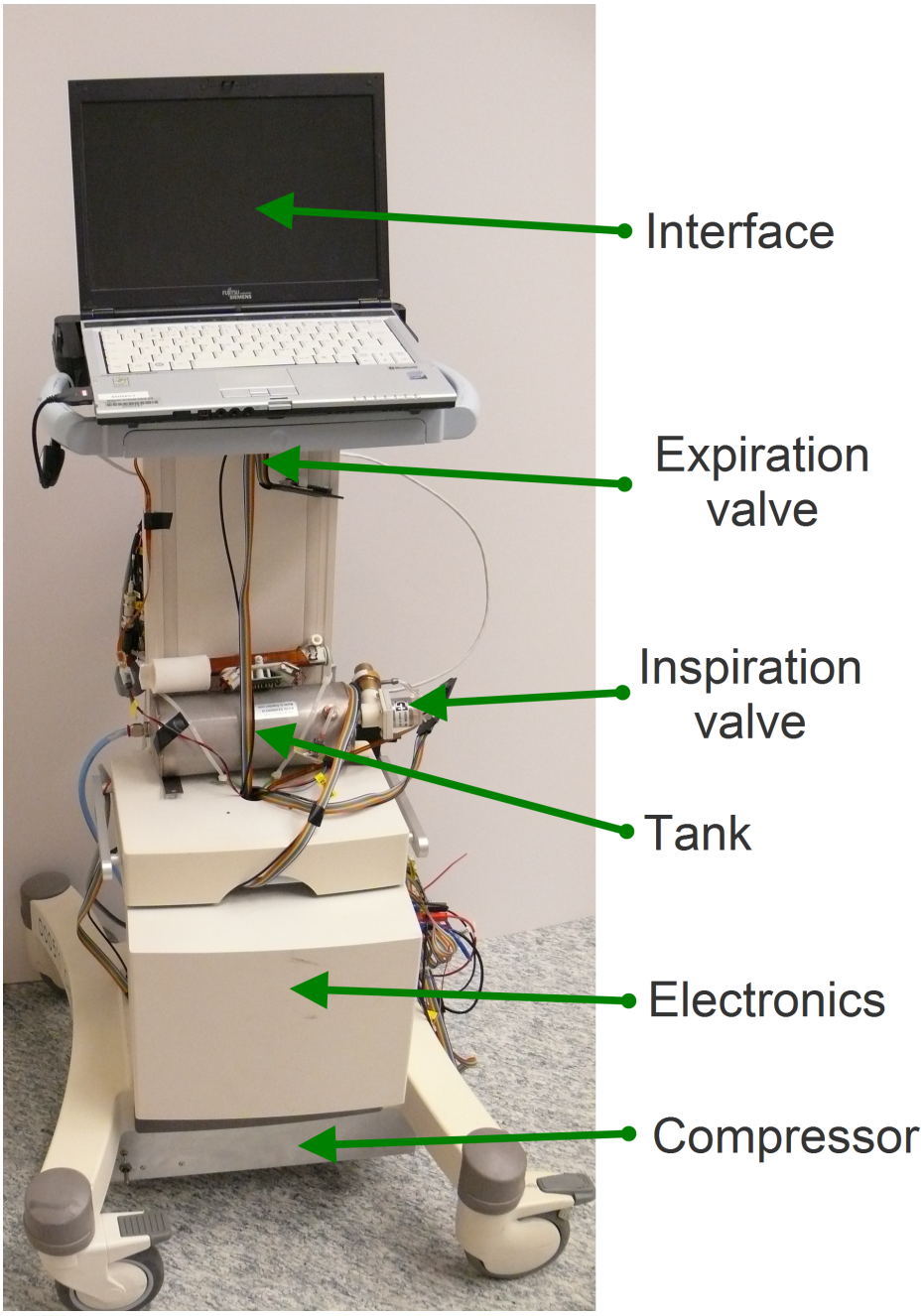

Figure 66: Developed ventilator.

5.2 Implemented Control Design

The control of the valves have been implemented using basic PI- and PID control algorithms. This was used as a first step in order to see how good manually tuned basic controllers could perform. This strategy gave more than enough performance for the fairly limited test cases used in this thesis.

The entire breath can be divided in to four different phases. The different phases can be seen in Figure 67.

In order to reduce the risk of controlling both actuators with the same error. The actuators were made to having feedback control one at a time. While one actuator has feedback control the other actuator only performs feed forward control.

The control algorithm used for the inspiration actuator is a PID regulator and for expiration a PI regulator. Both regulators have been manual tuned, to find suitable performance. Suitable performance meaning that is similar to Servo-i performance. A schematic picture of the control strategy is seen in Figure 68.

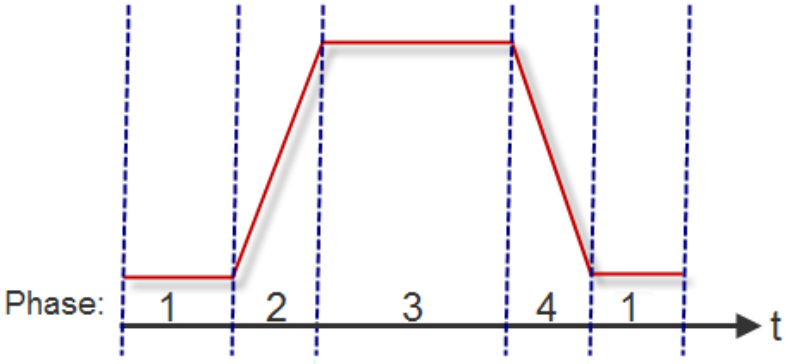

Figure 67: The implemented control phases.

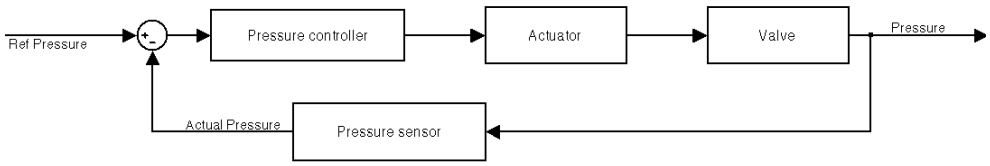

Figure 68: Schematic picture of control structure.

The control strategy has been implemented in MATLAB/Simulink and the corresponding model is described in Appendix E. The control structure has been implemented in Embedded MATLAB code. This code can be found in

Appendix F. By generating the model to c-code it can be executed in real time on DSpace.

5.2.1 Control Strategy

Below is a description of the different control phases that are implemented during a ventilated breath were PaP is peak airway pressure and PEEP is Positive End Expiratory Pressure.

Phase 1 - PEEP

Expiration: Control
Inspiration: Constant value
Here inspiration have a small flow leak to make it possible for expiration to control. Therefore make it possible to increase and decease the pressure.

Phase 2 - Rise from PEEP to PaP

Expiration: Constant value
Inspiration: Control
Expiration is set to a hold a constant PaP pressure.

Phase 3 - Pap

Expiration: Constant value
Inspiration: Control
Same idea as phase 2, where same control algorithm is used.

Phase 4 - Fall from PaP to PEEP

Expiration: Control
Inspiration: Closed
Inspiration is close to get out the specified volume as fast possible.

5.3 Testing

The major requirement in the implemented ventilator is to have a similar performance to the Servo-i, in a few test cases. These test cases are described below. There has also been some performance tests made to individual requirements for the inspiration valve as well as the expiration valve.

5.3.1 Patient Category Tests

The tests have been executed according to *Patient models and ventilation settings suitable for test* [15] document. Four different patients models have

been tested. The corresponding test parameters can be found in Table 3 [15]. A picture of a real test set-up are found in Appendix A.

The results of the tests are shown in Figure 69, 70, 71 and 72. Here it is seen that the implemented ventilator has a faster rise time than the Servo-i.

Table 4 give that the step time independent of the Pap value. The overshoot is less than in 10% in 75% of all cases.

Test TA4 where the overshoot is high, could had been lowered by making the control a bit slower. The settling time in test TA4 seen in Figure 72a is 0.3 s with error less than 2%. This makes it much faster to settle than Servo-i. This fast system is a consequence of the small moving mass in the actuator. Which makes i possible to control at higher frequency. In all tests PEEP level doesn't fall below set value, this is important because of risk of lung collapse.

Comparing PEEP level in test TA2 (Figure 70) a large drop in PEEP pressure in Servo-i can be seen compared to the demonstration ventilator.

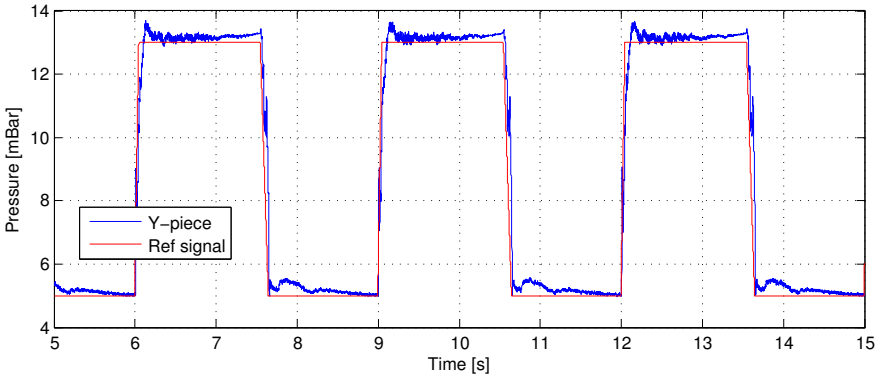

(a) Servo-X

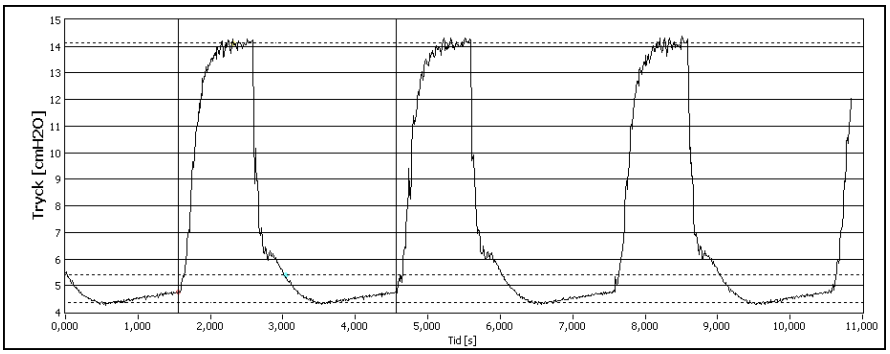

(b) Servo-i

Figure 69: Test with patient id TA1.

Table 3: Test set-up parameters.

Test id	Patient	Resistance [1/hPa(l/s)]	Compliance [1/ml hPa]	Breath rate [Bpm]	PEEP [hPa]	PaP [hPa]	Tidal volume [ml]
TA1	A1	5	50	20	5.0	8	500
TA2	A2	5	20	20	5.0	22	500
TA3	A3	20	50	20	5.0	12	500
TA4	A4	20	20	20	5.0	24	500

Table 4: Test result.

Test id	Tidal volume [ml]	Overshoot [hPa]	Overshoot relative %	Undershoot [hPa]	Undershoot relative %	Step time insp [ms]	Step time exp [ms]
TA1	405	13.7	8.6	12.9	1.5	5.6	11.1
TA2	463	29.1	9.5	26.0	4.6	5.6	11.1
TA3	500	17.5	4.1	16.7	2.8	5.6	11.1
TA4	502	32.3	13.7	27.4	6.6	5.6	11.1

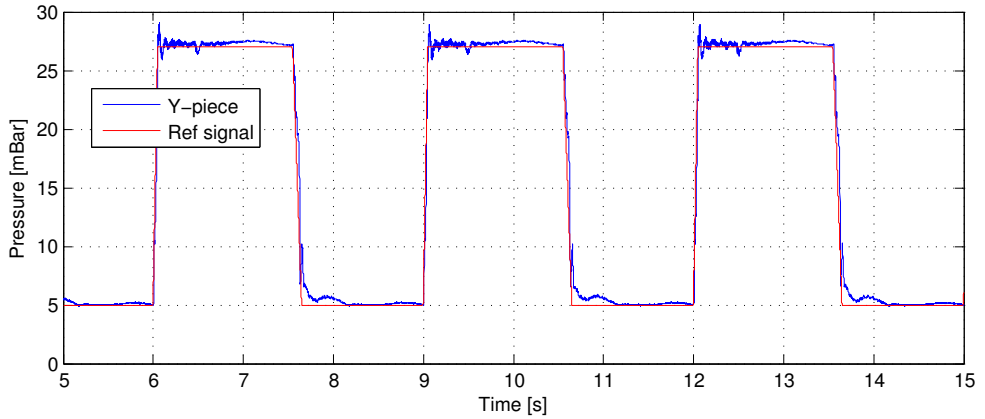

(a) Servo-X

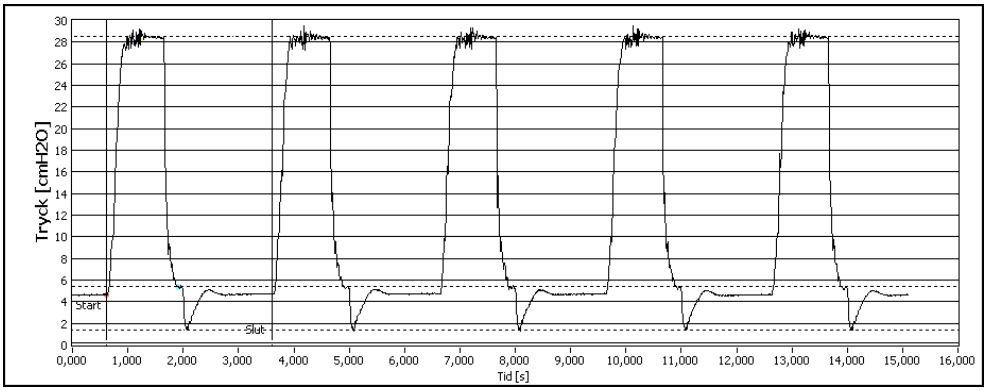

(b) Servo-i

Figure 70: Test with patient id TA2.

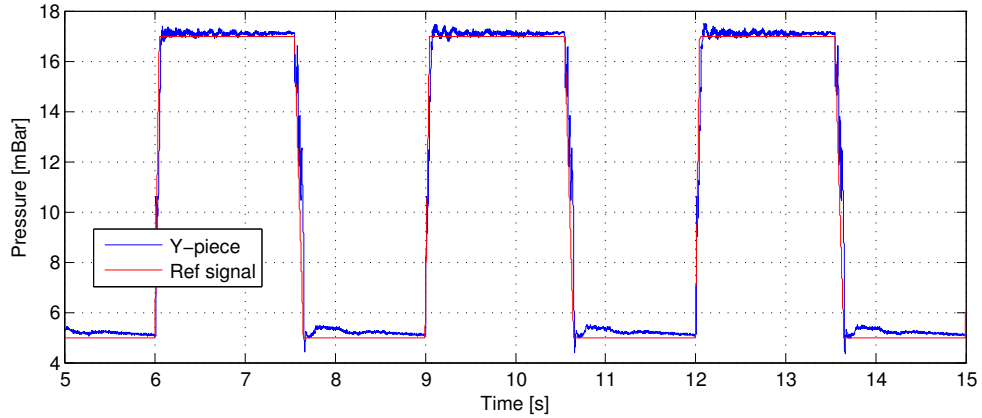

(a) Servo-X

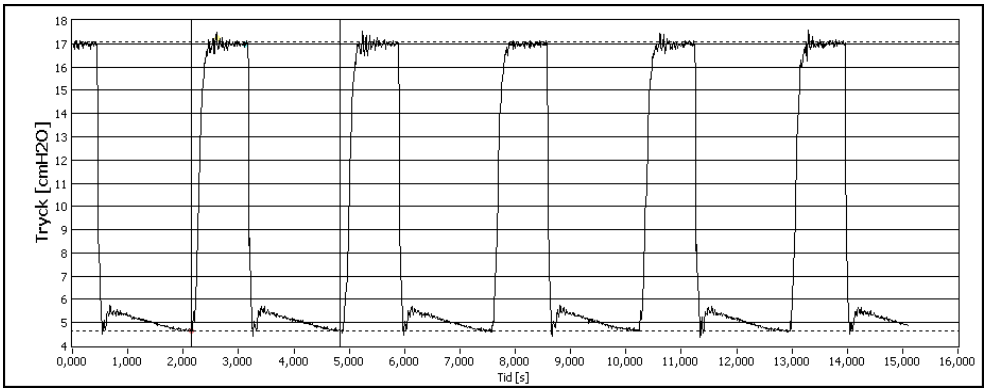

(b) Servo-i

Figure 71: Test with patient id TA3.

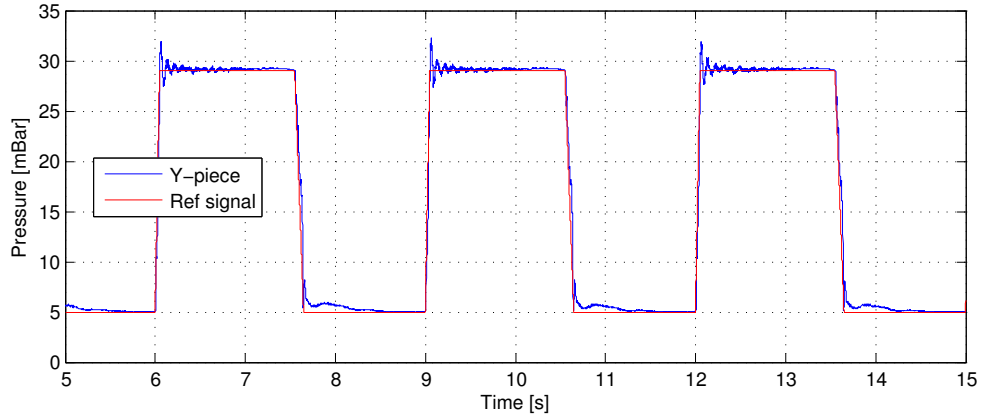

(a) Servo-X

Figure 72: Test with patient id TA4.

5.3.2 Pressure Drop over Expiration Cassette

This test is to verify that the pressure drop over the expiration cassette is according to requirements. Require that pressure drop need to be less than 6 hPa with flow of 30 lpm. According to requirements, the expiration cassette is allowed to half of this [17]. Result in Table 5 give that this standard is managed with margin. The setup of this test can be seen in Appendix A. The result also shows that pressure drop is lower in the developed expiration cassette than the current Servo-i because of the possibility to have active valve. The pressure drop is high when a passive valve is used. This is not as important as the active mode as long the standard is fulfilled.

Mode	Over	Pressure [hPa]
Active	Developed Expiration	0.5
Active	Current Expiration	0.9
Passive	Developed Expiration	2.1
Passive	Current Expiration	0.9

Table 5: Pressure drop over the expiration cassette 30 lpm with uTurn design.

5.3.3 Inspiration Rise and Fall

One of the requirement as to be able to change the flow from 0 to at least 180 lpm in less than 20 ms. The main purpose with this test was to get a rough idea of how fast the valve can be opened and closed. There were no demands for an optimized controlled step response. Figure 73 shows the measured step responses for the opening and closing of the *inspiration globe valve*. As seen, the time it takes from the reference change to a fully open or closed valve is about 5 ms. An inspiration valve with a membrane should have similar step response performance.

5.3.4 Power Consumption

The power consumption was estimated by using the applied voltage and known resistance of the VCM [36].

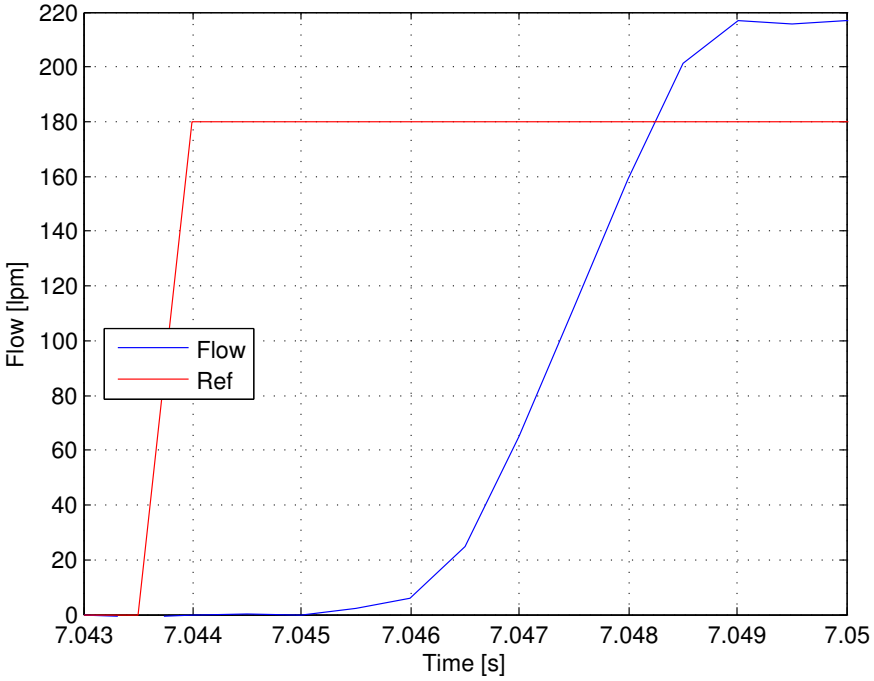

(a) Opening of the inspiration globe valve

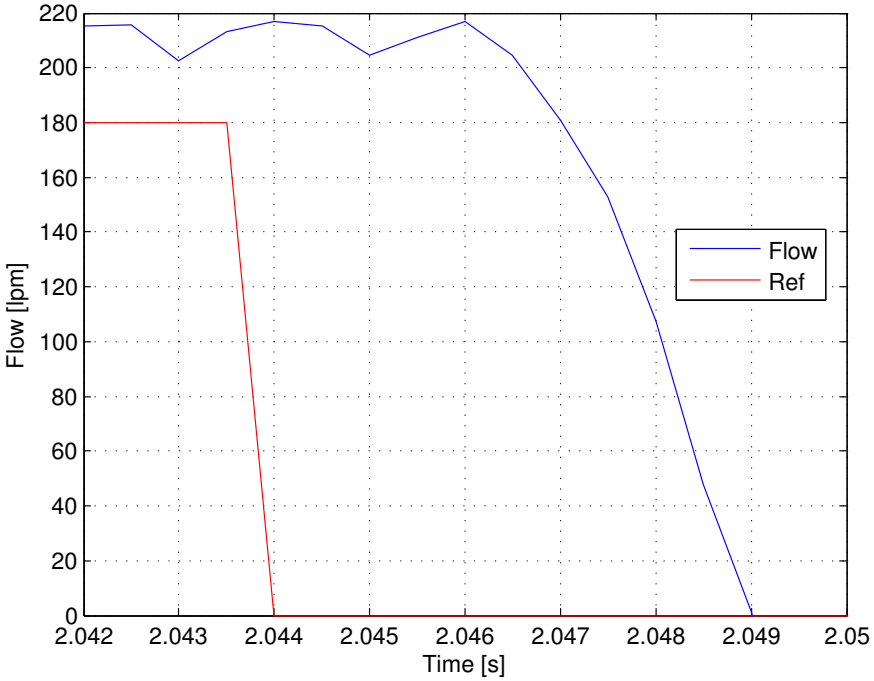

(b) Closing of the inspiration globe valve

Figure 73: Opening and closing of the inspiration globe valve.

What	Pressure [mBar]	Flow [ml/min]	Power [W]
Inspiration	1000	37	0
	500	0	0
	1500	498	0.049
	1500	17	0.14
	1000	180000	1.32
Expiration	120	511	2.00
	50	68	1.88

Table 6: Power consumption for different flows and pressure.

5.4 Cost

According to the requirements [16, 17], the final price for each valve should be less than 500 SEK .

Given the valves developed in this theses it is possible to use same actuator for both valves. This, due to the similarity in force demands. Currently there is a tender of an actuator that would fulfil force requirements [18] that has got an estimated cost of 3.42 USD per actuator. Even if this is not an optimal actuator it gives a guidance to the possible cost of an future actuator for these valves. It is likely that the cost of both the inspiration valve and expiration assembly will be much lower than 500 SEK.

There is no identified possible cost reduction of the inspiration valve, besides the actuator. As of now the inspiration valve consists of more parts than needed, this is due to prototype manufacturing constraints (see Section 3.1.6). Assuming that the valve seat can be made in one part it is believed that the valve seat will not be more expensive than the inspiration valve in the Servo-i.

Expiration assembly in current solution has two major drawbacks. The size of the cassette and the actuator, also the number of parts in the cassette assembly. With this new concept of expiration cassette there is less parts and the size can be reduced. There is also a possibility to have single use cassette with no electronics.

5.5 Discussion

Most of the requirements, on both the ventilator and the individual valves, have been fulfilled. There are a lot of optimizations possible but the important aspect of the thesis has been to prove the possibility to achieve some fundamental demands on a ventilator and its valves. It has been proven that a relatively simple control strategy is capable of good performance on certain patient categories and test cases.

6 Conclusions

The results in this report confirm that the aim of this thesis is fulfilled. All tested requirements are meet. Two of the developed inspiration valve prototypes - the membrane valve and the globe valve - fulfil the requirements and have similar performance. The two developed expiration valves have the required performance and fulfil all tested requirements.

Given that the bandwidth of the valve is measured from input voltage to output flow, both inspiration valves have a bandwidth of approximately 100 Hz. This coincides with the dynamic model of the valve. According to the model, lowering the moving mass or increasing the spring constant, would result in an increased bandwidth. As an example, lowering the mass by half increases the bandwidth to 134 Hz. Changing the electrical properties of the voice coil has an impact on the bandwidth of the valve. According to the model it is believed that the mechanical properties of the valve are predominating.

The expiration valve seat design "Flow" should be used if the investigation shows that it has better water trap functionality than the "uTurn". Performance of the two designs have shown to be similar. The benefit of the "uTurn" design is that it is more suited for manufacturing.

The actuator used in this thesis fulfil all requirements and in some aspects the force characteristics of this actuator is better than required. Hence there is room to optimize a voice coil that could be manufactured at a lower cost and consume less power. Another benefit of a custom made actuator would be that the moving mass of the actuator could be minimized in order to increase the bandwidth of the valves.

One purpose with building the ventilator prototype was to get an idea about the difficulties of designing a control system to the tank based ventilator as a whole and the valves specifically. Considering the relatively basic control strategy used, this ventilator has not shown to be difficult to control. With that said, the control strategy has only been tested on a relatively small number of patient categories and test cases.

The investigation into actuator suspension shows that flexures only are suitable for use in the inspiration actuator. They are not suited for the expiration actuator since the flexures needs to have a low spring constant remain stiff in non-moving direction. The low spring constant which is required to meet the demands of a passive valve.

The investigation of using lumped modelling with modal synthesis, has not been verified in this thesis. Modal synthesis is needed when the flow in the ventilator tubes needs to be modelled. It is important to have a good model of the tubes since the interaction of the tubes and the valves can produce standing waves that may cause the valve to become unstable. The study

has presented arguments that supports the theory that a lumped modelling approach - with modal synthesis - could capture the standing wave behaviour in the the gas chain.

7 Discussion

There are only a few requirements that have not been verified or not finalized.

The inspiration globe valve is exposed to the actuator and this might lead to extra requirements posed on the actuator and valve design. Therefore the inspiration membrane valve is the best suitable valve as of now.

The tests that have not been executed for the expiration valve that were difficult to test. These test were to prove some sub-functionality of the valve. These test included reverse flow and water trap functionality. The leakage test were the only tests that was executed but did not fulfil requirements. The probable cause of this was the use of material in the prototype valve. The valve entire valve made in low density and roughly surfaced 3D-printed plastic. It is likely that this problem can be fixed by manufacturing the valve in a more appropriate plastic material. Another test problem was that it was hard to center the test equipment properly during force tests.

Due to long lead times, an optimized actuator design has not been manufactured. Still it is likely that the cost and size of an optimized actuator will fulfil performance as well as cost requirements.

Simulating fluid dynamics with Solid Works have been the single most time consuming task in this thesis. The simulations did increase the understanding of the valve dynamics in general but the simulation results were not always in line with the measured result on the prototypes. Therefore it is questionable how much of the design optimization that had any substantial impact. Still, without fluid simulations it is unlikely that the same number of requirements had been fulfilled.

The method given by Maquet served as a good guidance throughout the entire thesis project. This guidance has been followed up by the supervisor at Maquet, this ensured that major deadlines were met. The ability to have regular follow-ups with the supervisor were of great benefit in order to fulfil the requirements and overall purpose with the thesis. This resulted in a thesis that many Maquet employees were satisfied with.

8 Future Work

This section highlights aspects of future work that could be done in order to develop the valves further.

The items below are prioritized with the most important items first.

- Actuator - Finish the process with external parter.
- Connection between expiration membrane and actuator - How to attach the actuator rod with the membrane without operators help.
- Gas chain modelling - The MATLAB/Simulink model of the valve and entire gas chain model should be compared to an equal set-up of an real system.
- Control theory - The control algorithm on the implemented ventilator could be improved in general. Mainly it can be made more robust and in order to handle an even wider range of patients. Further investigation could also be made into the choice of feedback to the valve controllers. Using pressure feedback seems to work well but there might be unforeseen problems with this.
- Placement of expiration membrane - Investigate the optimal placement of membrane to get a low pressure drop and still have the check valve functionality.
- The two inspiration valves have no identified performance differences. By studying these valves further it might be possible to identify some performance aspects were one valve proves to be better than the other.
- Expiration membrane - It might be a lot to gain in developing a custom made membrane. The used membrane originated from another type of valves that were available at Maquet.
- Water trap - Test the water trap functionality of the two expiration valve designs.
- Flexure - Manufacture different thickness and perform tests to compare with presented result.

Bibliography

Articles

[1] Jean-Philippe Bacher, Cédric Joseph, Reymond Clavel, (2002), *Flexures for high precision robotics.*, Industrial Robot: An International Journal, Vol. 29 Iss: 4 pp. 349 - 353

[2] James G. Skakoon. *There's the Rub* Mechanical Engineering, January 2009.

[3] N. Chen a, X. Chen b, Y.N. Wu b, C.G. Yang a, L. Xu a. *Spiral profile design and parameter analysis of flexure spring* Elsevier, 2005.

[4] Shorya Awtar, Alexander H. Slocum. *Parasitic Error-free Symmetric Diaphragm Flexure, and a set of precision compliant mechanisms based it: Three and Five DOF flexible torque couplings, Five DOF motion stage, single DOF linear/axial bearing.* MIT Confidential.

[5] A.S. Gaunekar, T. Giiddenhenrich and C. Heiden. *Finite element analysis and testing of flexure bearing elements* ELSEVIER, 1996.

[6] Z. S. Al-Otaibi and A. G. Jack. *SPIRAL FLEXURE SPRINGS IN SINGLE PHASE LINEAR-RESONANT MOTORS* Newcastle University, 20xx.

[7] C.J. Simcock. *Investigation of Materials for Long Life, High Reliability Flexure Bearing Springs for Stirling Cryocooler Applications* Honeywell Hymatic, University of Birmingham, 2007.

[8] Jin-Dong Hwang, Yong-Kil Kwak, Hong-Jung Jung, Sun-Ho Kim, and Jung-Hwan Ahn *Minimization of Modeling Error of the Linear Motion System with Voice Coil Actuator* International Journal of Control, Automation, and Systems, vol. 6, no. 1, pp. 54-61, February 2008

Books

[9] Bertil Jakobson *Medicin Och Teknik* Studentlitteratur, 1987.

[10] Jack W. Lewis *Modeling engineering systems: PC-based techniques and design tools* High Text Publications, Inc., 1994.

[11] Lennart Ljung, Torkel Glad *Modellbygge och Simulering* Studenlitteratur, 2005-2009.

Standard

[12] Swedish standard institute. *Elektrisk utrustning för medicinskt bruk – Del 2-12: Särskilda krav på grundläggande säkerhet och funktion på intensivvårdsventilatorer(ISO 80601-2-12:2011)* Swedish standard, 2011.

[13] Standard. *7396-1 Medical gas pipelines systems Part* Document identity Standard 7396-1

Internal Maquet Documents

[14] Carl Troili. *WGI ventilatorer, en genomgång av tillgängliga tekniker* Maquet, Document identity EVU-124966

[15] Carl Troili. *Patient models and ventilation settings suitable for test* Maquet, Document identity EVU-122916, 2009

[16] Carl Troili. *Specifikation av examensarbete inspirationsventil* Maquet, document identity EVU-130409, 2012.

[17] Carl Troili. *Specifikation av examensarbete expirationsventil* Maquet, document identity EVU-130410, 2012.

[18] A-TON. *Quotation of voice coil actuator*, Quotation no: SKMBT C45212020117360, 2012

[19] Maquet. *Servo-i User's manual* Order No: 65 14 942 E313E.

[20] *A Device for Accurate Tidal Volume Measurement* Master thesis.

[21] Carl Troili. *Expiratory pressure drop whole circuit at 60 lpm*, Test result.

[22] Carl Troili. *Tankar om Tankar*, Reasearch Studie, 2011.

Internet

[23] SolidWorks Help. *Analysis Solvers*, URL `http://help.solidworks.com/2011/english/SolidWorks/cworks/LegacyHelp/Simulation/Design_Studies/Analysis_Solvers.htm`
Retrieved 2012-06-11

[24] MathWorks. *MATLAB*, URL `http://www.mathworks.se/products/matlab/`
Retrieved 2012-06-11

[25] Euler–Bernoulli beam theory, URL http://en.wikipedia.org/wiki/Euler-Bernoulli_beam_equation
Retrieved 2012-04-20.

[26] Wikipedia. *Flexure bearing* URL http://en.wikipedia.org/wiki/Flexure_bearing
Retrieved 2012-04-20.

[27] SolidWorks. *SolidWorks Flow Simulation* URL http://www.solidworks.se/
Retrieved 2012-06-26.

[28] Ian Stokes-Rees *Introduction to FEA with FEMM.* TSS (UK) Ltd, 2004
URL http://www.femm.info/Archives/doc/femmtutor.pdf
Retrieved 2012-05-24.

[29] Al Prost *Picture describing the compliance characteristics of the lung*
URL http://alprost.blogspot.com/2010_12_20_archive.html
Retrieved 2012-04-20.

[30] FEMM. *FEA simulation program.* URL http://www.femm.info
Retrieve 2012-06-27.

[31] John Price *Acoustic Waveguides*
URL http://spot.colorado.edu/~pricej/pdf\%20docs/Acoustic\%20Waveguides.pdf University of Colorado, Boulder
Retrieved 2012-05-28.

[32] Federico Avanzini *Chapter 3. Sound modeling: source-based approaches*
CreativeCommons Attribution-NonCommercial-ShareAlike 3.0 license.
URL http://smc.dei.unipd.it/education/algo4smc_ch3.pdf
Retrieved 2012-05-28.

[33] SolidWorks. *SolidWorks Flow Simulation Instructor Guide* Presentation, 2010 URL
http://www.solidworks.fr/sw/images/content/Training/Flow_Simulation_Instructor_Guide_2010_ENG.ppt
Retrieved 2012-04-02.

[34] BEIKIMCO. *Actuators*, Applications & Product Selection Guide
http://www.beikimco.com/pdf/VCA\%20App\%20Product\%20Guide.pdf
Retrieved 2012-06-21.

[35] Engineers handbook. *frictioncoefficients*
URL http://www.engineershandbook.com/Tables/frictioncoefficients.htm
Retrieved 2012-06-05.

Data-sheets

[36] GeePlus. *Voice coil motors VM3334*, Datasheet,
URL http://www.geeplus.biz/FTPROOT/Voice_Coil_motor_VM3322\%20and\%20VM3334.pdf
Retrieved 2012-04-09

[37] TSI. *TSI 4040*, Datasheet,
URL http://testequipmentandtools.com/acatalog/TSI\%20_4040&4140_layout\%201_Layout\%201.pdf
Retrieved 2012-04-12

[38] Thommen. *Thommen digital manometer HM28*, Datasheet,
URL http://www.ingcapino.com.ar/productos/archivos-pdf/thommen/hm28.pdf
Retrieved 2012-03-30

[39] Honeywell. *Honeywell 40PC Series*, Datasheet,
URL http://datasheet.seekic.com/PdfFile/40P/Honeywell_40PC250G2A01143.pdf
Retrieved 2012-04-09

[40] PC1781. *Pressure sensor*, Datasheet,
URL http://www.maquet.com/content/Documents/Service_ProductEnd-of-Life/SERVOi_SERVEOL_MTS-07-0007_EN_ALL.pdf

[41] Mecmesin. *Mecmesin MultiTest 1-i*, Datasheet,
URL http://www.mecmesin.com/force-testing-products/force-test-systems/computer-controlled-test-systems/multitest-1-i-1kn
Retrieved 2012-04-17

[42] MAXIM. *MAX9736A Evaluation Kit*, Datasheet,
URL http://datasheets.maxim-ic.com/en/ds/MAX9736AEVKIT.pdf
Retrieved 2012-05-08

[43] Bio-Tek Instruments. *VT-2 Ventilator Tester*, User manual,
URL http://www.frankshospitalworkshop.com/equipment/documents/workshop_equipment/manuals/Bio-Tek\%20VT-2\%20Ventilator\%20Tester\%20-\%20User\%20manual.pdf
Retrieved 2012-06-18

[44] Imtmedical. *CITREX H4*,
URL http://www.imtmedical.com/en-us/products/mobiletestingdevices/citrexh4/Pages/index.aspx
Retrieved 2012-06-11

[45] D&E Glidlager Specialisten. *SBT Plain bearing*, Fact sheet
URL http://www.detrading.se/uploads/SBT_SWE\%20uppd_pdf_144.pdf
Retrieved 2012-06-21

[46] Maquet. *Compressor mini*, Fact sheet
URL http://www.maquet.com/content/Documents/DataSheet_OptionAccessory/CompMini_Data_6684417_R05_v0dot0_100406_EN_ALL.pdf
Retrieved 2012-08-10

A Appendix - The different test setup's

Test of Pressure Drop on Servo-i Expiration Cassette

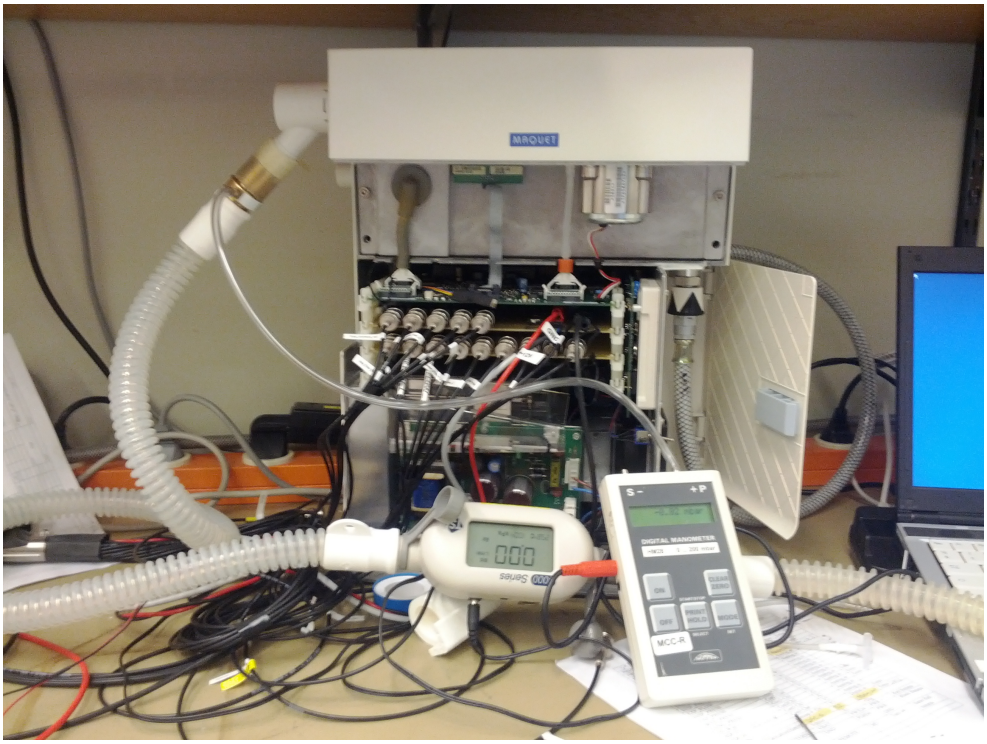

Figure 74: Test set up for measure ΔP on current expiration cassette.

Mecmesin test

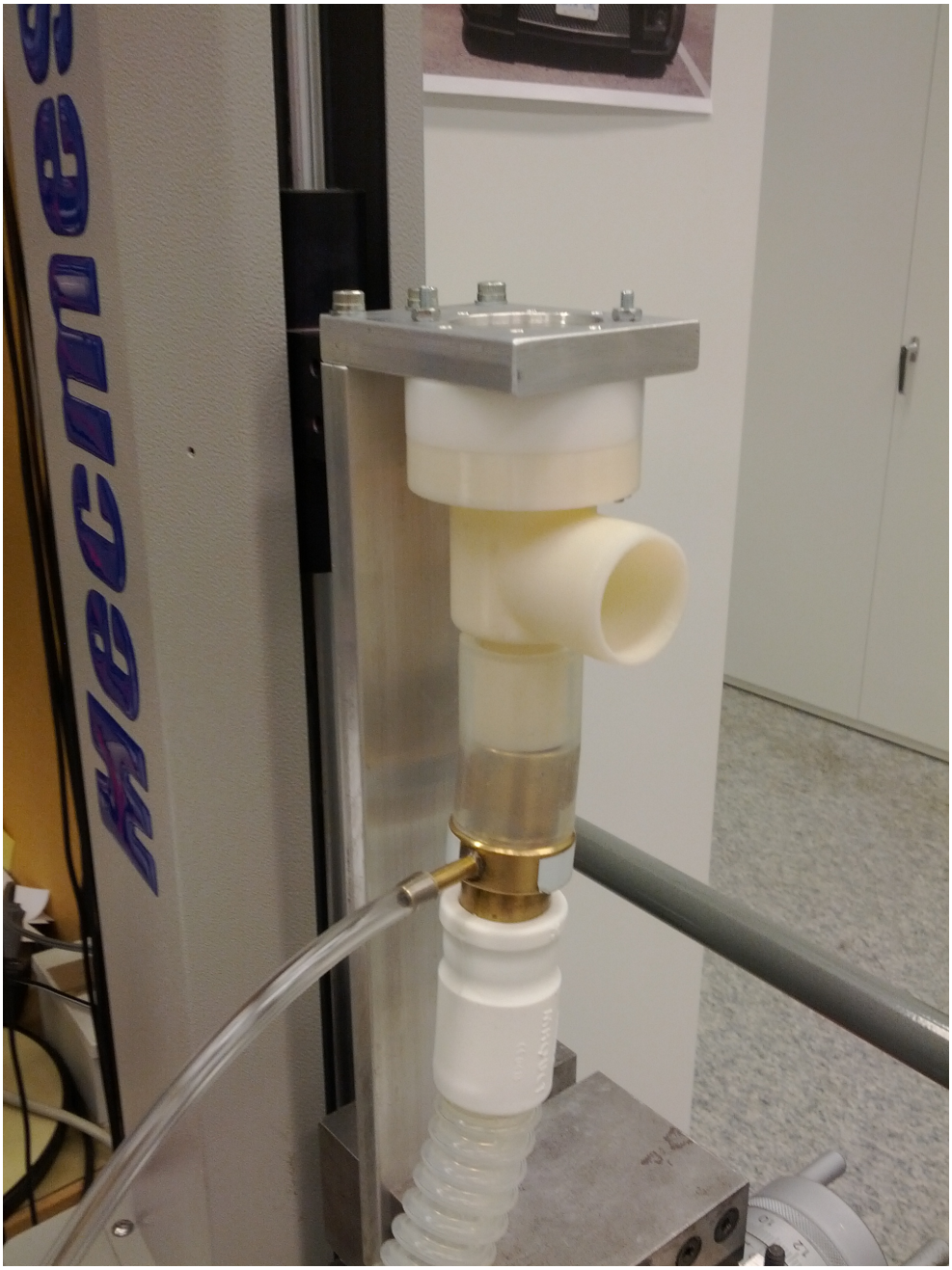

Figure 75: Test setup for expiration in Mecmesin force,flow and pressure test.

Test Set-up at Pressure Controlled Ventilation

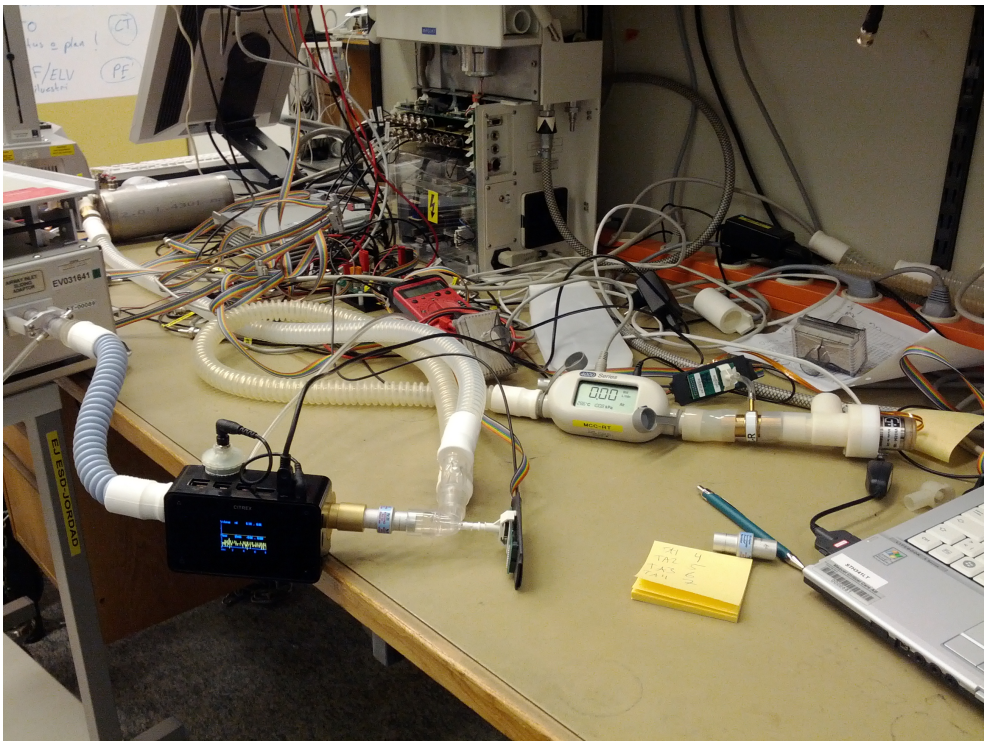

Figure 76: Overview of test set-up with pressure controlled ventilation.

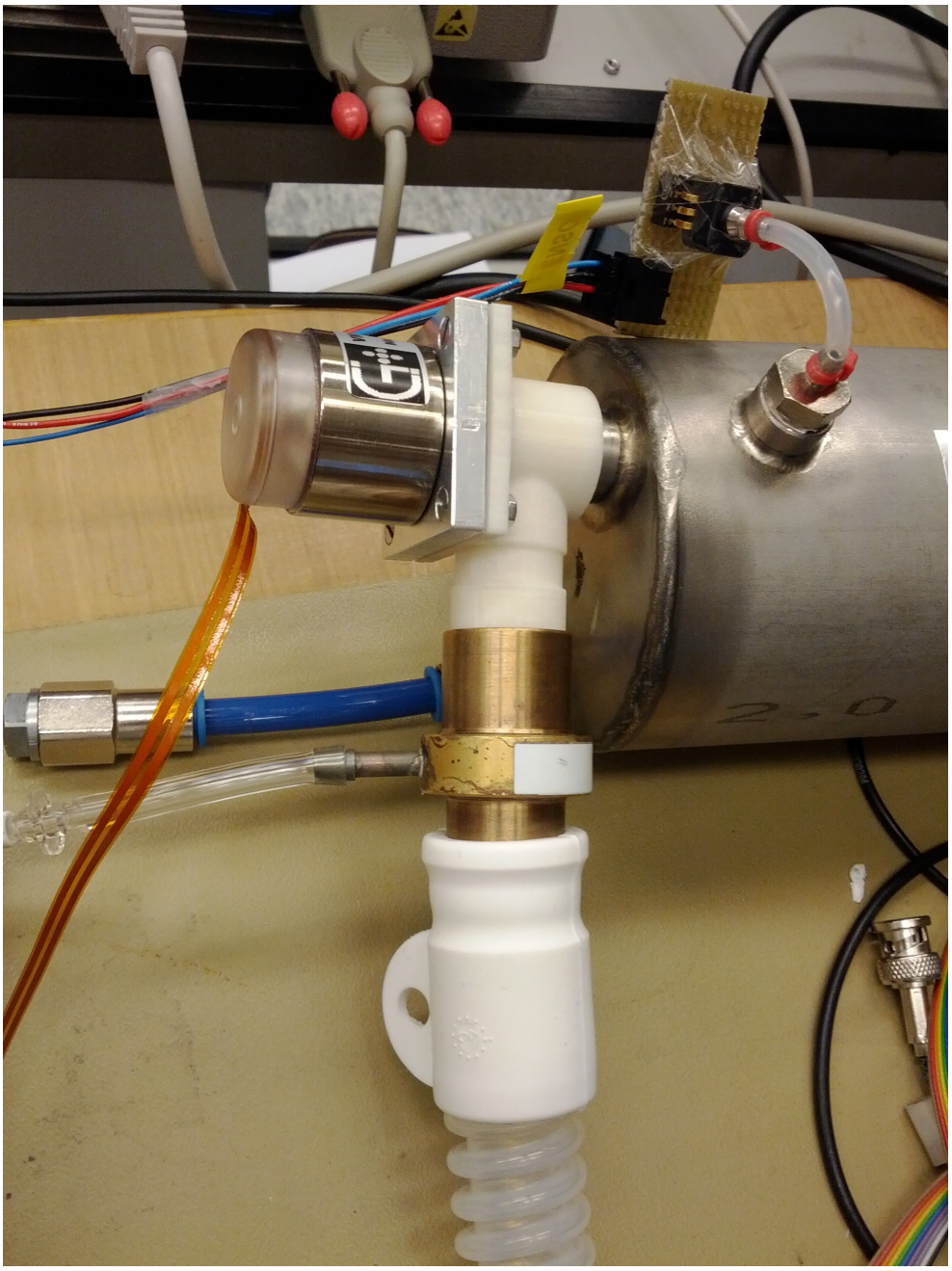

Figure 77: Inspiration valve and tank when testing pressure controlled ventilation.

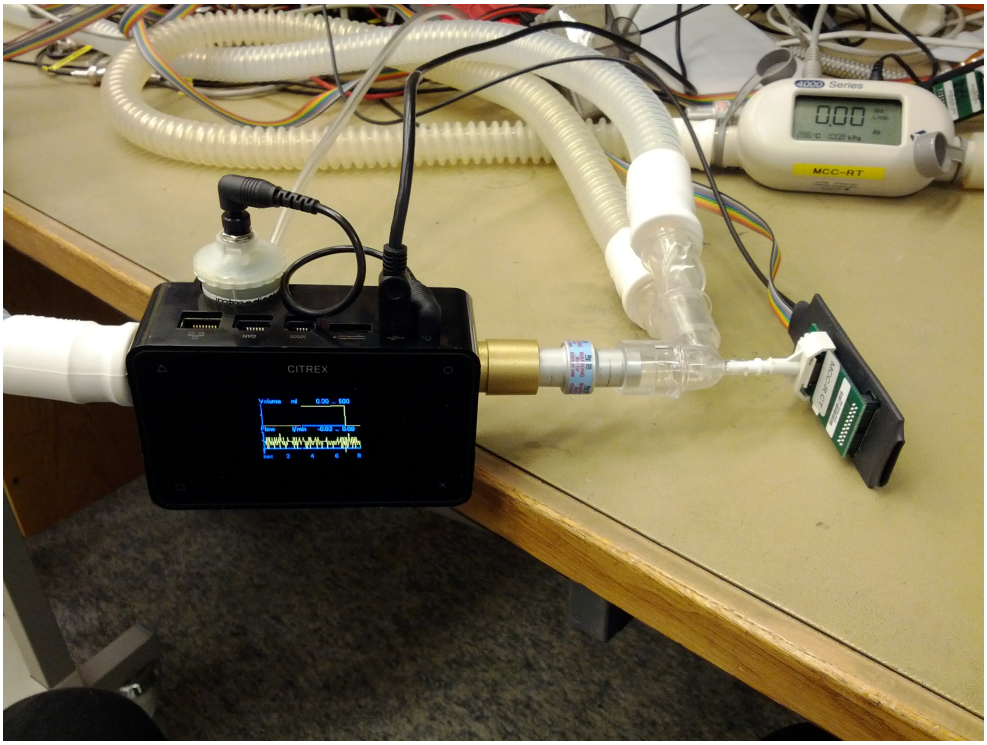

Figure 78: Y-piece when testing pressure controlled ventilation.

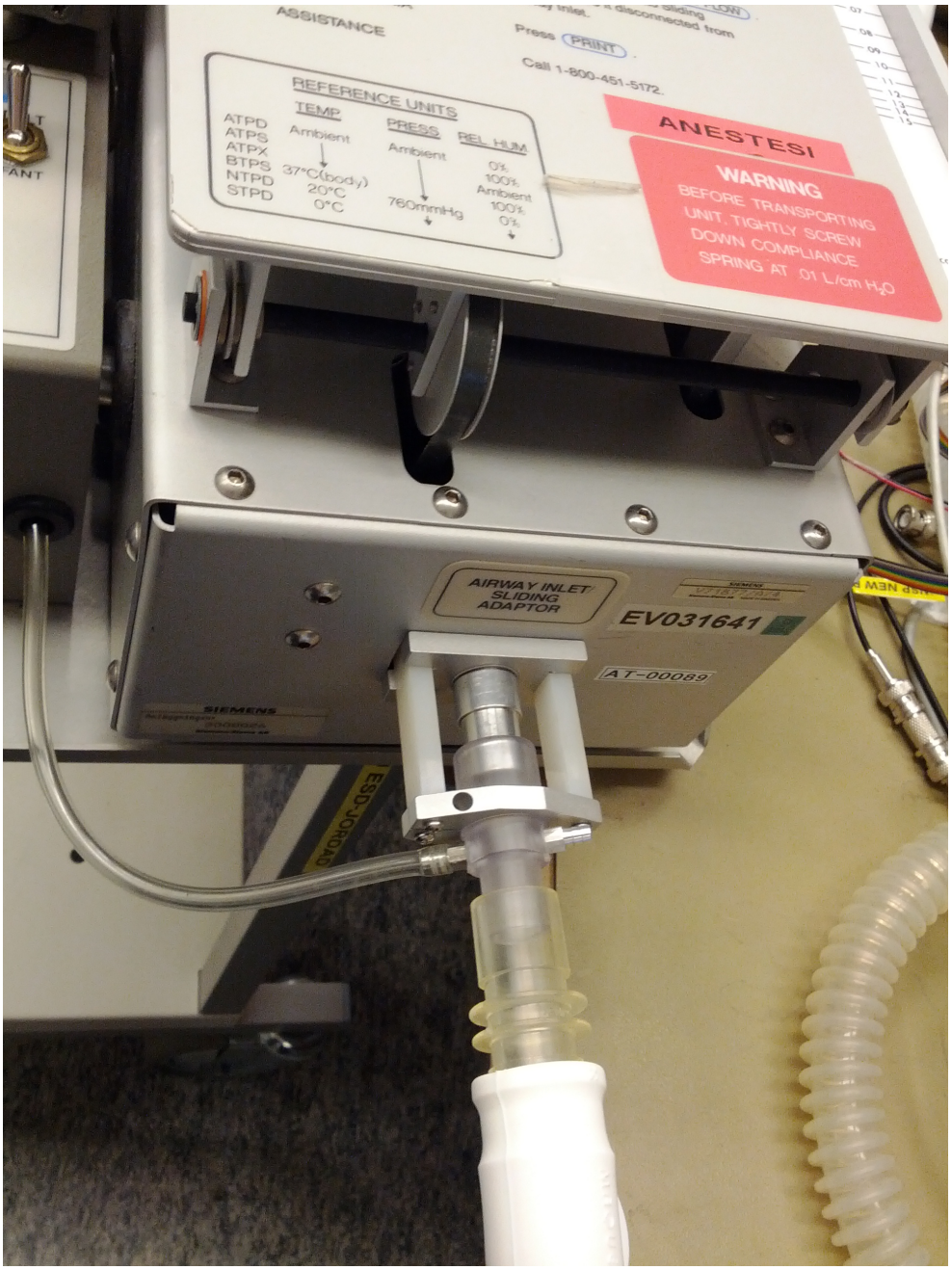

Figure 79: Test lung when testing pressure controlled ventilation.

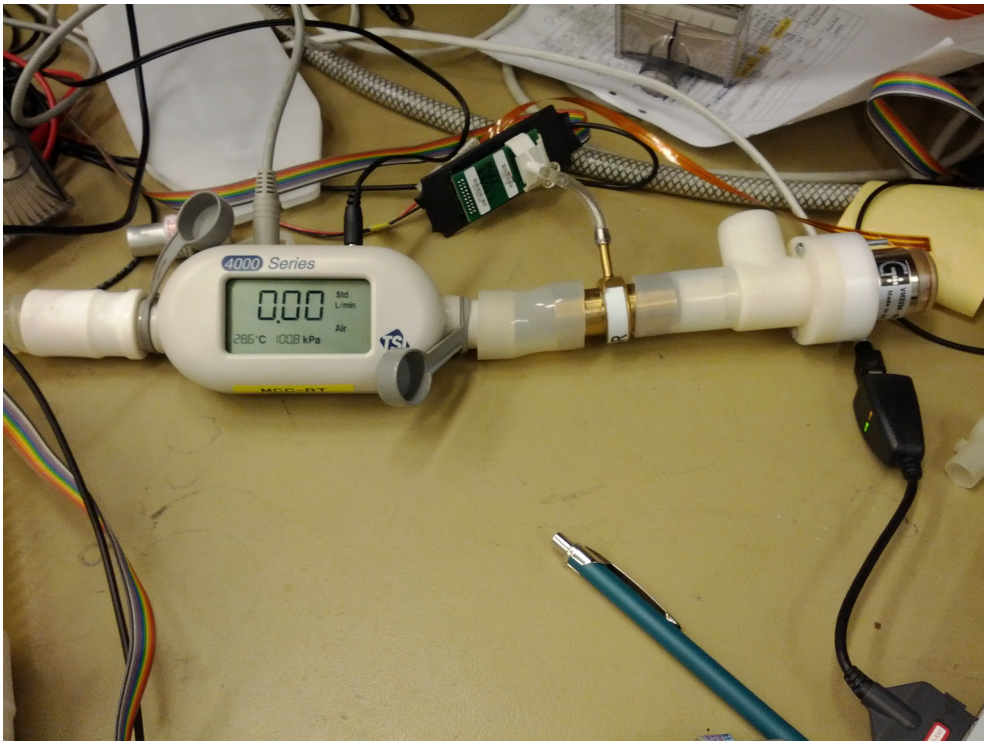

Figure 80: Expiration cassette when testing pressure controlled ventilation.

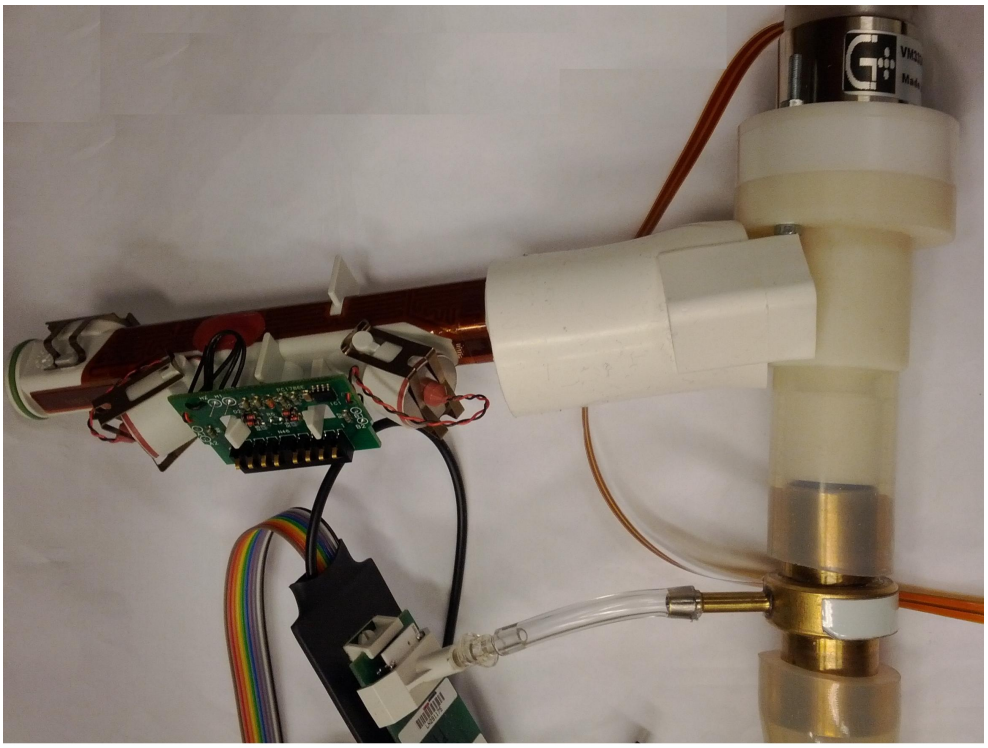

Figure 81: Test pressure drop over expiration cassette with exp flow sensor.

B Appendix - 'uTurn' Test Results

uTurn Mecmesin test results.

Inactive 30 lpm

Gap [mm]	3	1,12	0,6	0,38	0,26	0,21	0,18	0,16	0,12	0,1	0,08
dP [mBar]	2,52	3,3	5,8	11	20	30	40	51	78	106	136
Force [N]	0	0	0,05	0,14	0,28	0,44	0,6	0,77	1,21	1,65	2,14

60 lpm

Gap [mm]	3	1,3	1,12	0,76	0,54	0,42	0,35	0,3	0,25	0,2	0,18	0,16
dP [mBar]	4,24	5	6	11	20	31	39	48	64	94	113	128
Force [N]	0	0	0,03	0,13	0,27	0,41	0,5	0,67	0,9	1,4	1,7	1,9

120 lpm

Gap [mm]	3	2,5	1,69	1,37	1,01	0,82	0,61	0,53	0,47	0,39	0,34	0,31	0,26
dP [mBar]	6,37	5,47	9,7	14	24	34	51	60	71	89	101	109	138
Force [N]	0	0	0,1	0,18	0,32	0,48	0,75	0,9	0,95	1,3	1,4	1,5	1,9

180 lpm

Gap [mm]	3	2,64	1,75	1,4	1,17	0,87	0,73	0,64	0,57	0,48
dP [mBar]	8	10	20	29	39	64	81	100	111	130
Force [N]	0,05	0,08	0,3	0,49	0,65	1	1,2	1,4	1,7	1,85

Active

30 lpm

Gap [mm]	3	1,55	0,85	0,7	0,59	0,34	0,22	0,11	0,07	0,03	0,01	-0,03	-0,03	-0,09
dP [mBar]	0,32	0,99	3,15	4,55	6,02	11,45	18,76	30,76	39,5	52,06	63,76	91,8	102,66	122,24
Force [N]	0	0,08	0,13	0,16	0,19	0,28	0,41	0,61	0,75	0,97	1,2	1,67	1,9	2,27

60 lpm

Gap [mm]	3	1,32	0,93	0,63	0,49	0,35	0,24	0,18	0,1	0,08	0,01
dP [mBar]	1,22	4,78	8,37	14,68	21,17	31,45	45,4	59,35	95,93	104,37	124,53
Force [N]	0,01	0,14	0,21	0,32	0,41	0,59	0,79	0,97	1,54	1,69	1,99

120 lpm

Gap [mm]	3	1,93	1,4	1,12	0,84	0,68	0,51	0,41	0,36	0,35	0,29	0,19
dP [mBar]	4,39	8,36	13,64	19,02	29,4	39,17	57,11	73,72	85,8	88,36	105,75	123,43
Force [N]	0,067	0,2	0,29	0,38	0,58	0,72	0,96	1,2	1,39	1,41	1,69	1,89

180 lpm

Gap [mm]	3	2,22	1,67	1,36	1,11	0,93	0,79	0,7	0,58	0,51	0,42
dP [mBar]	8,94	13,62	20,91	28,74	39,48	51,61	66,54	76,49	88,88	99,83	122,24
Force [N]	0,17	0,29	0,46	0,58	0,79	0,95	1,2	1,4	1,5	1,6	1,86

Leak test

20 mBar

Flow [lpm]	0	0	0	0	0,04	0,12	0,16	0,33	0,63
Force[N]	4,66	1,39	1,24	1,03	0,83	0,67	0,6	0,55	0,46

30 mBar

Flow [lpm]	0	0	0	0,01	0,53	0,54	0,61	0,79	0,99
Force[N]	3,26	2,17	1,65	0,95	0,69	0,71	0,67	0,64	0,61

60 mBar

Flow [lpm]	0,03	0,03	0,03	0,04	0,05	0,17	0,35	0,9	1,15
Force[N]	5,43	4,72	3,7	2,98	2,02	1,52	1,4	1,21	1,18

120 mBar

Flow [lpm]	0,11	0,11	0,11	0,12	0,19	0,23	0,27	0,4	0,99	1,63
Force[N]	5,4	3,79	3,6	3,58	2,94	2,82	2,76	2,55	2,38	2,27

C Appendix - 'Flow' Test Results

Flow Mecmesin test results.

Inactive

30 lpm

Gap [mm]	3	0,96	0,62	0,38	0,22	0,16	0,13	0,07	0,06	0,03	0,01
dP [mBar]	3,14	3,18	4,99	9,7	20,87	37,56	47,88	59,95	77,06	108,53	133,99
Force [N]	0	0	0,05	0,13	0,32	0,58	0,76	1	1,3	1,9	2,38

60 lpm

Gap [mm]	3	2,53	1,42	0,97	0,83	0,52	0,41	0,3	0,18	0,15	0,12	0,1
dP [mBar]	4,39	4,4	4,78	8,64	10,87	21,37	27,31	40,22	65,25	84,59	112,21	126,77
Force [N]	0	0	0	0,08	0,13	0,28	0,39	0,6	1	1,32	1,78	2

120 lpm

Gap [mm]	3	2,04	1,77	1,09	0,8	0,66	0,53	0,49	0,35	0,3	0,27	0,24
dP [mBar]	7,48	7,7	9,56	20,51	32,2	42,02	54,9	59,1	78,35	102,89	112,83	132,61
Force [N]	0,02	0,03	0,09	0,3	0,5	0,63	0,79	0,85	1,1	1,48	1,66	2

180 lpm

Gap [mm]	3	2,69	1,73	1,32	1,04	0,9	0,82	0,77	0,65	0,53	0,44	0,4
dP [mBar]	8,95	10,18	19,64	28,75	41,45	51,3	56,92	63,21	76,27	91,1	107,98	121,36
Force [N]	0,04	0,1	0,31	0,48	0,64	0,81	0,94	1	1,2	1,33	1,55	1,76

Active

30 lpm

Gap [mm]	3	0,66	0,38	0,21	0,15	0,12	-0,05	-0,08	-0,1	-0,13
dP [mBar]	0,29	5,03	10,29	19,87	29,28	37,81	58,55	81,65	96,87	120,19
Force [N]	0,01	0,2	0,3	0,47	0,64	0,79	1,15	1,63	1,98	2,49

60 lpm

Gap [mm]	3	1,68	0,66	0,38	0,21	0,15	0,12	-0,05	-0,08	-0,1	-0,13
dP [mBar]	0,29	0,97	5,03	10,29	19,87	29,28	37,81	58,55	81,65	96,87	120,19
Force [N]	0,01	0,08	0,2	0,3	0,47	0,64	0,79	1,15	1,63	1,98	2,49

120 lpm

Gap [mm]	3	2,56	1,73	1,03	0,8	0,61	0,47	0,42	0,23	0,19	0,15	0,12
dP [mBar]	4,44	5,56	9,94	21,11	31,19	43,78	62,1	70,46	80	96,16		
Force [N]	0,1	0,14	0,26	0,44	0,63	0,82	1,06	1,2	1,31	1,53	1,84	2,1

180 lpm

Gap [mm]	3	2,58	1,62	1,16	0,95	0,78	0,7	0,58	0,57	0,45	0,38	0,28
dP [mBar]	8,12	10,05	19,28	30,53	41,34	52,9	60,52	72,41	75,8	88,81	100	125,41
Force [N]	0,17	0,22	0,44	0,64	0,82	0,99	1,1	1,28	1,3	1,44	1,58	1,97

Leak test

20 mBar

Flow [lpm]	0,96	0,68	0,45	0,38	0,28	0,17	0,06	0,01	0	0
Force[N]	0,76	0,99	1,16	1,32	1,61	1,94	2,36	2,96	3,01	4,931

30 mBar

Flow [lpm]	0,95	0,75	0,66	0,46	0,39	0,23	0,19	0,1	0,03	0,01	0
Force[N]	1,15	1,32	1,39	1,63	1,74	1,97	2,11	2,61	3,02	3,45	4,41

60 mBar

Flow [lpm]	0,83	0,76	0,53	0,4	0,33	0,25	0,15	0,08	0,03	0,02	0,01
Force[N]	2,16	2,26	2,49	2,62	2,87	2,93	3,08	3,57	4,54	5,1	6,72

120 mBar

Flow [lpm]	0,79	0,61	0,49	0,4	0,35	0,24	0,16	0,13	0,07	0,06
Force[N]	3,67	3,89	3,93	4,15	4,27	4,56	4,72	4,84	5,68	6,54

D Appendix - Ventilator to DSpace Connections Chart

Picture/table of connections from system to DSpace multibox.

Device	Connector Simulink	Connector Dspace	Type	Comment
Pressure regulator	DAC4	C2	Analog out	
Actuator insperation	DAC5	B1	Analog out	VM3334
VCM expiration	DAC6	B2	Analog out	VM3334
Tank pressure	Con3 Ch1	b2	Analog in	Honeywell40PC
Insp pressure	Con3 Ch2	Z2	Analog in	PC1781
Exp pressure	Con2 Ch4	V1	Analog in	PC1781
Y-piece	Con2 Ch1	b1	Analog in	PC1781
Flow sensor 1	Con1 Ch3	Y1	Analog in	TSI 4040
Flow sensor 2	Con2 Ch3	X1	Analog in	Net flow sensor

E Appendix - Ventilator Simulink Model

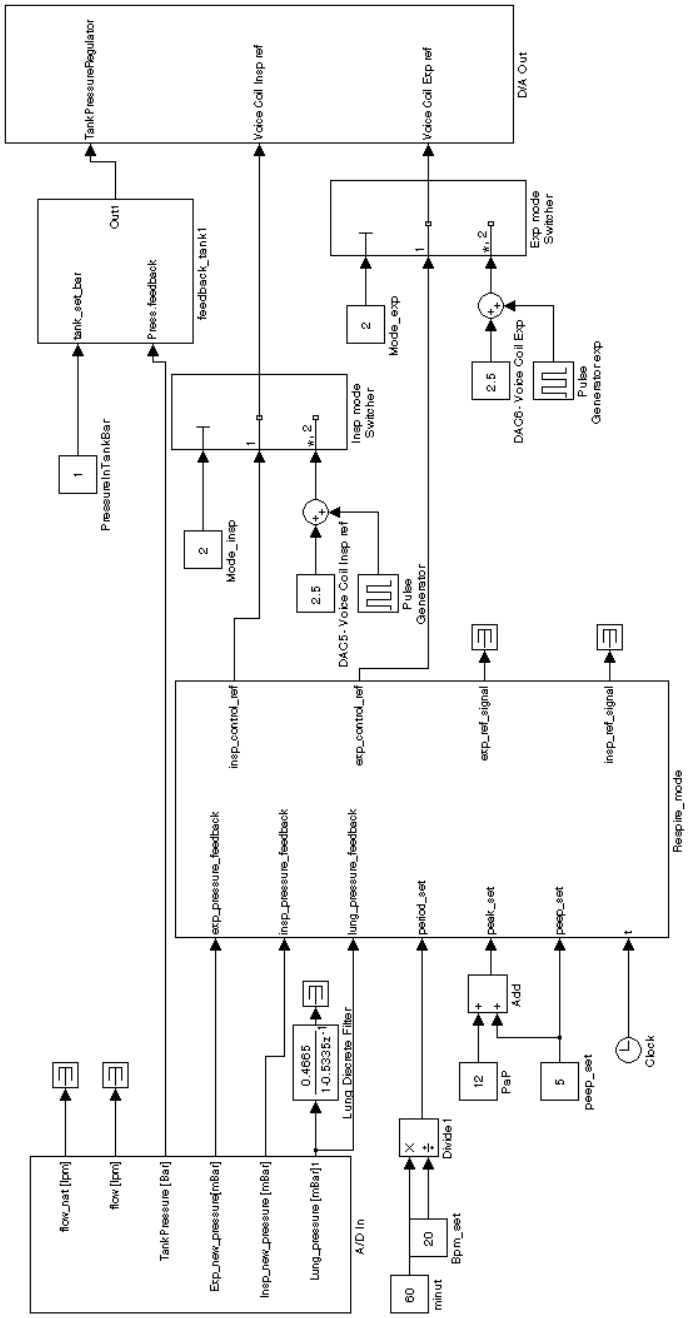

Figure 82: Main view of MATLAB/Simulink blocks.

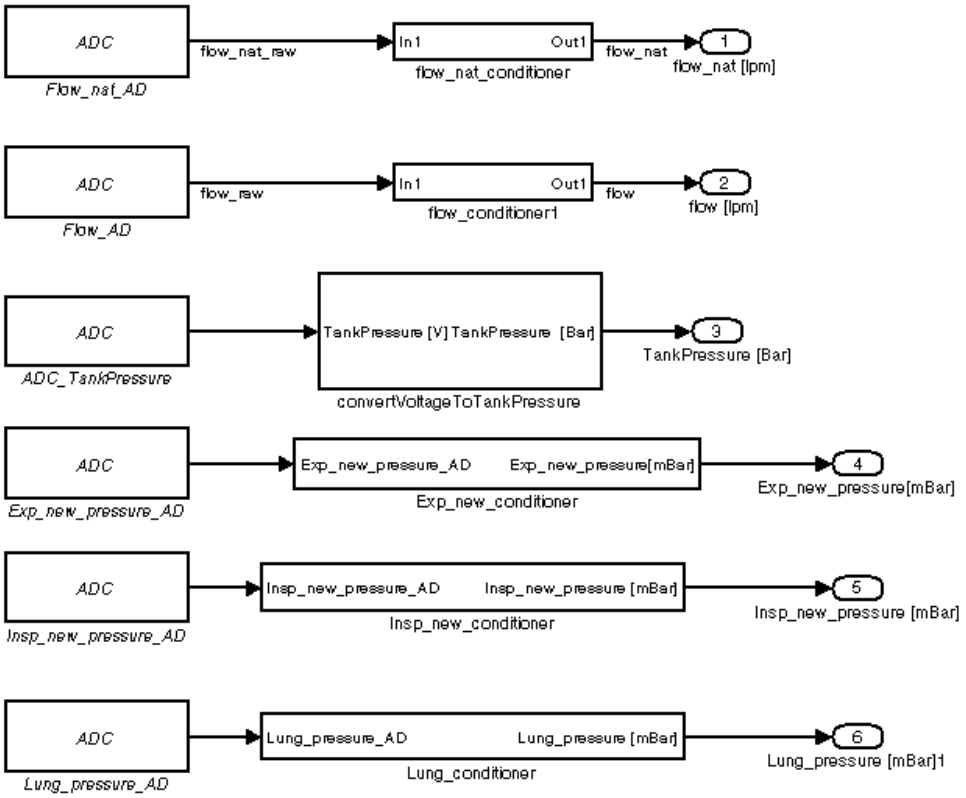

Figure 83: Analogue input to MATLAB/Simulink.

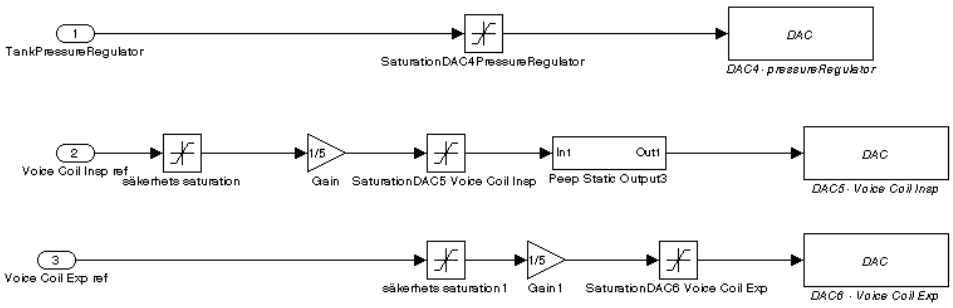

Figure 84: Analogue output from MATLAB/Simulink.

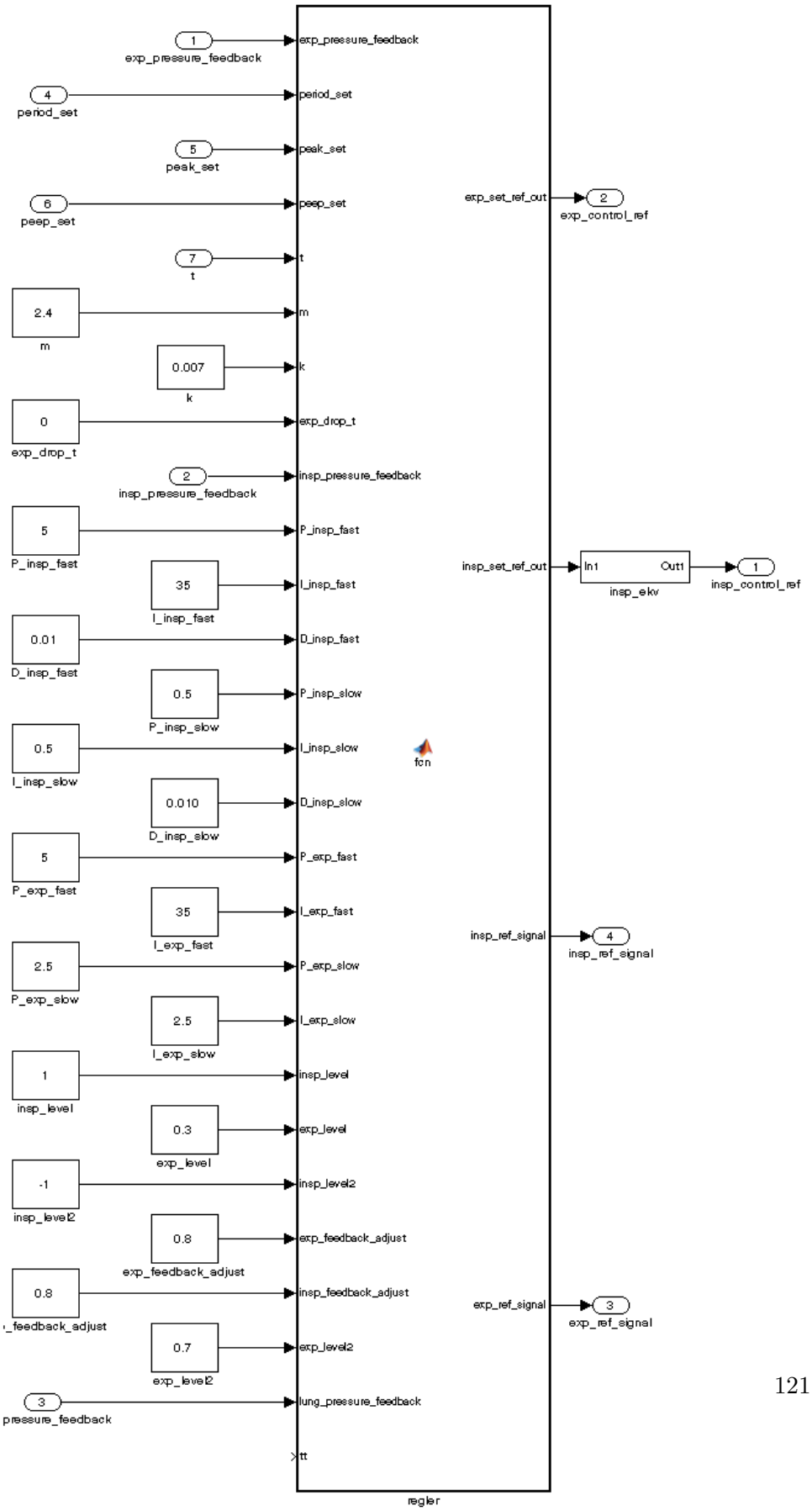

Figure 85: Embedded matlab code controller code can be found in Appendix F.

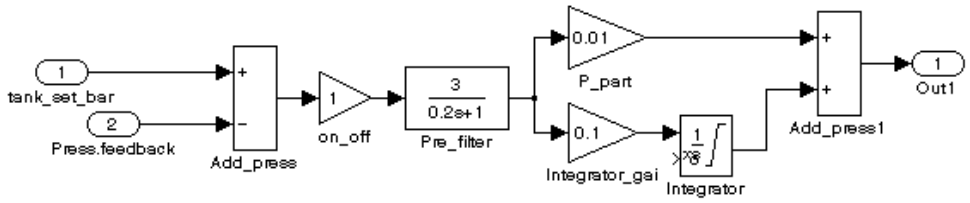

Figure 86: Tank pressure control.

F Appendix - MATLAB/Simulink embedded code

MATLAB/Simulink embedded code

```
function [exp_set_ref_out, insp_set_ref_out, insp_ref_signal, exp_ref_signal] = ...
    fcn(exp_pressure_feedback, period_set, peak_set, peep_set, t, m, k, exp_drop_t, ...
    insp_pressure_feedback, P_insp_fast, I_insp_fast, D_insp_fast,...
    P_insp_slow, I_insp_slow, D_insp_slow, P_exp_fast, I_exp_fast, P_exp_slow, ...
    I_exp_slow, insp_level,exp_level,insp_level2,exp_feedback_adjust,...
    insp_feedback_adjust, exp_level2,lung_pressure_feedback,tt)


persistent old_time time exp_set_ref insp_set_ref I_part_exp I_part_insp;
persistent insp_t exp_t peak_t insp_rise_k exp_rise_k last_phase;
persistent previous_error_insp ;

if isempty(old_time)
    exp_set_ref=0;
    insp_set_ref=0;
    time=0;
    old_time=0;
    I_part_exp=0;
    I_part_insp=0;
    previous_error_insp=0;
    last_phase=1;
end

delta_t=0.0005;
exp_pressure_feedback = exp_pressure_feedback*exp_feedback_adjust + ...
    lung_pressure_feedback*(1-exp_feedback_adjust);
insp_pressure_feedback = lung_pressure_feedback*(1-insp_feedback_adjust) + ...
    insp_pressure_feedback*insp_feedback_adjust;

if time>period_set
    old_time=old_time+period_set;
end
time = t- old_time;

insp_t = period_set*0.5*(1/3);
exp_t = period_set*0.5*(2/3);
peak_t = period_set*0.5;

insp_rise_k = (peak_set-peep_set)/(insp_t*0.1);
exp_rise_k = (peak_set-peep_set)/(exp_t*0.1*(1-exp_drop_t));
% Fas 1
if time<(insp_t*0.9)
    insp_set_ref = peep_set;
    exp_set_ref = peep_set;
    phase=1;
% Fas 2
elseif time<insp_t
    insp_set_ref = insp_rise_k*(time-insp_t*0.9)+ peep_set;
```

```
    exp_set_ref = insp_rise_k*(time-insp_t*0.9) +peep_set;
    phase=2;
% Fas 3
elseif time<(peak_t+insp_t)
    insp_set_ref = peak_set;
    exp_set_ref = peak_set;
    phase=3;
% Fas 4
elseif time<(exp_t*0.1+peak_t+insp_t)
    insp_set_ref = peak_set-exp_rise_k*(time-insp_t-peak_t);
    exp_set_ref = peak_set-exp_rise_k*(time-insp_t-peak_t);
    phase=4;
% Fas 5
elseif time<(exp_t+peak_t+insp_t)
    insp_set_ref = peep_set;%
    exp_set_ref = peep_set;
    phase=5;
else
    phase=1;
end
insp_ref_signal=insp_set_ref;
exp_ref_signal=exp_set_ref;

exp_error=exp_set_ref-exp_pressure_feedback;

insp_error = insp_set_ref-insp_pressure_feedback;


%Controller Exp
if (time>(peak_t+insp_t))||time<(insp_t*0.1)
    P_exp = P_exp_fast;
    I_exp = I_exp_fast;
else
    P_exp = P_exp_slow;
    I_exp = I_exp_slow;
end

%Generate Control Signal Exp
P_part_exp = P_exp*exp_error;

if (last_phase==3)&&(phase==4)
    I_part_exp=0;
elseif (last_phase==1)&&(phase==2)
    I_part_exp=0;
else
    I_part_exp = I_part_exp + I_exp*exp_error*delta_t;
end

%Controller Insp
if (time>(insp_t*0.9))&&(time<(peak_t+insp_t))
    P_insp = P_insp_fast;
    I_insp = I_insp_fast;
    D_insp = D_insp_fast;
else
```

```
    P_insp = P_insp_slow;
    I_insp = I_insp_slow;
    D_insp = D_insp_slow;
end

%Generate Control Signal Insp
P_part_insp = P_insp*insp_error;

if (last_phase==3)&&(phase==4)
    I_part_insp=0;
elseif (last_phase==1)&&(phase==2)
    I_part_insp=0;
else
    I_part_insp = I_part_insp + I_insp*insp_error*delta_t;
end

D_part_insp = D_insp*(insp_error-previous_error_insp)/delta_t;

if (phase==1)||(phase==5)

    control_signal_insp_pressure = insp_level*2.99;
    control_signal_exp_pressure = P_part_exp + I_part_exp;
elseif(phase==4)
    control_signal_insp_pressure = insp_level2*(peak_set- ...
        exp_rise_k*(time-insp_t-peak_t));
    control_signal_exp_pressure = P_part_exp + I_part_exp
elseif(phase==3)
    control_signal_insp_pressure = P_part_insp + I_part_insp + D_part_insp;
    control_signal_exp_pressure = exp_level2*peak_set;
else
    control_signal_insp_pressure = P_part_insp + I_part_insp + D_part_insp;
    control_signal_exp_pressure = exp_level*peak_set;
end

%Save values
last_phase=phase;
previous_error_exp = exp_error;
previous_error_insp = insp_error;

exp_set_ref_out = k*control_signal_exp_pressure+m;
insp_set_ref_out = control_signal_insp_pressure;
```

G Appendix - Sensors Description

This part short describe which sensor have been used in this project and basic facts about them.

Flow sensor

Measure flow are complex and hard to know how good the measurement is. We have used TSI 4040 for flow measurement, that has a four millisecond repose time and accuracy of 2% of the flow rate [37].

Pressure sensor

Measure ΔP is perform by measure the difference between a chosen place and atmosphere. In test we have used Thommen digital manometer HM28 with a reading 20 times/second and measure from zero to 300 mbar [38]. For measure overpressure Honeywell 40PC series have been used with a sensitivity of 266.6 mV/psi and measure up to 15 psi [39]. In the prototype we have used PC1781 to measure with[40]. To get better pressure measurements a piezometer ring was used at all ΔP measurements. This measure pressure in a circular pattern evenly distributed around a pipe [20].

Force measuring test system

Force test have been made with Mecmesin MultiTest 1-i with a 40 N loadcell that have an accuracy of +/-0.1% of full scale [41].

Amplifier

To drive VCM, the class D Maxim MAX9736A Evaluation Kit [42] speaker amplifier was used. Where capacitor C11 and C12 where short-circuit to enable DC output and the amplifier where driven in Stereo mode to be enable to control both valves with same amplifier.

Ventilator tester

We have used passive test lung system from Bio-Tek Instruments VT-2 Ventilator Tester[43]. This system makes it possible to change compliance and resistance of the lung.

Volume/flow sensor

CITREX H4 is a ventilator tester that can measure flow, pressure, volume and more [44].

H Appendix - Suspension of Actuator

When controlling a voice coil friction may become a problem. Particular when you want micrometer precision. Friction occurs among other things from the suspension of the voice coil. This part will go through ways to reduce or eliminate this friction. To make a system that can be controlled better at short movement.

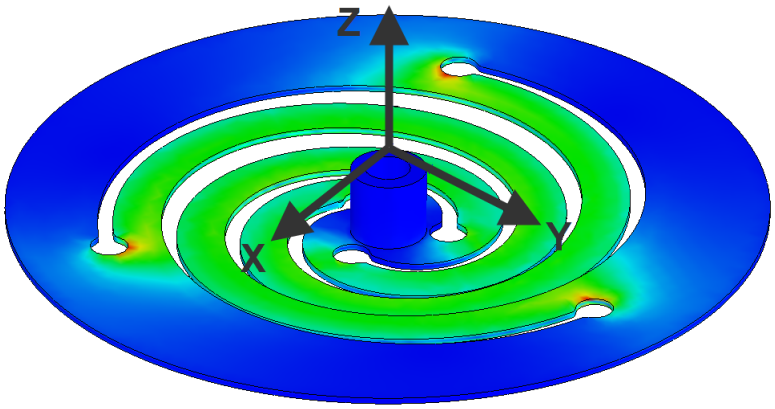

Figure 87: Coordinate system of flexure.

Flexures

A very effective and many times ignored solution is to use flexures[2]. Flexure is a type of linear bearing that allows linear motion by bending the material that the flexures are made by. This gives a non friction suspension that is suitable for small movement. They also require no maintenance and lubrication if they are designed correctly. Flexures are also used in current inspiration actuator. The basic principle can be described with Euler-Bernoulli bending theory see Equation (10) and (11) describe the deflection and (12) is the plastic deflection in the material [25].

$$E \cdot I \frac{d^4 w(x)}{dx^4} = q(x) \tag{10}$$

$$\delta = \frac{F \cdot L^3}{3 \cdot E \cdot I} \tag{11}$$

$$e \approx L \left(\frac{w}{L} \right)^2 \tag{12}$$

Flexures have some limitations where one is stroke length[1]. In this application desirably stroke length is *1.5* and *3.0 mm* for inspiration respective expiration actuator, this is describe more in part *Valve seat design*. Flexures are today uses in many different areas like measurement devices [3, 26]. To get the most out from from the VCM the distance between the coil and permanent magnet shall be as small as possible this is describe in chapter *Actuator design*. Hence the aliment of the coil in x and y see Figure 87 need to be stiff and movement in z as linear as possible. Flexure are where stiff in axial direction[4] but when the material is deformed a torque around z axis is created. That want rotate the axle. To reduce this symmetric arms can be used this use the plastic forces to opposing to each other to reduce this problem [4]. Appearance of this design can be see in Figure 88b. There are many ways to manufacturing flexure sheet-metal stamping, laser cutting, etching and water-jet cutting.

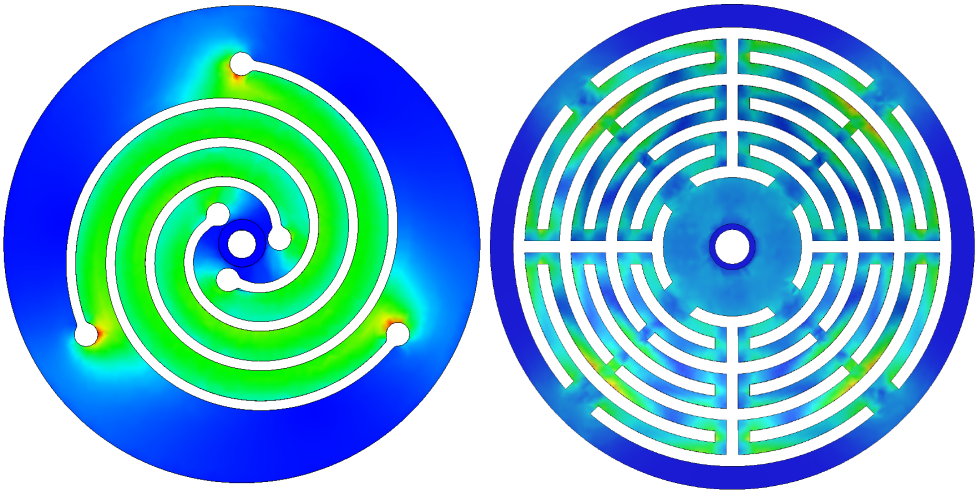

(a) Design 1 (b) Design 2

Figure 88: Flexure for inspiration VCM.

Flexure Design

To analyse the flexure with finite element analysis have show to give good result compared to reality testing [5, 3, 6, 7]. FEA analyse where performed with SolidWorks Simulation. The goal is to find a stiffness of the flexure that are suitable with the resulting valve from *Valve design* and *Actuator design*. To reduce risk of bend fracture the maximum of stress in the material need to be keep to *60*% of the Ultimate Tensile Strength (UTS) [7]. This have been proven with a test cycle of 10^6 times. Different thickness where analysed

to find a suitable stiffness. From the requirements the ventilator need to be enable to handle a G force of *+/-15G* [19].

Inspiration Suspension

From the test in chapter *Valve design* we get that the actuator need to be equipped with a spring that is pre-tensioned. There is a possibility to assembly the flexures with this pretension and not need a extra spring for pretension. From test in chapter *Actuator design* a appropriate spring constant will be something between *2-3 N/mm*. Spring constant will be distributed over two flexures coupled together by the coil see Figure 89. First design is based on equation (13) and (14) and this design can be seen in Figure 88a [3]. Second design seen i Figure 88b made to reduce z torque.

$$x_0 = a \cdot (cos(\phi - \frac{\alpha}{2}) + \phi \cdot sin(-\frac{\alpha}{2})) \tag{13}$$

$$y_0 = a \cdot (sin(\phi - \frac{\alpha}{2}) - \phi \cdot cos(-\frac{\alpha}{2})) \tag{14}$$

Expiration Suspension

According to Swedish standard[12] the ΔP need to be less than *6 cmH20* from the patient connection to outlet of expiration valve, when system have lost power supply . Expiration valve can't stand for more than half of the ΔP. In chapter *Expiration Valve* a selection where made to use valve as check valve. This gives problem when the system has lost power and it's no longer possible to run the valve active. Given this and Equation (15) the maximum force that can open the valve is *0.0462 N*. From test found in appendix B and C give that at *30 lpm* to have a ΔP less than *3 cmH2O* you need to open valve to minimum *1 mm*. Using Equation (16) give that a spring constant for expiration flexure need to be k_{flex} *= 0.0059 N/mm*. This is ten times smaller than spring constant in membrane, that from measurements been define to $F_{membrane}$ *= 0.0343 N/mm*.

$$F_{3cmH20} = P \cdot A \tag{15}$$

$$F_{3cmH20} = x\,(2 \cdot k_{flexure} + k_{membrane}) \tag{16}$$

To evaluate how thin flexure need to be to fulfil requirement for F_{3cmH20} calculations and simulations where made. If you make the flexure as a beam fix in both ends and point load in the middle. Half of F_{3cmH20} can be from $k_{flexure}$, shared on two flexure hence quarter of F_{3cmH20} and δ = 1 mm. Given Equation (17) and b = 1.32 , L = 370mm, F = 3.8mN, E= 210GPa and

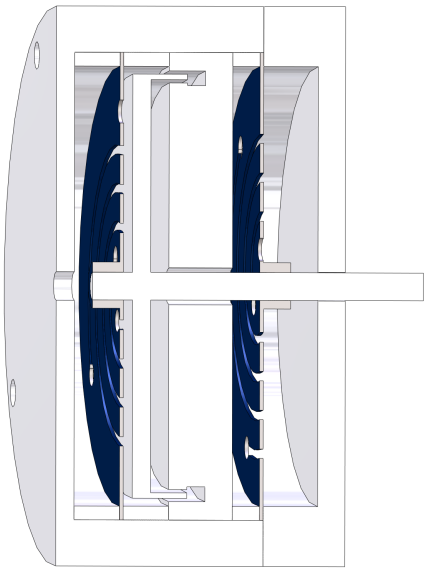

Figure 89: Actuator with two flexures.

$I = b \cdot h^3/3$. This give a thickness of 0.26mm will give right stiffness. Compare this to result from SolidWorks Simulation with *Design 1* and parameters a angle sweep from *200*°to *800*°gives external diameter of 60 mm and 186 mm long arms. This gives a thickness of 0.13 mm to evaluate stiffness x and y direction a force of 0.02 N where applied. This give a stiffness of $k_{flexure_x} =$ 0.0684 N/mm. This is not stiff enough to handle the required g forces.

$$\delta = \frac{F \cdot L^3}{192 \cdot E \cdot I} \tag{17}$$

One other way to solve this is to have plain bearings which have the problem friction and wear. Different bearing material gives different friction coefficient by choosing material with low friction this force can be made relative small and because of the low mass of the coil the wear can be seen as rather small. Using steel in axis and Teflon(PTFE) in the holding part. Friction in this combination is *0.04* [35, 34]. Combining equation (1) and (18) gives the theoretical smallest current differences that can be applied see equation (19).

$$F_f \leqslant \mu F_N \tag{18}$$

$$i = \frac{F_f}{B \cdot l} = \frac{m \cdot g \cdot \mu \cdot F_N}{B \cdot l} \tag{19}$$

Finite Element Analysis of Flexures

To make it less complex to simulate there have been proven you can simulate only one flexure [3]. And if you whan't more than one in final assembly you multiply with wanted numbers of flexures. First design where sweep from *50°*to *540°*with a = *1 mm* thick cut and α = *0.035 m*. Second design seen in Figure 88b has cut and arm of *1 mm*. Analysis where preformed with different thickness to find a suitable stiffness. This was preformed in SolidWorks Simulation where stress and displacement as output result seen in Figure 90 and91. Material that has been used is Steel 1045 cold drawn. Both design's have same external diameter *42 mm* and axial hole of *3 mm*.

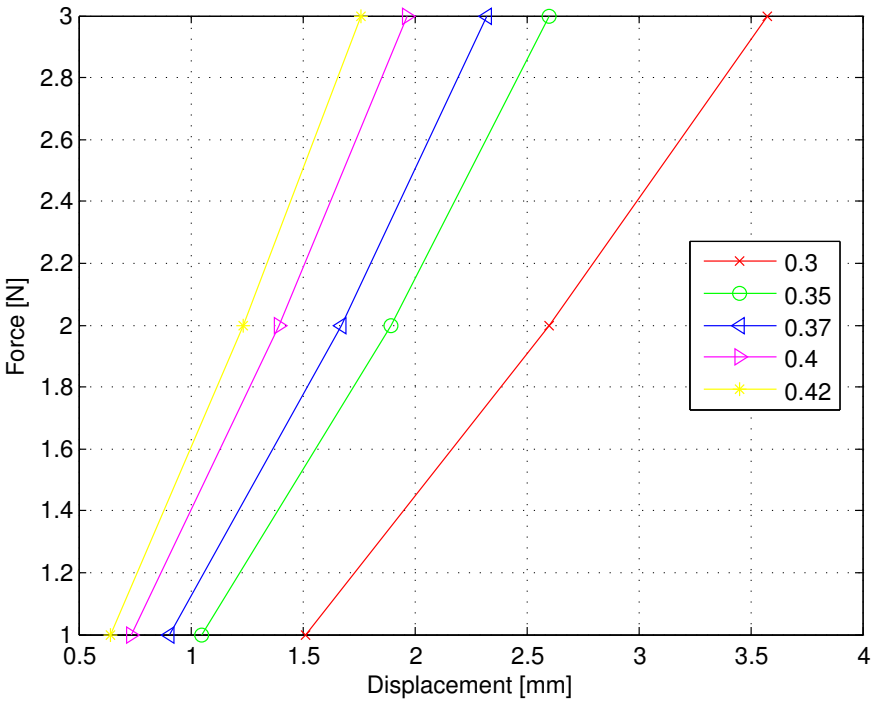

(a) Design 1: Test for different thickness of flexure.

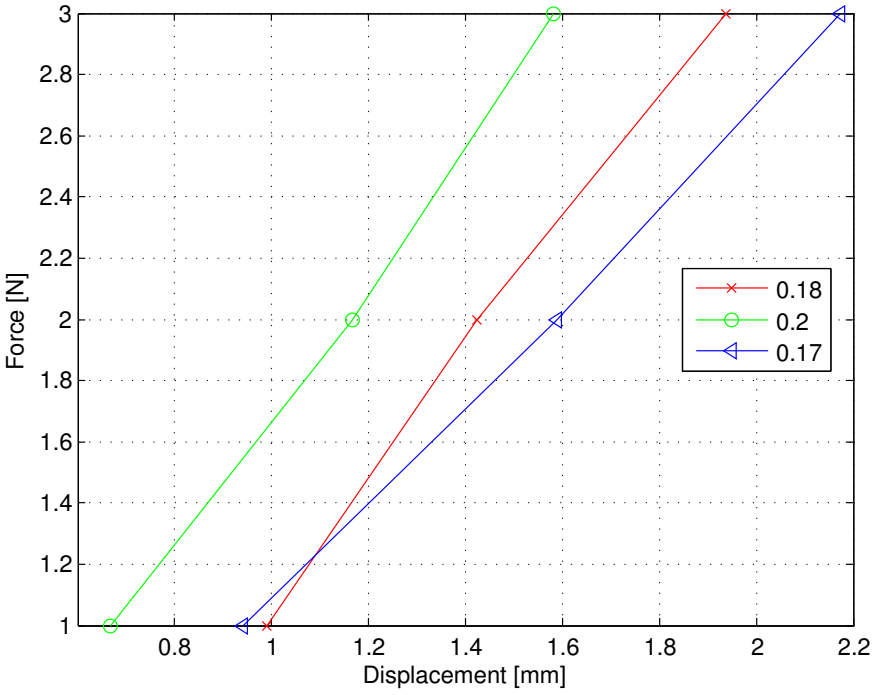

(b) Design 2: Test for different thickness of flexure.

Figure 90: Result from Finite Element Analysis of Flexures.

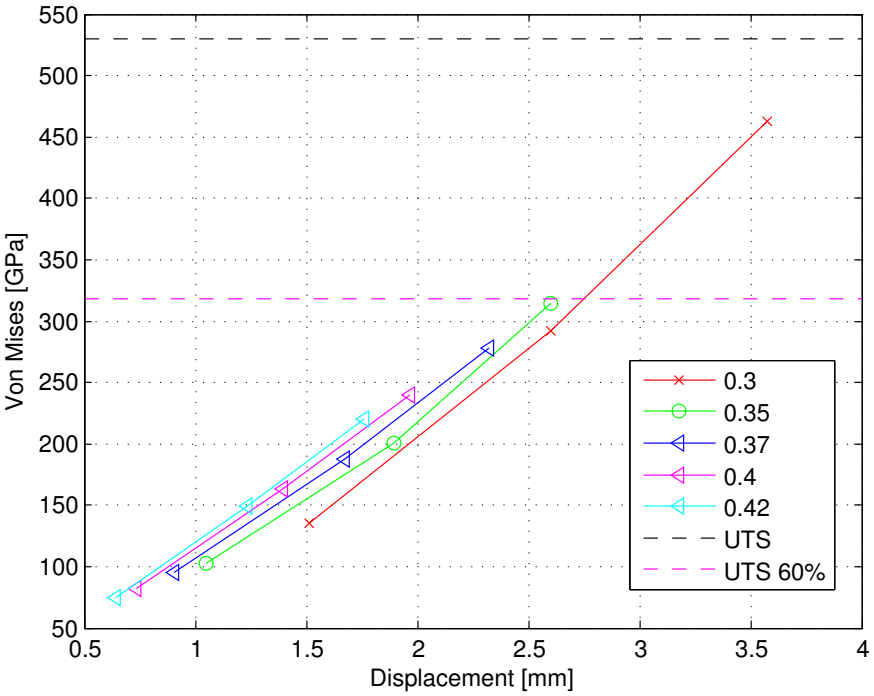

(a) Design 1: Von Mises stress in material.

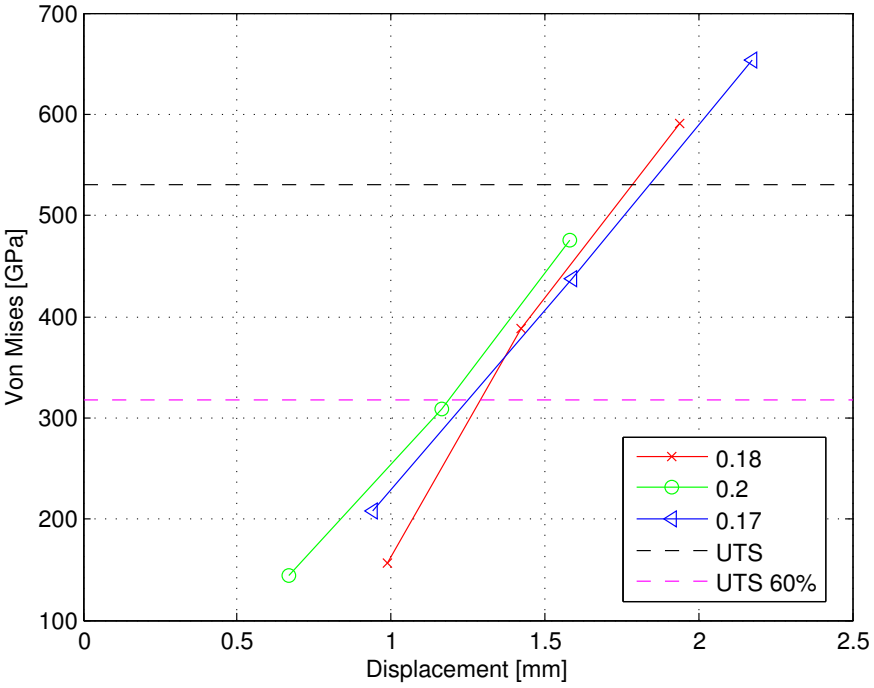

(b) Design 2: Von Mises stress in material.

Figure 91: Result from Finite Element Analysis of Flexures.

Discussion

Result from FEA test show in Figure 91a shows that Design 1 have low stress maximum compared to *Design 2* shown in Figure 91b. With design 1 a thickness of *0.3 mm* have a stress level that are close to the 60% of UTS. Thickness over this will be suitable to use in inspiration actuator. As see in Figure 90a stiffness are between *1* to *1.5 N/mm*. To proven that simulation correspond to reality next step will be to manufacturing those and measure stiffness. If need of smaller diameter it's possible be reduced diameter and still have similar stiffness by chose thinner material and still have stress max smaller than 60% of UTS. *Design 2* have very high stress levels and are not suitable for low stiffness and are not a good option for this purpose. If there a need to reduce the torque it's possible to place flexure *Design 1* reversed to each other and in this way reduce the torque. Expiration suspension with plain bearings is a more straightforward way to go and here use Steel and Teflon, this give little friction force. If skip to use valve as check valve. Place the zero point of the membrane 3 mm from the valve seat. The develop flexure *Design 1* for the inspiration actuator will be suitable design to use with some modification to find an optimal stiffness and stress level.

I Appendix - Implemented Gas Chain Model

An overview of the gas chain model is seen in Figure 92. The model runs and produces results that are within the range of reason. There were not enough time to verify this model any further. The main model building blocks are: voice coil to the inspiration valve, the inspiration valve seat, the inspiration tube, lung and expiration tube. The input to the model is the voltage to the voice coil.

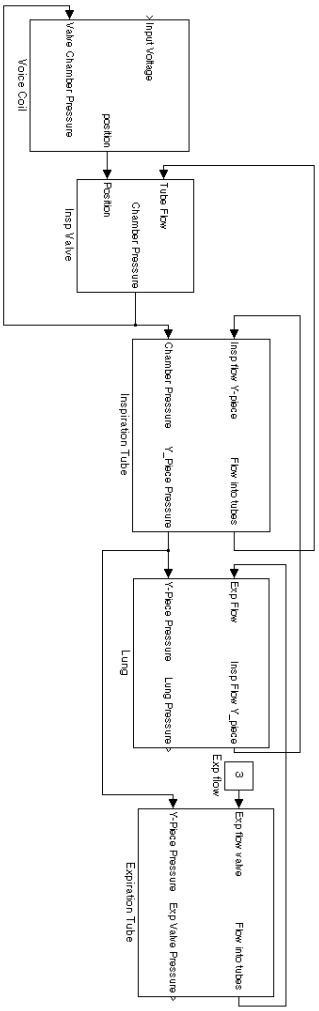

Figure 92: An overview of the gas chain model.

Voice coil

The model of the voice coil is shown in Figure 93. This voice coil is connected to the inspiration valve seat. The voice coil itself is divided according to the different states in the voice coil. The voice coil model has two inputs, the voltage to the voice coil and the valve chamber pressure.

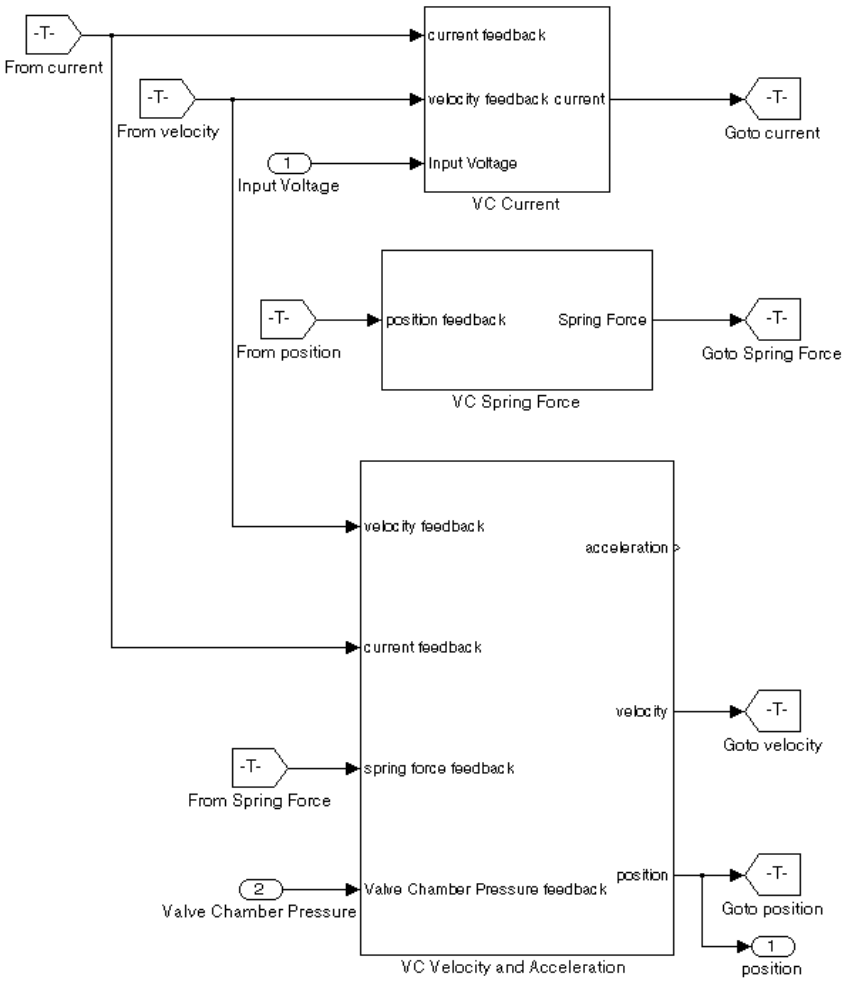

Figure 93: The simulink model of the Voice coil.

The current state equations are illustrated in Figure 94.

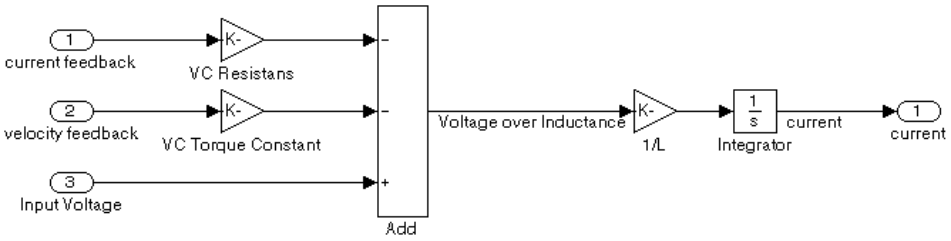

Figure 94: The current state model.

The spring force state equations are illustrated in Figure 95.

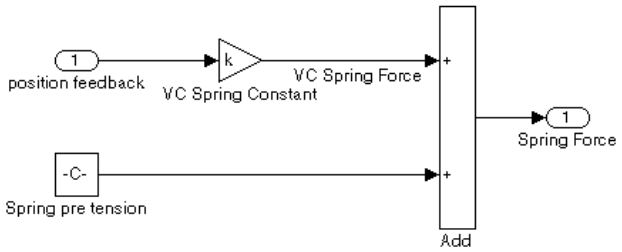

Figure 95: The spring state model.

The position and velocity state equations are illustrated in Figure **??**.

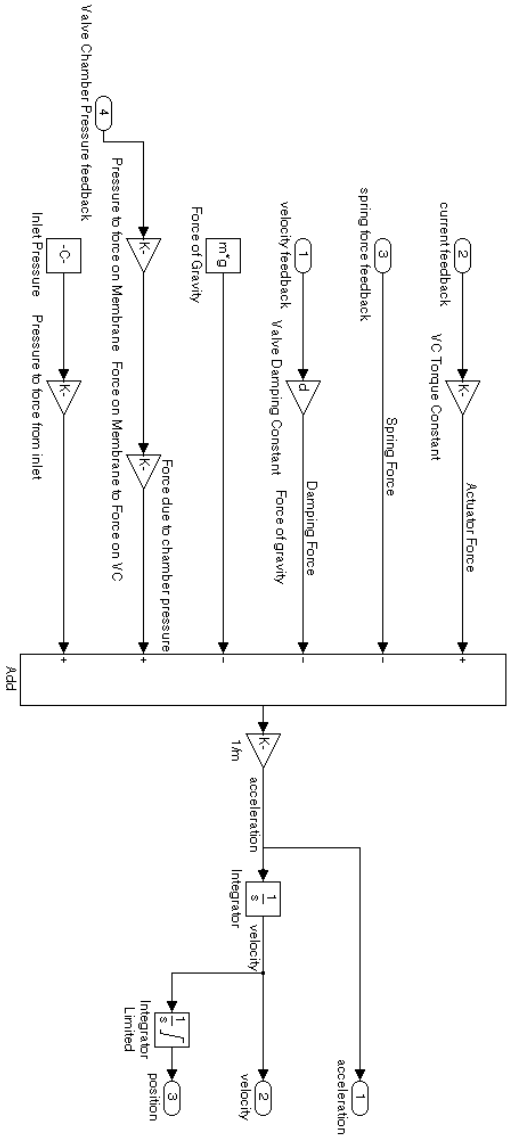

Figure 96: The position and velocity state model.

Inspiration Valve Seat

The valve seat equations are illustrated in Figure 97. The input to this model is the flow in the tubes and the position of the voice coil. The flow into the valve is a linear function of the position of the voice coil. This is one of the major simplifications in the model. The valve seat chamber is modelled as having a compliance resulting in a valve chamber pressure as output.

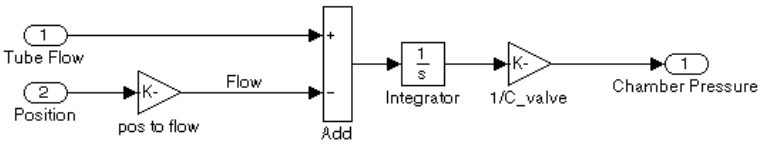

Figure 97: The model if the inspiration valve seat.

Tubes

Both the inspiration tube and the expiration tube are made up by eight RLC-tube sections seen in Figure 98. The difference between the inspiration tube and the expiration tube are the inputs and outputs from the tubes. The inputs and outputs for each tube can also be seen in Figure 92. The inspiration tube has - the flow out of the tube as well as the pressure at the valve chamber - as inputs. The outputs from the inspiration tube are the flow that is present at the inlet to the tube as well as the pressure at the Y-Piece. The Y-Piece is where the lung, the expiration tube and the inspiration tube meet.

The expiration tube has the flow out of the tube as well as the pressure at the Y-Piece as inputs. As of now the out of this tube is set as a constant of 5 lpm. The outputs from the expiration tube are the flow that is present at the inlet to the tube as well as the pressure at the end of the tube.

The inlet of the inspiration tube is defined as the end that is connected to the inspiration valve. The inlet of the expiration tube on the other hand is defined as the end that is connected to the Y-Piece.

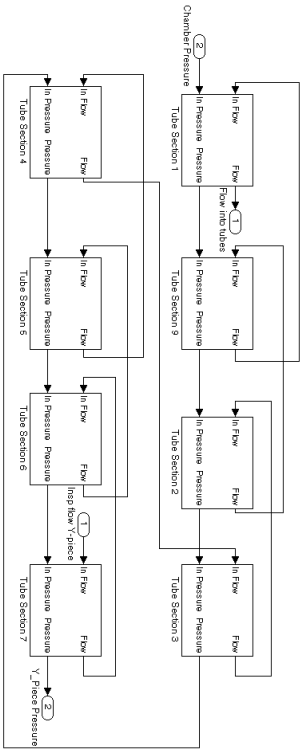

Figure 98: The tube that consists of eight coupled RLC-oscillators.

Each tube section, i.e RLC-oscillator is shown in Figure 99. The inputs to this system are the pressure present at the previous section as well as the flow present in the next section. The outputs from this system are the flow and the pressure, present at this tube section.

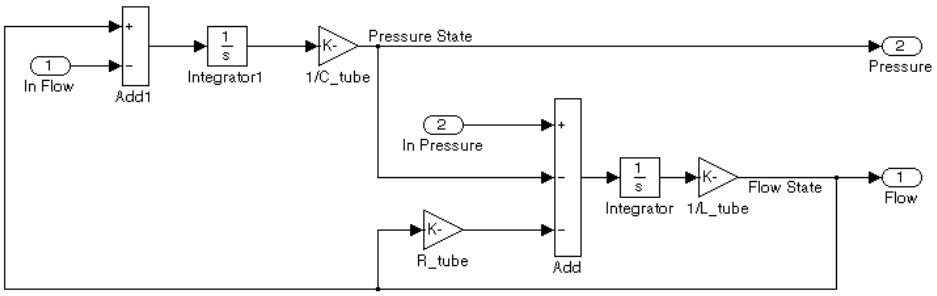

Figure 99: The RLC-oscillator.

Lung

The lung is modelled as an RC-circuit and is seen in Figure 100. The inputs to this model is the current flow into the expiration tubes as well as the pressure present at the Y-Piece. The output from this model is the pressure in the lung as well as flow present at the outlet to the inspiration tube.

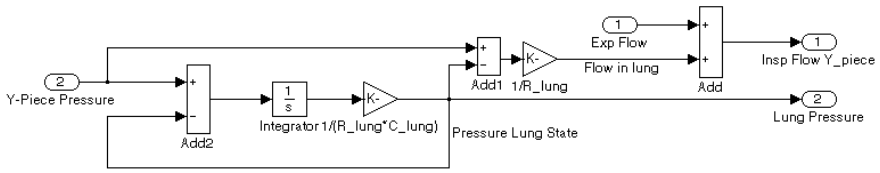

Figure 100: The simulink model of the lung made up by a RC-circuit.

J Appendix - Ventilator Prototype

Pictures of ventilator prototype concept.

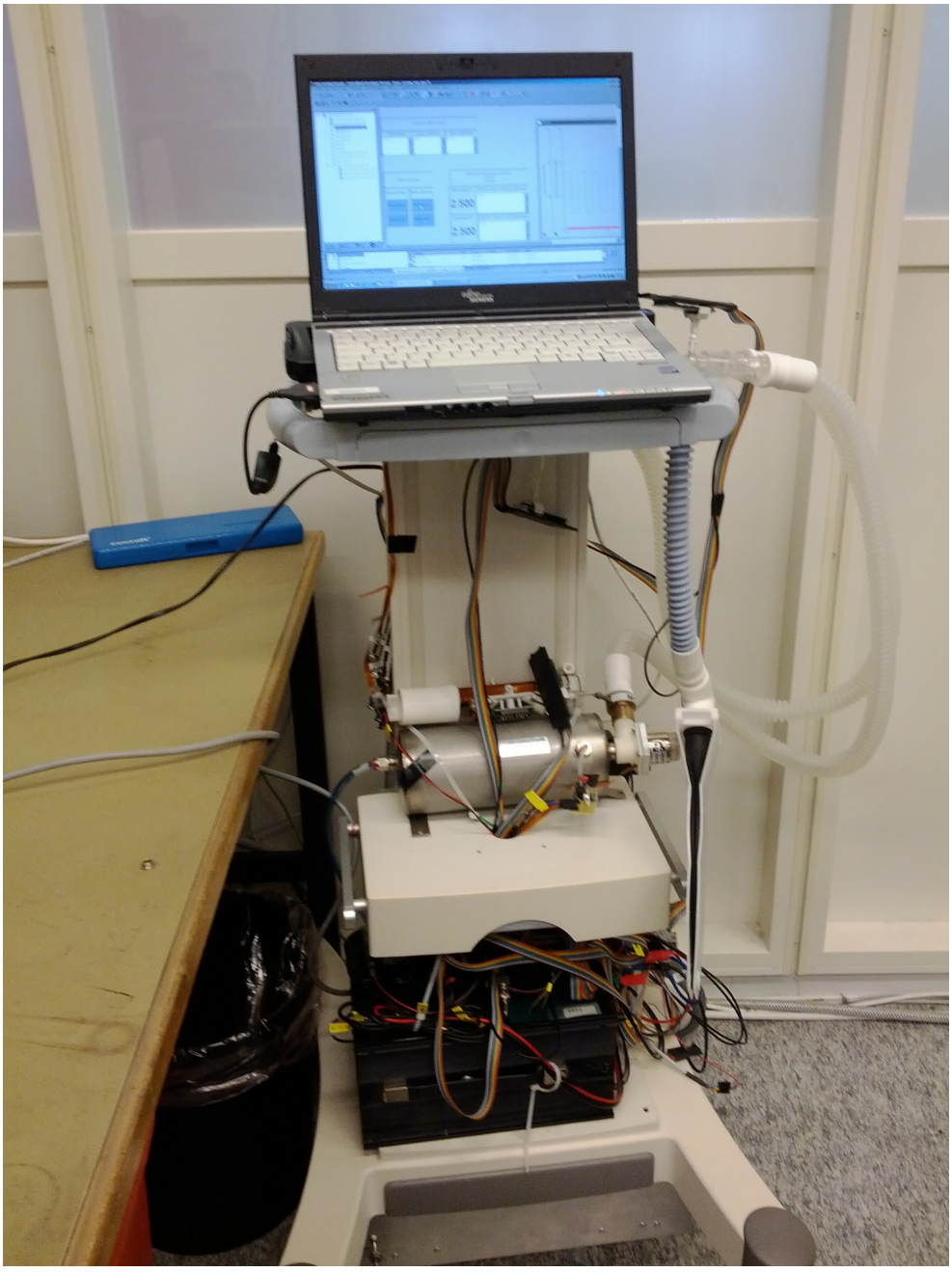

Figure 101: Prototype ventilator.

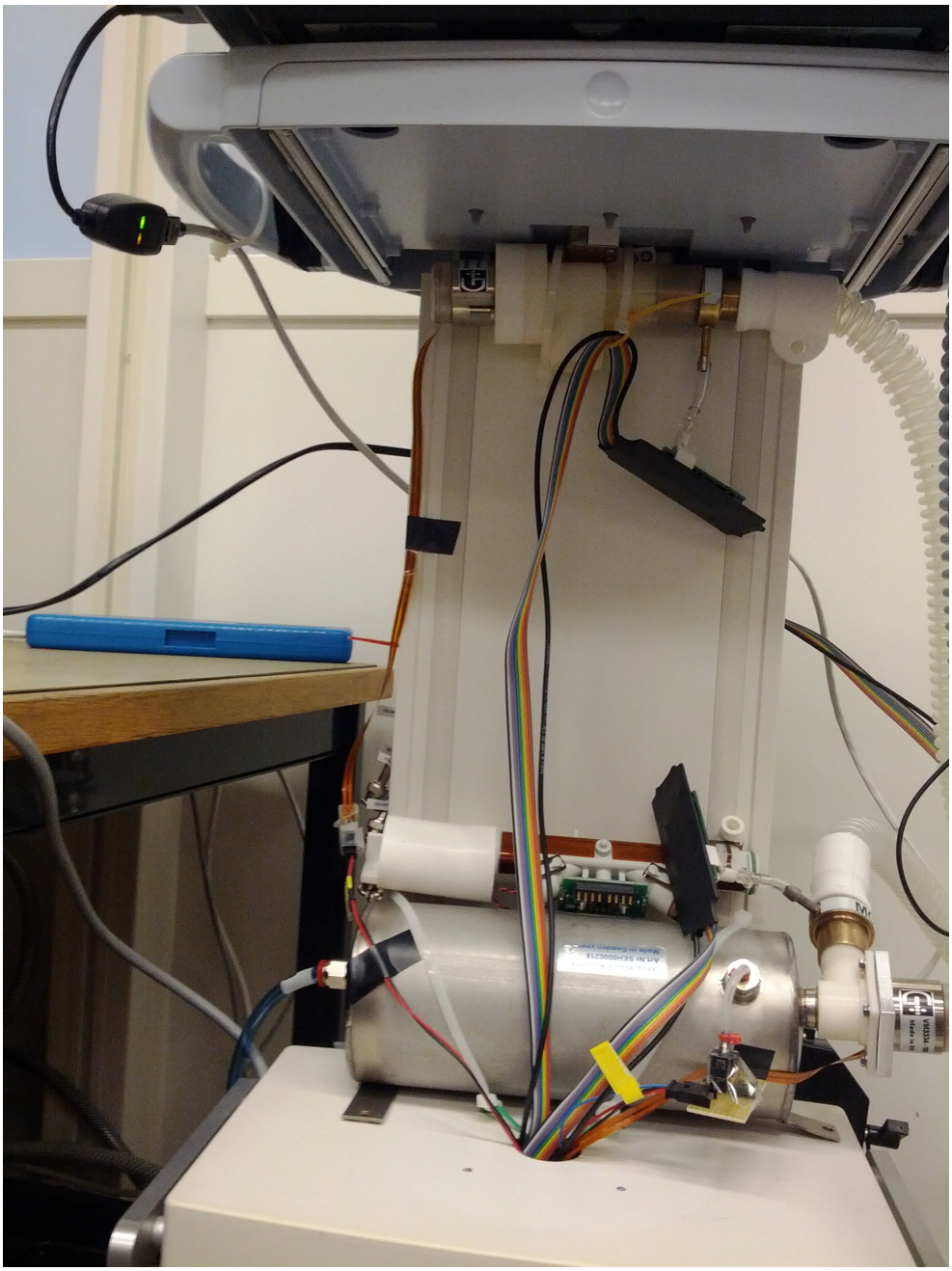

Figure 102: Inspiration valve with tank and expiration valve.

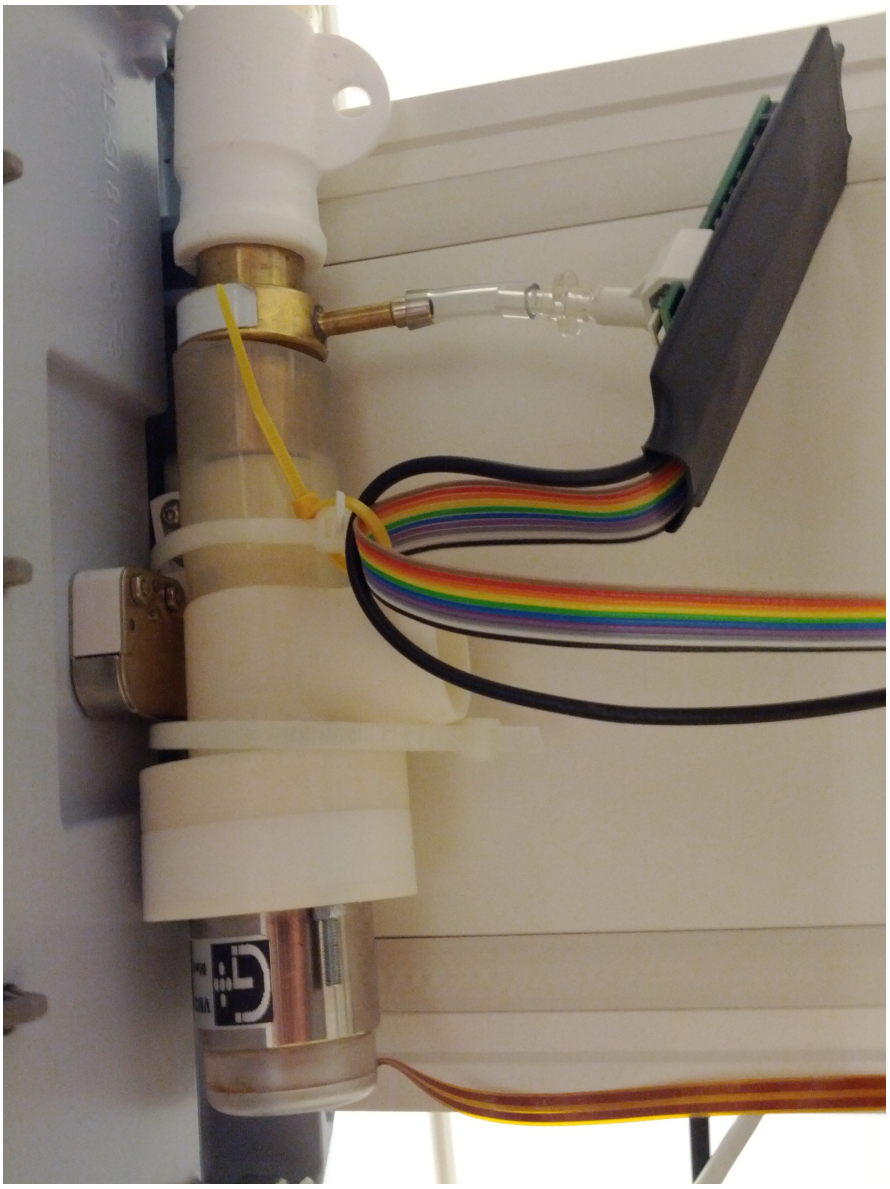

Figure 103: Expiration valve.

K Appendix - Model of the Voice Coil Motor

The electrical system, shown in the S-junction to the left in Figure 104, has the current i as state variable. Since it is a series electrical circuit - S-junction - the current is the same trough all components. The interaction between the electrical and mechanical systems is done in accordance with a gyrator with

$$U_{ind} = K_b \cdot v \qquad\qquad F_{VC} = K_f \cdot i$$

The velocity of the VCM induces a voltage proportional to the counter-electromotive force constant K_b and the current in the VCM produces a force proportional to the motor constant K_f.

In the S-junction to the right the mechanical system consists of two states. The force on the spring F_s - with spring constant k - and the velocity, v of the VCM. Since it is a S-junction, the velocity is the same for all forces acting on the actuator.

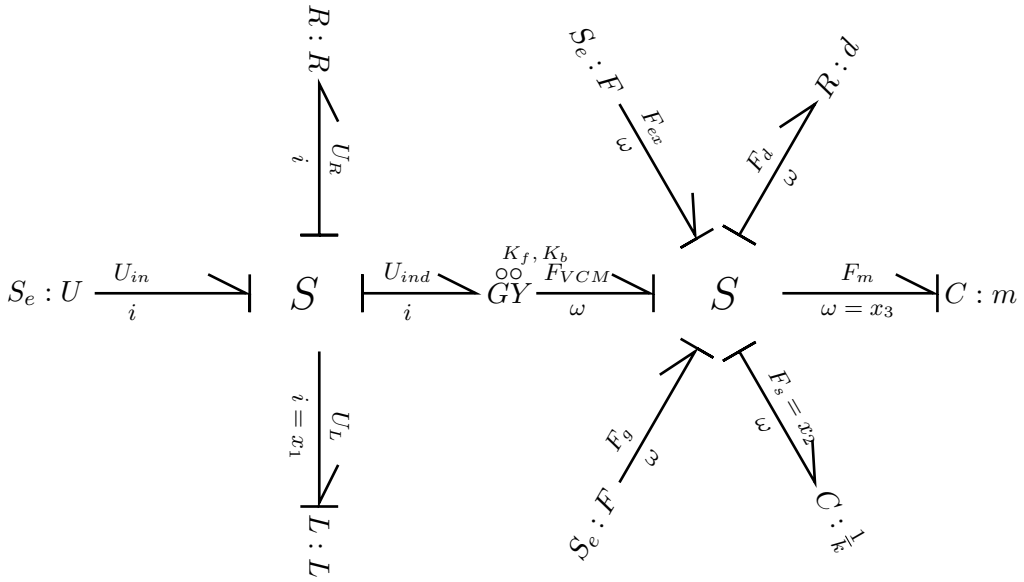

Figure 104: Bond graph model of the VCM actuator in a valve setup.

The state derived from the Bond Graphs in Figure 104 are shown in (20).

$$\begin{bmatrix} i\,(t) \\ F_s\,(t) \\ \omega\,(t) \\ \int \omega\,(t) \end{bmatrix} = \begin{bmatrix} x_1\,(t) \\ x_2\,(t) \\ x_3\,(t) \\ x_4\,(t) \end{bmatrix} \tag{20}$$

Since the position of the actuator determines the flow generated from the valve, this state is added simply by integrating the velocity state. The corresponding state space equations for the system is shown in (21).

$$\begin{bmatrix} \dot{x}_1(t) \\ \dot{x}_2(t) \\ \dot{x}_3(t) \\ \dot{x}_4(t) \end{bmatrix} = \begin{bmatrix} -\frac{R}{L} & 0 & -\frac{K_b}{L} & 0 \\ 0 & 0 & k & 0 \\ \frac{K_F}{m} & -m^{-1} & -\frac{d}{m} & 0 \\ 0 & 0 & 1 & 0 \end{bmatrix} \cdot \begin{bmatrix} x_1(t) \\ x_2(t) \\ x_3(t) \\ x_4(t) \end{bmatrix} + \begin{bmatrix} \frac{U_i}{L} \\ 0 \\ -g - \frac{F_p}{m} \\ 0 \end{bmatrix} \tag{21}$$

L Appendix - Ventilator Concept

The main purpose of this chapter is to show suggestions of possible ventilator designs. This to get a feeling for size and component placement. In Figure 105 and 106 their is a over view of the system and in Figure 107 their is a close up of the ventilator.

The main valves are shown in Figure 108. Figure 109 shown a top view with PCB, battery, tank and touch screen marked. Cross cut of the tank in the ventilator is shown in Figure 110.

In Figure 111 a cross section of the inspiration assembly is shown where basic parts are marked. In Figure 112 the expiration assembly basic parts are marked. Flow direction through cassette is also marked.

Figure 105: Front view of ventilator concept.

Figure 106: Backside of ventilator concept.

Figure 107: Close up of the ventilator concept.

Figure 108: Main valves in the ventilator.

Figure 109: Top view of the ventilator concept.

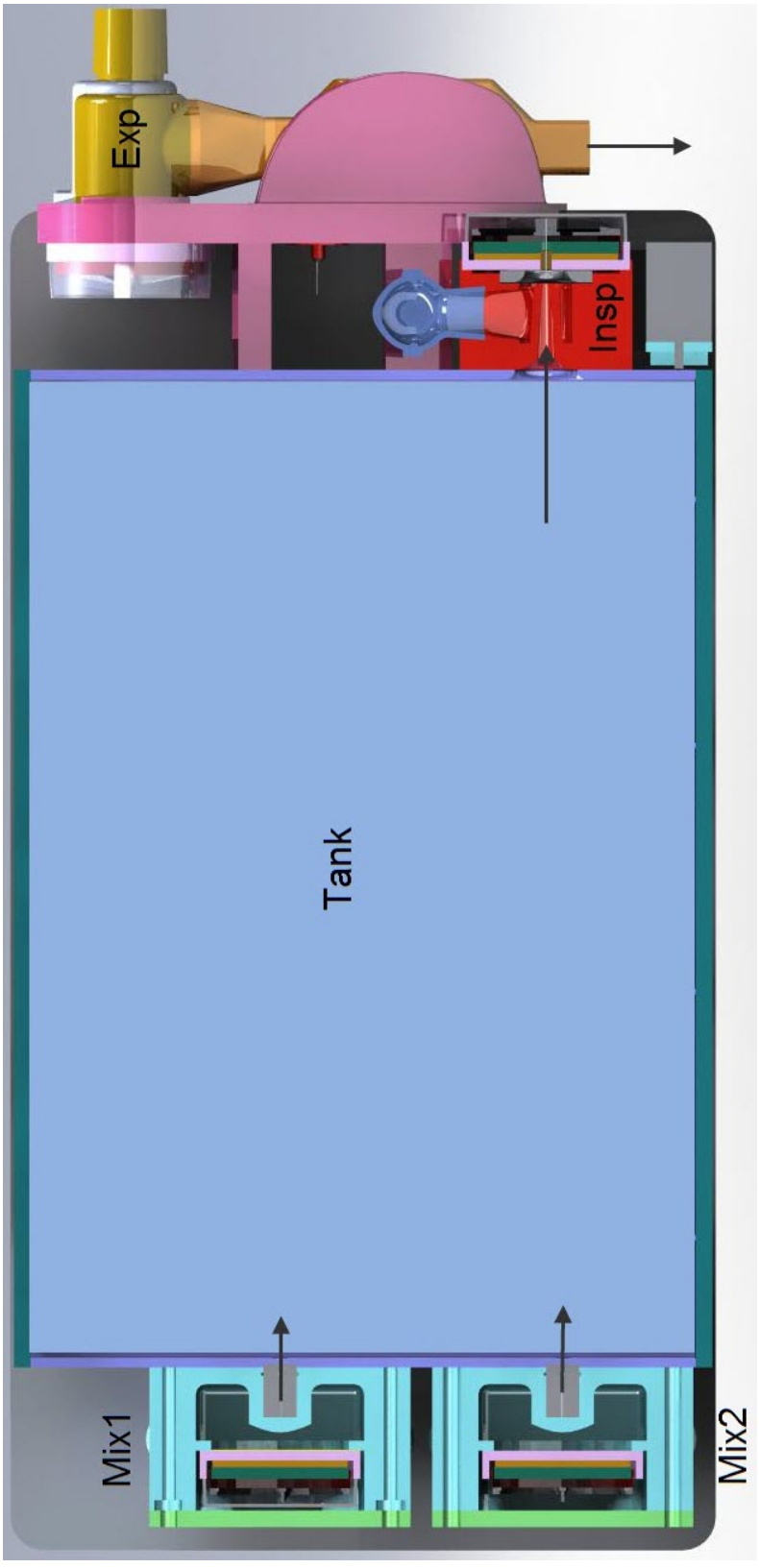

Figure 110: Flow direction in the system.

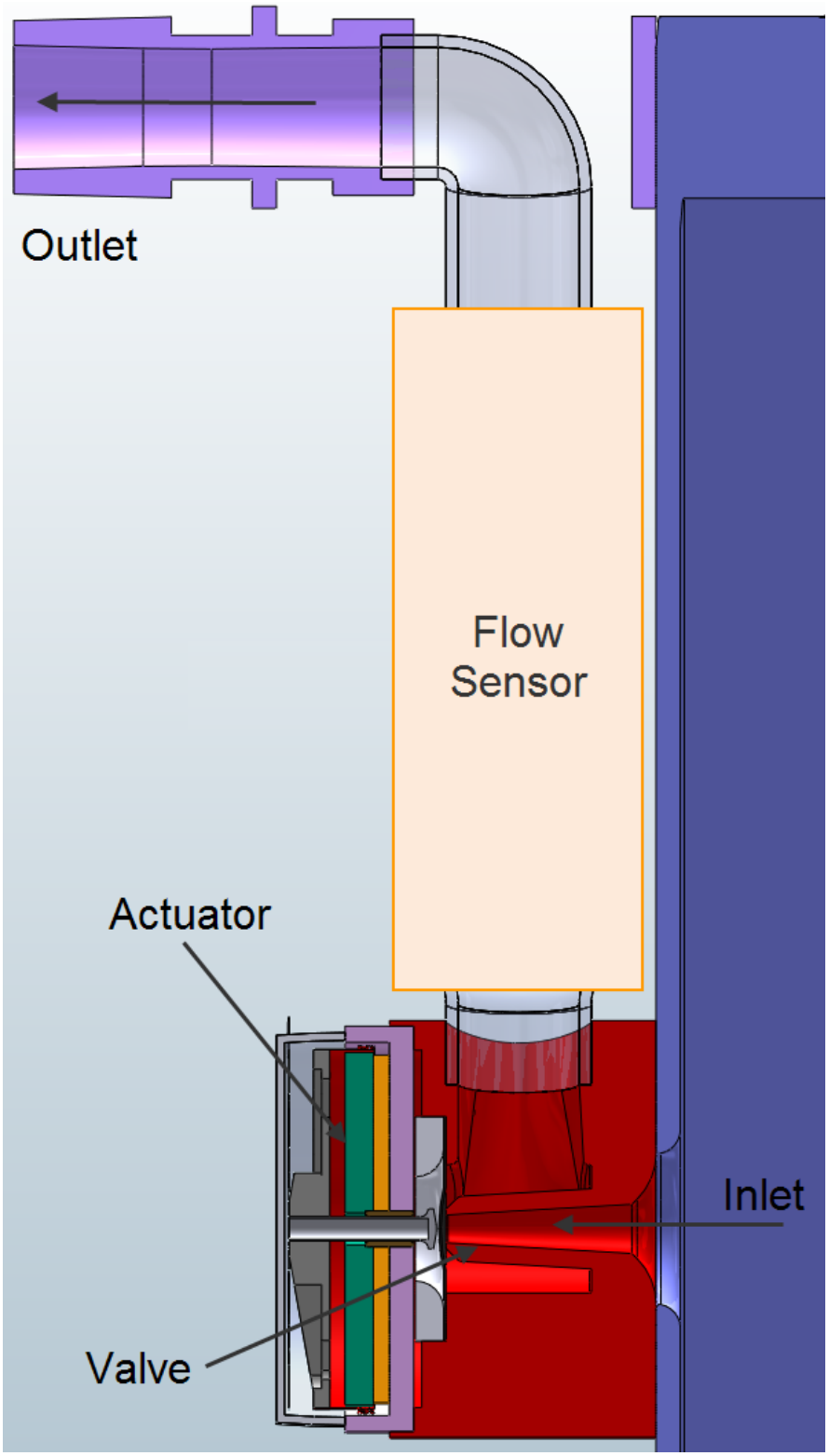

Figure 111: Inspiration assembly with basic parts.

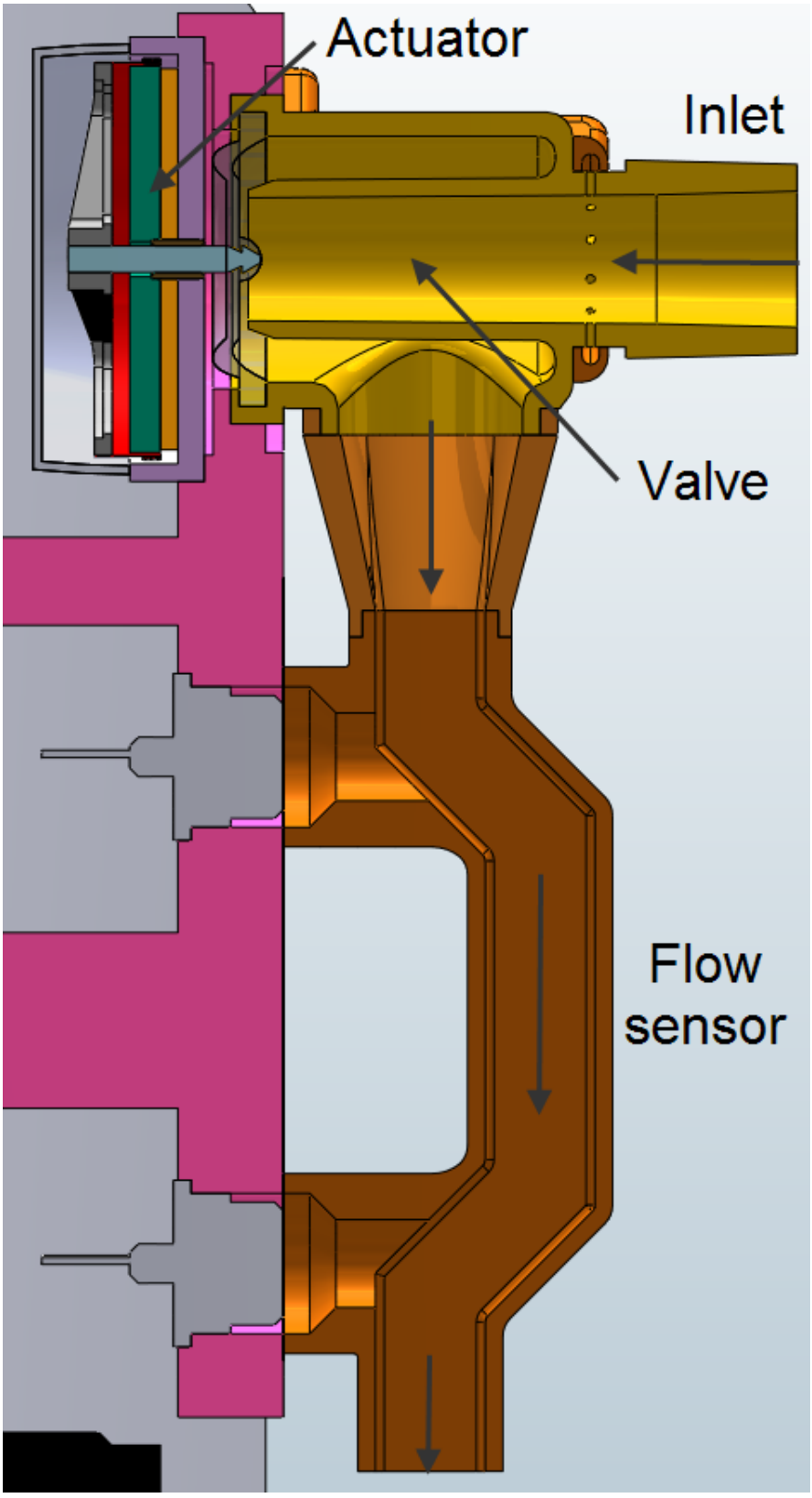

Figure 112: Expiration assembly with basic parts.

M Appendix - Optimization for Inspiration- and Expiration Actuator

Inspiration Actuator

The aim for the design of the inspiration actuator is to make the actuator as small as possible and have a stroke of 1.2 mm and the maximum force can be defined by selection of a suitable spring as describe in *Valve seat design* chapter. From this we get that a pretension of 1.9 N and spring constant of 2 N/mm is required. This will be the force limit what the actuator need to be enable to deliver at a 10% duty cycle. This curve has been determined from worst case for inspiration valve. The corresponding curve *Force 10% Duty cycle* can be seen in Figure 113a. The two other force curves in that Figure 113a represent the continuous needed force. This have been the ground when design the actuator.

After simulated different measurements a final size were selected. The selected measurements and chosen materials can be found in Table 7a. Result is shown as first a flux field graph which show the intensity of the magnetic field found in Figure 113b and second as a force curve at two different power consumptions modes show in Figure 113a. Where continuous drive consumes 1.6 W and with a 10% duty cycle consuming 3.5 W and the coil have a resistance of 1.6 ohm.

	Insp	Exp
A	20	10
B	1.3	1,3
C	2	3
D	19.7	9,7
a	2	3
b	2	3
c	3	3
Coil	0.6x2	0.6x3
Wire	0.2	0.2
Turns	20	30

(a) Inspiration and expiration measurements of voice coil motor in mm.

Name	Material
Magnet	NdFeB 52
Steel	Steel 1018
Coil	Copper, Ø = 0.2m

(b) Voice coil material

Discussion

As describe earlier this is used as a base for a discussion with an external partner, they will investigate this more. There are things in this simulations

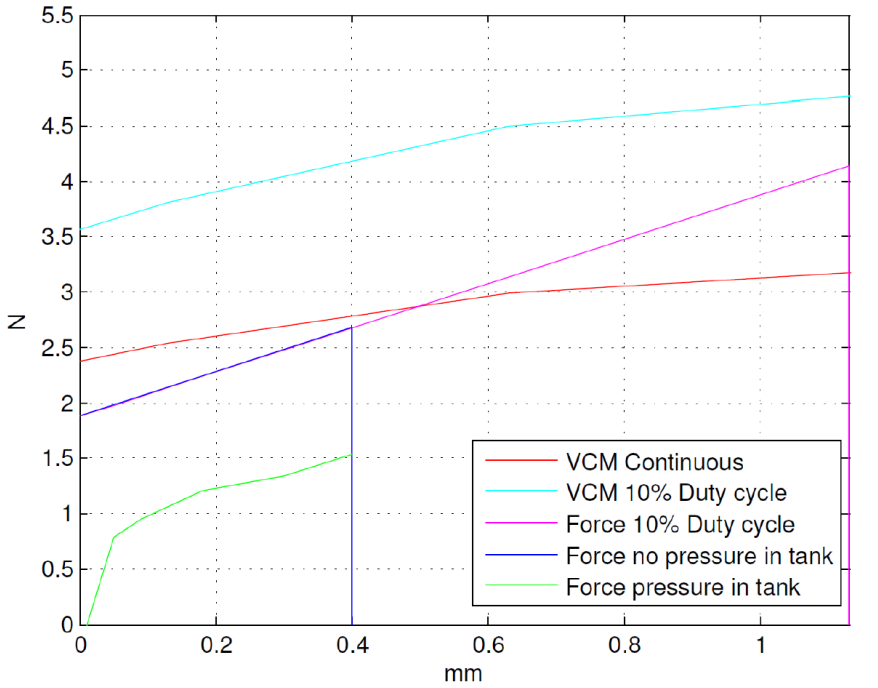

(a) Force characteristics.

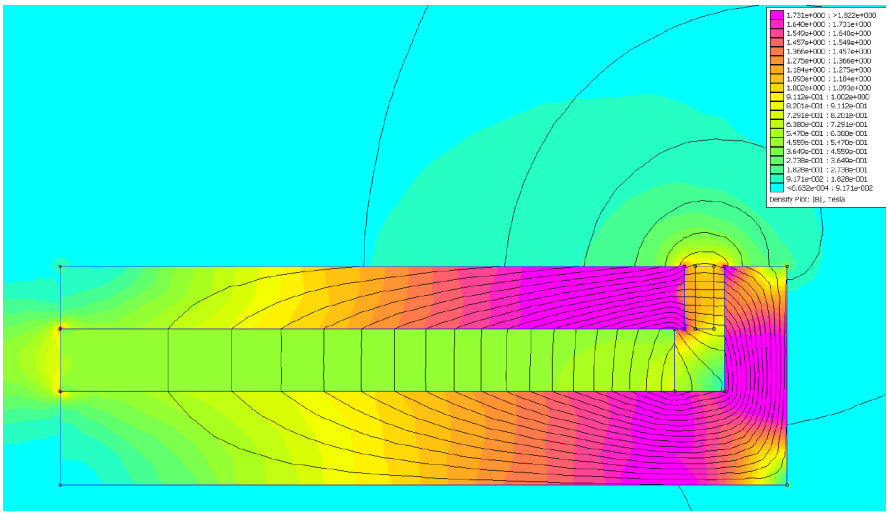

(b) Flux field intensity.

Figure 113: Result from FEMM simulation of inspiration actuator.

that not have been taken into account when design the actuator, like the temperature that arise when driven it a high power.

There would have been more optimal to have the peak force of the voice coil place where the continuous mode has the peak instead of where 10 % duty cycle has it. This to get the most out from the voice coil in the normal mode and assure that in can mange the peak force at 10 % duty cycle.

Expiration Actuator

Expiration actuator used in current assembly has three main problems: price, size and speed. Because of the new design of the valve seat the force requirements have been reduced hence it possible to use a smaller actuator. The measured force characteristics of the valve seat can be seen in Figure 114, where gap zero is when the valve is closed. These test results were performed with valve seat design uTurn and run as an inactive valve.

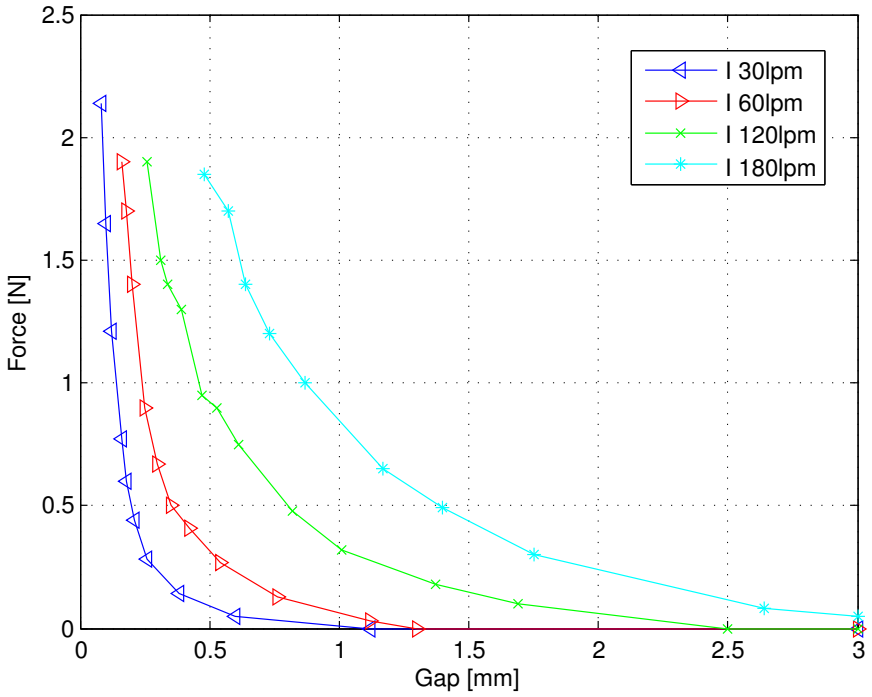

Figure 114: The force characteristics of uTurn valve seat design at different flows.

The conclusion from this is that, 0-1 mm is the stroke range where the high force demands are located. Other stroke part is the required force is relative small. This result is summarize in Figure 115a. Where actuator has two different modes continuous drive and 10% duty cycle, the big peak on the

10% duty cycle force curve is when the membrane is deforming against the valve seat.

The design has been performed with same procedures as describe in *Inspiration Actuator* part. Measurements for the final design can found in Table 7a and chosen material in Table 7b. This resulting in flux field intensity graph show in Figure 115b and a force curve at two different power consumptions modes show in Figure 115a. Where continuous drive consumes 1.9 W and with a 10% duty cycle consuming 3.4 W and the coil have a resistance of 1.3 ohm. From this we also get that the ferromagnetic material volume is 1.3 cm^3.

Discussion

Requirements that are given for the actuator is: Continuous power consumption lower than 5 W, ferromagnetic material half of current solution [17]. This is no problem to meet all given requirements. Because of the low power consumption extra power can without any problem be applied if needed as requirements say peak power can be up to 15 W.

This is not an optimal solution for example use for three layers of coil wire dose not use the air gap in an optimal way. The continuous mode can be lowered more and from this place the peak force to get out the maximum from the voice coil when required. It would be possible to have a force curve that is steeper to get an even better efficiency.

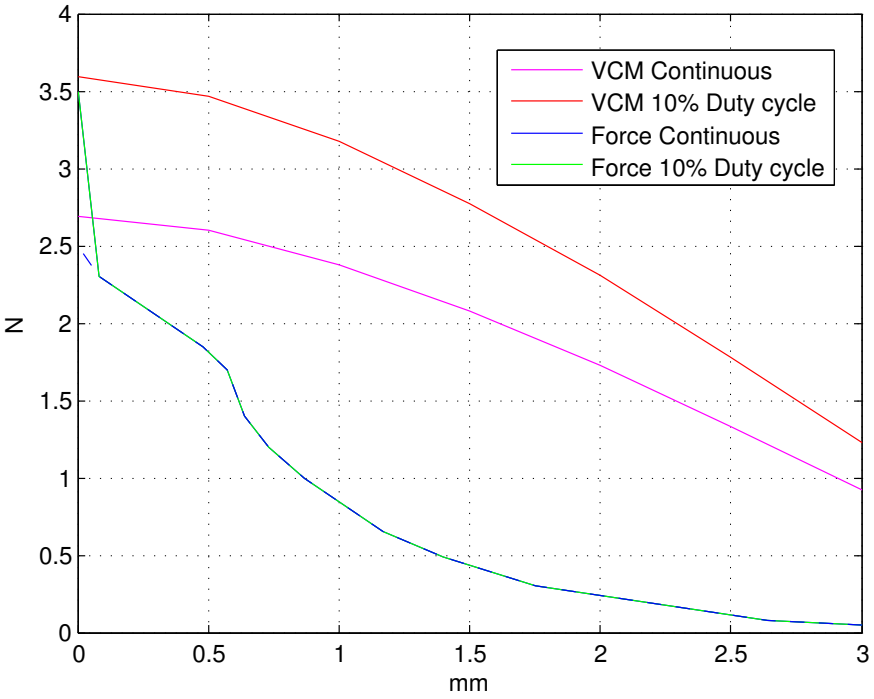

(a) Force characteristics.

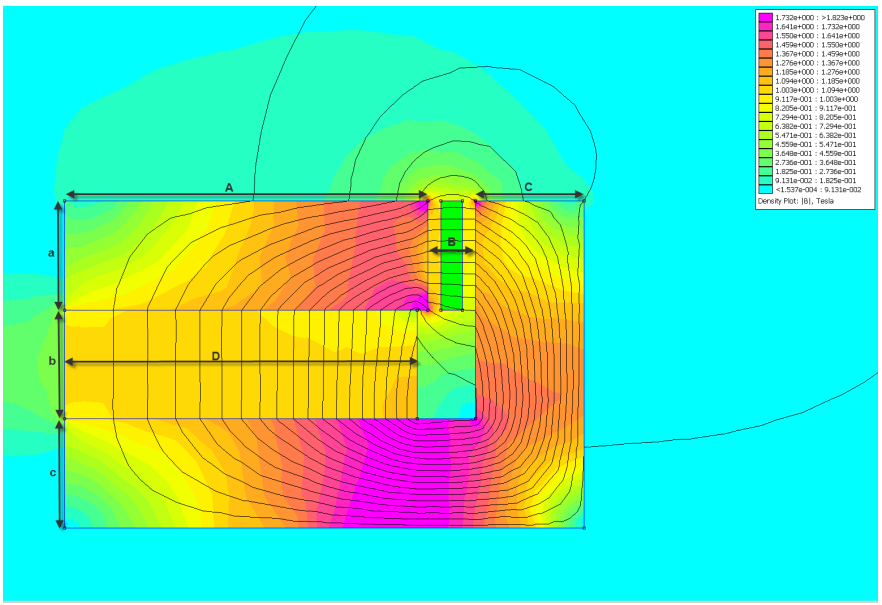

(b) Flux field intensity.

Figure 115: Result from FEMM simulation of expiration actuator.